

**Genetic Manipulation of the Cross-talk between Abscisic  
Acid and Strigolactones and Their Biosynthetic Link  
during Late Tillering in Barley**

Dissertation

zur Erlangung des  
Doktorgrades der Naturwissenschaften (Dr. rer. nat.)

Der  
Naturwissenschaftlichen Fakultät I  
Biowissenschaften  
der Martin-Luther-Universität Halle-Wittenberg,

vorgelegt  
von Herrn M.Sc. Hongwen Wang  
geb. am 10.02.1985 in Gaomi, China

Gutachter:

1. Prof. Dr. Nicolaus von Wirén
2. Prof. Dr. Klaus Humbeck
3. Prof. Dr. Harro J. Bouwmeester

Datum der Verteidigung: 27.04.2017, Halle (Saale)

## Contents

1. Introduction .....	1
1.1 Genetics of tillering in barley .....	1
1.2 Functional role of abscisic acid in branch or tiller development .....	4
1.3 Abscisic acid biosynthesis and metabolism.....	5
1.4 Functional role of strigolactones in branch or tiller development .....	7
1.5 Biosynthetic pathway of strigolactones .....	8
1.6 The cross-talk between abscisic acid and strigolactones biosynthetic pathways .....	10
1.7 Aim of the present study .....	11
2. Materials and methods .....	13
2.1 Materials .....	13
2.1.1 Plant materials .....	13
2.1.2 Bacterial strains .....	13
2.1.3 Plasmid and Vectors .....	13
2.1.4 Primers .....	13
2.1.5 Chemicals .....	14
2.1.6 Enzymes and kits.....	15
2.1.7 Special instruments .....	15
2.1.8 Media.....	15
2.2 Methods .....	16
2.2.1 Plant growth conditions for Golden Promise and LOHi3/236/272 lines .....	16
2.2.2 Histological analysis .....	17
2.2.3 RNA isolation from tissues .....	17
2.2.4 Quality check of the RNA using NanoDrop.....	18
2.2.5 cDNA synthesis and quality of the cDNA .....	18
2.2.6 Quantitative real time polymerase chain reaction (qPCR).....	19
2.2.7 Extraction and analysis of ABA .....	19
2.2.8 Extraction and analysis of strigolactones .....	20
2.2.9 Basic cloning methods and sequencing.....	21
2.2.10 Phylogenetic analyses .....	22

2.2.11	Vector constructions of <i>pAtD27::HvD27</i> and <i>35S::HvMAX1</i> .....	24
2.2.12	Stable transformation of Arabidopsis and generation of transgenic plants .....	25
2.2.13	Genomic DNA extraction .....	25
2.2.14	Plant growth conditions for VIGS experiments .....	26
2.2.15	Vector constructions of VIGS- <i>HvD27</i> , VIGS- <i>HvCCD7</i> and VIGS- <i>HvCCD8</i> .....	26
2.2.16	<i>In vitro</i> transcription and BSMV inoculation .....	27
2.2.17	Statistical analysis .....	27
3.	Results .....	28
3.1	Silencing <i>HvABA 8'-hydroxylase</i> gene provokes a late-tillering phenotype.....	28
3.2	ABA accumulation in stem bases and roots of LOHi lines .....	33
3.2.1	Expression analysis of ABA biosynthesis and degradation genes .....	33
3.2.2	ABA levels in wild type and LOHi antisense lines .....	37
3.3	Investigations on strigolactone biosynthesis in wild-type plants and <i>ABA 8'-hydroxylase</i> antisense lines.....	38
3.3.1	LC-MS/MS analysis and quantification of strigolactones .....	38
3.3.2	Identification of putative strigolactone biosynthesis pathway genes in barley .....	40
3.3.3	Gene expression analysis of putative strigolactone biosynthesis genes.....	45
3.4	Functional characterization of the <i>HvD27</i> gene by virus-induced gene silencing in barley .....	51
3.5	Functional characterization of the <i>HvCCD7</i> gene by virus-induced gene silencing in barley .....	55
3.6	Functional characterization of the <i>HvCCD8</i> gene by virus-induced gene silencing in barley .....	58
3.7	Functional characterization of the <i>HvMAX1</i> gene by a genetic complementation approach.....	61
4.	Discussion .....	64
4.1	The signaling role of strigolactones in barley shoot architecture .....	64
4.2	The $\beta$ -carotene isomerase DWARF27 links abscisic acid with the strigolactones biosynthesis.....	69
4.3	Crosstalk between the biosynthetic pathways of ABA and strigolactones .....	71

5. Summary .....	76
6. Zusammenfassung .....	78
7. References .....	80
8. Appendix .....	93
9. Abbreviations .....	103
10. Acknowledgements .....	106
11. Curriculum Vitae .....	108
12. Affirmation/Eidesstattliche Erklärung.....	110

## 1. Introduction

### 1.1 Genetics of tillering in barley

On a global scale, the most important cereal crops are maize (*Zea mays L.*), rice (*Oryza sativa L.*), wheat (*Triticum aestivum L.*) and barley (*Hordeum vulgare spp. vulgare*), with a total of 2.6 billion tons produced in 2013 (FAOSTAT, 2013). The demand for cereals may double by 2050, which will require an average yield increase of 2.4% per year for the major cereals (Ray *et al.* 2012, Tilman *et al.* 2011). Tillering in barley is a key component in yield formation because these specialized grain-bearing branches strongly influence final grain number. Tillers are formed from ABs (axillary buds), located in the leaf axils at the base of many grasses (Sreenivasulu and Schnurbusch 2012). Tillering is a plastic trait of agricultural importance that is modified by intrinsic signals and environmental cues to form shoot architecture (Agusti and Greb 2013). However, a large number of tillers coincides often with low fertility and seed filling. Thus, balancing the number of tillers is important, as unproductive tillers cost assimilates and nutrients that get lost whenever tillers are reduced. The development of new plant ideotypes, which follows the concept of idealized plant architecture (IPA), has been proposed as a means to enhance yield potential. Lower tiller numbers with few unproductive tillers, more grains per inflorescence, and thick and sturdy stems have been identified as most important characteristics of future high-yielding varieties (Jiao *et al.* 2010).

The vast diversity in above-ground plant architecture found in cereal crop species is largely governed by shoot branching or tillering. Shoot branching/tillering is determined by the number and activity of axillary meristems (AXMs) and subsequent dynamics in branch/tiller growth. During vegetative development, the shoot apical meristem (SAM) gives rise to all aerial structures of plants, including the primary shoot, leaves, nodes, internodes, inflorescence and the AXMs (DeCook *et al.* 2006, McSteen and Leyser 2005, Sussex 1989). When a branch originates from a leaf axil of an elongated internode, it is called an aerial branch, whereas the tiller is a side-branch developing from a basal leaf axil (Kebrom *et al.* 2013, McSteen and Leyser 2005). Barley only exhibits basal branches in acropetal succession with primary tillers growing out of leaf axils of the SAM, secondary tillers develop in the leaf

axils of primary tillers, and so on (Counce *et al.* 1996). Classically, tiller development in grasses has been divided into three stages: (i) initiation of an AXM in the leaf axil, (ii) development of leaf primordia from the AXM to produce an AB, which may remain dormant; or (iii) outgrowth of AB to form a tiller (Schmitz and Theres 2005). In barley, the first AXMs are initiated during embryogenesis. The mature barley embryo generally contains two ABs, one in the axil of the coleoptile and one at the first leaf primordium (Kirby and Appleyard, 1987).

To gain insights into the genetic regulation of the AXM initiation, a number of mutants have been identified in several species. These phenotypes can fall into two general classes (Oikawa and Kyozyuka 2009). One class restricts the AXM formation in conjunction with other abnormalities, such as defects in SAM formation (*pinhead* mutant), leaf polarity and vascular development (Raman *et al.* 2008) in *Arabidopsis thaliana* and leaf patterning (*uniculme4* mutant) in barley (Tavakol *et al.* 2015). The second class exhibits AXM-specific defects, including as mutants in *Arabidopsis thaliana*, *lateral suppressor (las)*, *regulator of axillary meristems (rax)* and *excessive branches1 (exb1)*; in tomato (*Solanum lycopersicum*), *lateral suppressor (ls)* and *blind (bl)*; in maize (*Zea mays*), *barren stalk1 (ba1)*, and in rice (*Oryza sativa*), *monoculm1 (moc1)* and *lax panicle1 (lax1)*. All the underlying affected genes are critical for AXM formation (Greb *et al.* 2003, Guo *et al.* 2015, Keller *et al.* 2006, Li *et al.* 2003, Muller *et al.* 2006, Oikawa and Kyozyuka 2009, Schmitz *et al.* 2002).

Another important branching or tillering event is the outgrowth of lateral buds after AXM establishment. The formation of ABs is mostly under genetic control, while bud outgrowth is determined by a complex interplay between differential gene expression, hormonal and environmental factors (Hussien *et al.* 2014, Kebrom, Spielmeier and Finnegan 2013, McSteen and Leyser 2005). Plant hormones, such as auxin, cytokinins (CK), and strigolactones (SLs), are major players in the control of axillary bud growth. The hormone auxin is mainly synthesized in the shoot apex in young leaves and subsequently transported basipetally in the polar auxin transport stream (PATS), which is responsible for apical dominance (Agusti and Greb 2013, Ljung *et al.* 2001). Auxin upregulates genes required for

strigolactone biosynthesis, and the subsequent inhibition of bud outgrowth by SLs. (Arite *et al.* 2007, Brewer *et al.* 2009, Hayward *et al.* 2009). Meanwhile, auxin suppresses cytokinin biosynthesis via transcriptional down-regulation of the genes required for biosynthesis. Hence, cytokinins cannot promote bud outgrowth any longer (Ferguson and Beveridge 2009).

Several mutants with altered tillering have been identified, and the corresponding barley genes may promote or repress tiller development by affecting AXM initiation or AB formation and outgrowth (Babb and Muehlbauer 2003, Dabbert *et al.* 2009, Hussien *et al.* 2014) (Table 1). These tillering mutants have been divided into two general classes (Bennett *et al.* 2006). The first class of genes is characterized by mutations that exhibit a low-tillering phenotype and promote AXM activity. These mutations include: *low number of tillers1 (lnt1)*, *absent lower laterals1 (als1)*, *intermedium-b (int-b)*, *uniculm2 (cul2)*, *uniculm4 (cul4)*, and *semibrachytic (uzu)*. The mutant *uniculm2 (cul2)* fails to develop ABs and carries no tillers. It is a well-studied example with a phenotype similar to that of the *moc1* mutant in rice (Babb and Muehlbauer 2003). Because of compromised axillary bud outgrowth, *low number of tillers1 (lnt1)*, *absent lower laterals1 (als1)* and *uniculme4 (cul4)* mutants show a low-tillering phenotype (Babb and Muehlbauer 2003, Dabbert *et al.* 2009, Dabbert *et al.* 2010). There are mutants with modestly reduced tillering, including the *intermedium-b (int-b)* and *semibrachytic (uzu)* mutants (Babb and Muehlbauer 2003). More aspects about gene mutation, function, and signaling have been addressed and updated in Hussien *et al.* (2014). Additionally, mutations in barley row type genes may have pleiotropic effects on tillering. It has been shown that one group of mutants with an increased number of seeds has a significant effect on tiller number at early development or reduced tillering only at full maturity. Another group of mutants is characterized by a reduction of seeds per spike and in tiller number and includes all alleles of *vrs3 (six-rowed spike 3)*, *int-c*, *int-f*, *vrs4*, and *vrs1* (with exception of *vrs1 (int-d.11)*). These lines show a negative correlation between tillering and seed number per spike. This group can be further divided into two subgroups: (a) low tillering already before maturity (*vrs3*, *int-c*, *int-f*) and (b) low tillering only at maturity (*vrs1*, *vrs4*). Another group contains all alleles of *als*, *lnt1*, *int-b*, and *vrs1 (int-d.11)*. These mutants show reduced tillering and reduced seed number per spike (Liller *et al.* 2015).

**Table 1.** List of barley tillering mutants. For each mutant, the chromosomal position and relevant references are indicated, along with the corresponding (candidate) gene and rice ortholog when known. Updated from Hussien *et al.* (2014).

Barley mutant	Map position	Mutant phenotype	Gene (rice ortholog)
<i>uniculm2 (cul2)</i>	6HL	no tiller, irregular INF	ND
<i>low number of tillers1 (Int1)</i>	3HL	few tillers, irregular INF	<i>JuBel2 (qSH1)</i>
<i>absent lower laterals1 (als1)</i>	3HL	few tillers, irregular INF	ND
<i>uniculme4 (cul4)</i>	3HL	few tillers	<i>NPR5</i>
<i>intermedium spike-b (int-b)</i>	5HL	reduced tillering, irregular INF	ND
<i>semibrachytic (uzu)</i>	3HL	reduced tillering and plant height, shorten spike	<i>HvBR11 (OsBR11)</i>
<i>granum-a (gra-a)</i>	3HL	high tillering, dwarf, shorten spike	ND
<i>intermedium-c (int-c)</i>	4HL	high tillering, reduced lateral spikelet development	<i>HvTB1 (OsTB1)</i>
<i>many noded dwarf1.a (mnd1.a)</i>	7HL	high tillering, dwarf, irregular INF	ND
<i>many noded dwarf6 (mnd6)</i>	5HL	high tillering, short spike	ND
<i>semidwarf1 (sdw1)/denso</i>	3HL	high tillering, reduced plant height	SD1
<i>intermedium spike-m (int-m)</i>	ND	high tillering, irregular INF	ND

INF, inflorescence; ND, not determined.

## 1.2 Functional role of abscisic acid in branch or tiller development

For many years abscisic acid has been postulated to have a role in the development of lateral branches or tillers. Previous studies indicated that the hormone abscisic acid (ABA) inhibits bud outgrowth as shown after exogenous ABA treatment in pea, Arabidopsis, Ipomoea spp., tomato, or sunflower (Chatfield *et al.* 2000, Cline and Oh 2006), or by the application of the ABA biosynthesis inhibitor fluridone in rose (*Rosa spp.*) (Le Bris *et al.* 1999), or in excised nodes of transgenic ABA-insensitive poplars (*Populus spp.*) (Arend *et al.* 2009). A negative correlation between ABA levels and the developmental status of buds was found in a wide range of plant species (Gocal *et al.* 1991, Knox and Wareing 1984, Mader *et al.* 2003, Tamas *et al.* 1979, Tucker 1977, Tucker and Mansfield 1971). The possibility that ABA may control branch development has been more widely explored. After decapitation of plants in a variety of species, ABA abundance in dormant ABs has been found to decrease (Gocal *et al.* 1991, Knox and Wareing 1984, Mader *et al.* 2003). When plants were exposed to light with high



R:FR ratio, usually decreasing ABA levels, bud outgrowth was stimulated in *Xanthium strumarium* and tomato (Tucker 1977, Tucker and Mansfield 1971). Recently, a study has also shown that ABA-related gene expression patterns increased in bud-containing tissues of *Arabidopsis* under low R:FR light, which led to a general reduction in branch numbers (Gonzalez-Grandio *et al.* 2013). Finally, Yao and Finlayson Scott (2015) have provided evidence that endogenous ABA exerts a direct effect on regulating axillary bud outgrowth in intact *Arabidopsis*, acting as a general inhibitor (Yao and Finlayson 2015).

### **1.3 Abscisic acid biosynthesis and metabolism**

As indicated in Figure 1, ABA is known to be synthesized from the isoprene derivative isopentenyl pyrophosphate (IPP) in plants (Schwartz *et al.* 1997b). The pathway uses the methylerythritol phosphate (MEP) pathway as a source of IPP. The MEP pathway seems to exist in all photosynthetic eukaryotes (Lichtenthaler 1999).

Most of the enzymes involved in ABA biosynthesis have already been identified (Cutler *et al.* 2010, Nambara and Marion-Poll 2005) by characterization of ABA auxotrophic mutants of *Arabidopsis* and corn (Koornneef *et al.* 1982, Koornneef *et al.* 1998, Schwartz *et al.* 1997a, Schwartz *et al.* 2003, Tan *et al.* 2003). ABA biosynthesis occurs in plastids with the exception of the last two steps where xanthoxin is converted to ABA in the cytosol (Marin *et al.* 1996, Seo *et al.* 2006, Tan *et al.* 2003). The first biosynthetic step in ABA biosynthesis is the conversion of zeaxanthin a C40 carotenoid precursor to all-*trans*-violaxanthin, a two-step epoxidation process catalyzed by zeaxanthin epoxidase (ZEP/AtABA1) (Audran *et al.* 2001). The enzyme(s) involved in the conversion of all-*trans*-violaxanthin to 9-*cis*-violaxanthin or 9'-*cis*-neoxanthin have not yet been identified. 9-*cis*-epoxycarotenoid dioxygenase (NCED) catalyzes the next step, which represents an oxidative cleavage of 9-*cis*-violaxanthin and/or 9'-*cis*-neoxanthin to produce xanthoxin and is considered to be the rate-limiting step (Chernys and Zeevaart 2000, Iuchi *et al.* 2001, Qin and Zeevaart 2002). Xanthoxin is eventually exported to the cytosol and converted to abscisic aldehyde by a short-chain dehydrogenase/reductase (SDR/AtABA2) (Cheng *et al.* 2002, Gonzalez-Guzman *et al.* 2002). Abscisic aldehyde is then oxidized to ABA by aldehyde oxidase (AAO/AO). AO needs the

sulfurylated form of a molybdenum cofactor (moco/AtABA3) for its activity (Bittner *et al.* 2001).

In contrast to ABA biosynthesis, there is less knowledge about its catabolism. As previously reported, the hydroxylation of ABA occurs in three different ways to form hydroxylated ABA that retains substantial biological activity. The spontaneous cyclization of the hydroxylated ABA results in phaseic acid (PA) which is further reduced to dihydrophaseic acid (DPA) by a soluble reductase. This spontaneous cyclization leads to a significant reduction of the biological activity in the form of PA and to zero activity in the form of DPA. The majority of ABA is converted to its inactive form via hydroxylation at the 8' position, which is carried out in barley by a cytochrome P450-type protein, ABA 8'-hydroxylase1/2/3 in barley (Seiler *et al.* 2011, Zhou *et al.* 2004, Zou *et al.* 1995).

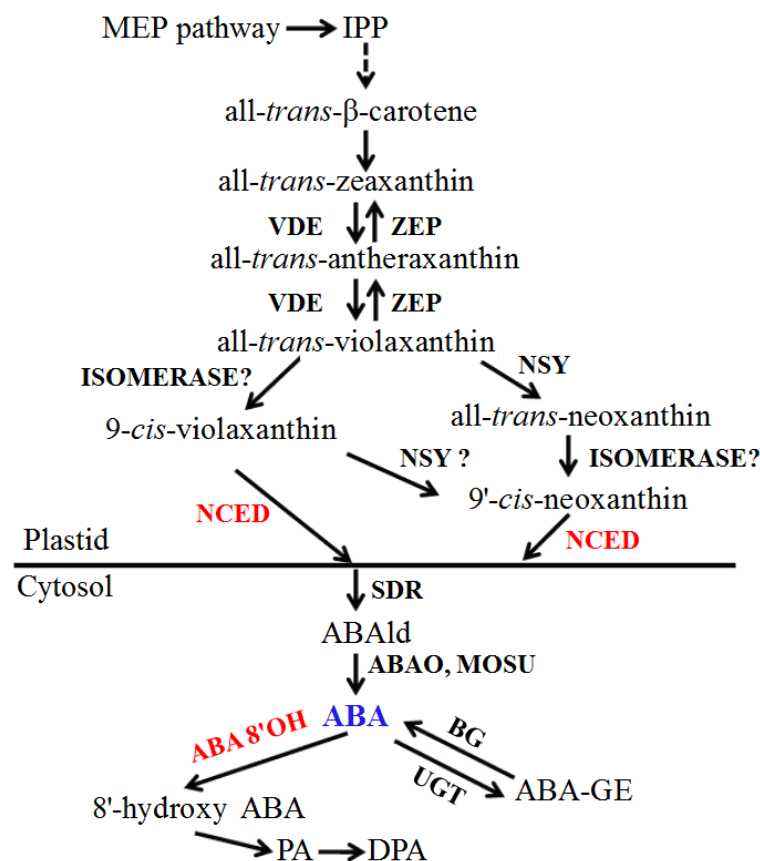


**Figure 1.** The ABA pathway in higher plants. The ABA precursor, a C40 carotenoid, is synthesized from IPP originating from the MEP pathway. *Solid arrows* indicate one-step modification of an intermediate and *dashed arrows* represent multistep modifications of an intermediate. Enzyme names are given in **bold**. Abbreviations: *IPP* isopentenyl pyrophosphate, *ZEP* zeaxanthin epoxidase, *VDE* violaxanthin de-epoxidase, *NSY* neoxanthin

synthase, *NCED* 9-*cis* epoxy-carotenoid dioxygenase, *SDR* short-chain dehydrogenase/reductase, *ABAO* abscisic aldehyde oxidase, *MOSU* molybdenum cofactor (MoCo) sulfurase, *ABAld* abscisic aldehyde, *ABA 8'OH* ABA 8'-hydroxylase, *BG* beta-glucosidase, *UGT* uridine diphosphate (UDP) glucosyltransferase, *PA* phaseic acid, *DPA* dihydrophaseic acid, *ABA-GE* ABA-glucose ester.

#### **1.4 Functional role of strigolactones in branch or tiller development**

Insights into the function of SLs in the regulation of lateral branches or tiller development have arisen from mutational analysis of branching in a variety of plant species (Al-Babili and Bouwmeester 2015). Restricted shoot branching by SLs was the first scientific proof (Gomez-Roldan *et al.* 2008, Umehara *et al.* 2008). Several mutations have been identified that are affected in SL biosynthesis or signaling, such as *ramosus (rms)* in pea, *decreased apical meristem (dad)* in petunia, *more axillary growth (max)* in Arabidopsis, or *dwarf (d)/high tillering dwarf (htd)* in rice. All these mutations show enhanced shoot branching phenotypes (Arite *et al.* 2007, Booker *et al.* 2004, Drummond *et al.* 2009, Johnson *et al.* 2006, Simons *et al.* 2007, Sorefan *et al.* 2003, Wen *et al.* 2016, Zheng *et al.* 2016, Zou *et al.* 2006 ).

Two compatible models have been proposed to explain SL interactions with auxin and cytokinins: the second-messenger and the canalization model. In line with the second-messenger model, auxin mediates the role of SL-CK antagonism in regulating bud outgrowth. Based on decapitation and girdling experiments it has been postulated that growing lateral branches or buds have an effect on auxin sink strength and their responsiveness to SLs. An elevated auxin abundance in the stem can inhibit bud outgrowth by maintaining locally high SL and low CK levels. It has also been found that both SL and CK can act locally in buds to control bud outgrowth, converging at a common target in the bud, possibly the TCP transcription factor, BRANCHED1 (BRC1) (Brewer *et al.* 2009, Dun *et al.* 2012, Ferguson and Beveridge 2009). The canalization-based model proposes that an initial auxin flux from an auxin source (shoot apex or buds) to an auxin sink (root) is gradually canalized into cell files by the action of PIN-type auxin transporters. These cell files will subsequently differentiate into vascular tissue, through which auxin will be transported (Domagalska and Leyser 2011). Auxin export from buds is correlated with the initiation of

bud outgrowth and therefore it is believed that buds need to export auxin in order to be activated [reviewed by (Muller and Leyser 2011)]. Leyser's group carried out computer modeling to study how SLs affect auxin transport, in which different processes regulating polar auxin transport were simulated. The results from this study suggested that SL may modulate PIN cycling between the plasma membrane and endosomes (Prusinkiewicz *et al.* 2009). Computer modeling provided additional support for the canalization-based model for shoot branching control by SL [reviewed by (Cheng *et al.* 2013)].

### **1.5 Biosynthetic pathway of strigolactones**

Over the past eight years, remarkable advancements in SL research have been made since their discovery as a new class of plant hormones in 2008 and as inhibitors of shoot branching (Gomez-Roldan *et al.* 2008, Umehara *et al.* 2008). It has been shown that 5-deoxystrigol is a common precursor of most of the natural SLs (Rani *et al.* 2008, Zwanenburg *et al.* 2009).

As shown in Figure 2, strigolactones are derived from the carotenoid biosynthetic pathway, of which all-*trans*- $\beta$ -carotene acts as the precursor for SLs biosynthesis and is converted into 9-*cis*- $\beta$ -carotene by the  $\beta$ -carotene isomerase DWARF27 (D27) (Alder *et al.* 2012, Lin *et al.* 2009, Waters *et al.* 2012). 9-*cis*- $\beta$ -carotene is cleaved by carotenoid cleavage dioxygenase 7 (CCD7) that is encoded by the gene *MAX3/RMS5/D17(HTD1)/DAD3* (Bookeretal *et al.* 2004, Drummondetal *et al.* 2009) into a 9-*cis*-configured aldehyde. The carotenoid cleavage dioxygenase 8 (CCD8) enzyme is encoded by the gene *MAX3/RMS5/D17(HTD1)/DAD3* (Bookeretal *et al.* 2004, Drummondetal *et al.* 2009) and incorporates three oxygens into 9-*cis*- $\beta$ -*apo*-10'-carotenal and performs molecular rearrangement, linking carotenoids with SL and producing carlactone (CL), a compound with strigolactone-like biological activities (Alder *et al.* 2012). A rice homolog of Arabidopsis *more axillary growth1* (*MAX1*), encodes a cytochrome P450 CYP711 subfamily member that acts as a CL oxidase to stereoselectively convert CL into *ent*-2'-*epi*-5-deoxystrigol, the presumed precursor of rice SLs. A protein encoded by a second rice *MAX1* homolog then catalyzes the conversion of *ent*-2'-*epi*-5-deoxystrigol to orobanchol (Zhang *et al.* 2014). More aspects about SL biosynthesis, perception, and signaling as well as structure-function relationships have been

nicely addressed and updated in the review by Janssen and Snowden (2012).

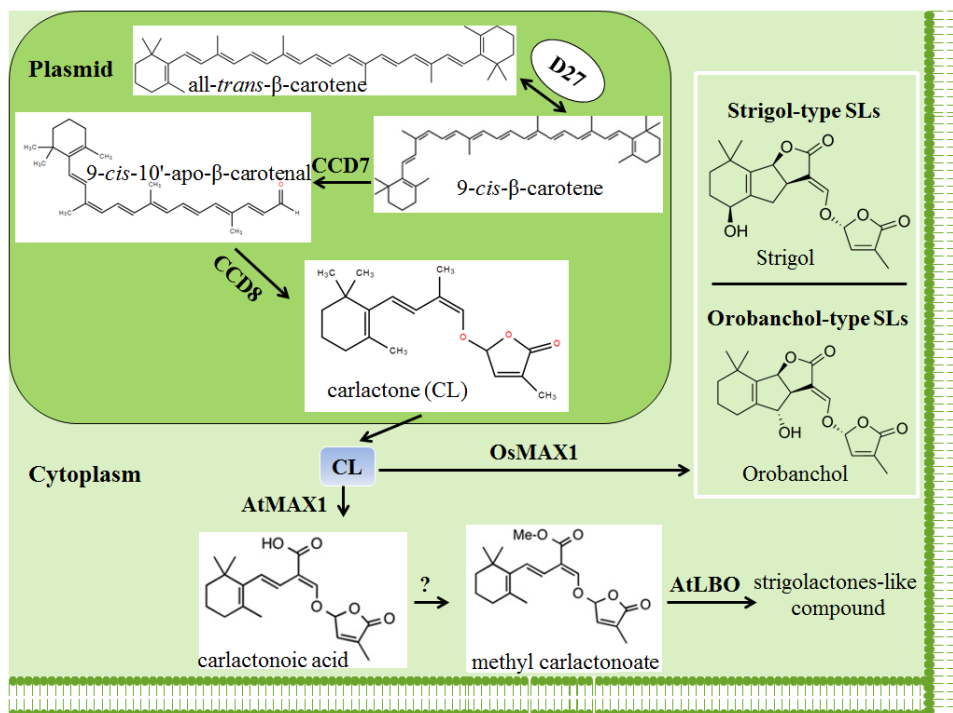


**Figure 2.** The biosynthesis of strigolactone (SL) in higher plants. SL biosynthesis involves an isomerase (D27) and two dioxygenases (CCD7, CCD8) that successively convert all-*trans*- $\beta$ -carotene into carlactone (CL), a key intermediate in SL biosynthesis. These enzymatic activities are occurring in the plasmid. CL is then transported into cytosol where it can be converted into SL-like compounds by more axillary growth1 (MAX1) and lateral branching oxidoreductase (LBO).

To date, more than 20 SLs have been isolated and characterized from root exudates of various plant species. All natural SLs contain a tricyclic lactone ring system (ABC part) that connects via an enol ether linkage to a butenolide moiety (D ring) (Xie *et al.* 2010). These SLs have different substituents on the A/B ring but the same C-D moiety and possess an *R*-configuration at C-2', which has been described to be important structural features for inducing high germination of root parasitic plant seeds (Zwanenburg *et al.* 2009). The natural SLs can be divided into two types based on the stereochemistry or orientation of the C ring. Strigol-type SLs have a  $\beta$ -oriented C ring and include strigol (2), sorgolactone (4), sorgomol (5) and strigone (7) which are derived from 5-deoxystrigol (1). The other includes orobanchol-type SLs carrying an  $\alpha$ -oriented C ring, including orobanchol (11), fabacol (13),

7-oxoorobanchol (15) and solanacol (17), which are derived from 4-deoxyorobanchol (*ent*-2'-*epi*-5-deoxystrigol, 10) as shown in Figure 3.

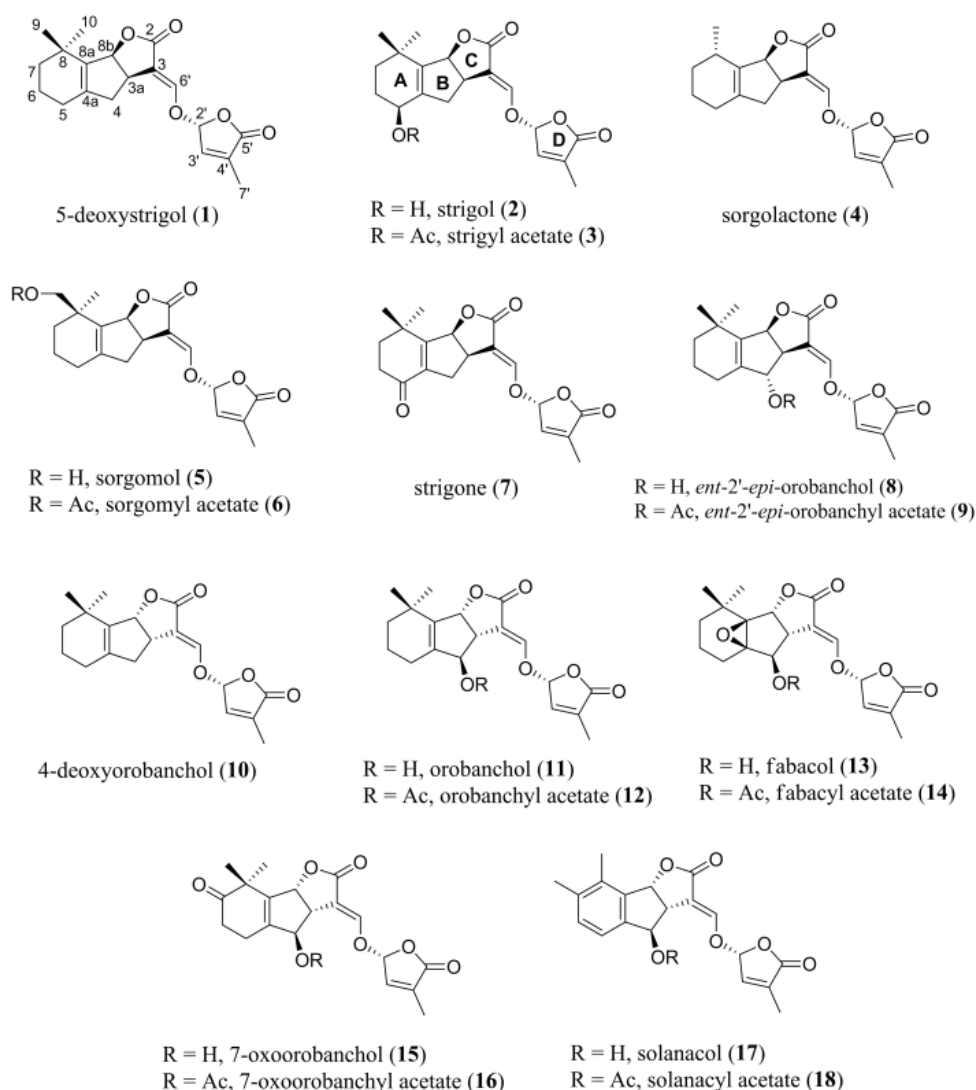


**Figure 3.** Structures of natural strigolactones.

## 1.6 The cross-talk between abscisic acid and strigolactones biosynthetic pathways

Both ABA and SL are derived from the carotenoid pathway from which they are hypothesized to diverge at all-*trans*- $\beta$ -carotene and lead from all-*trans*- $\beta$ -carotene to all-*trans*-violaxanthin (Al-Babili and Bouwmeester 2015). Due to these common precursors, it is tempting to speculate that both hormones depend on each other and that induction of ABA biosynthesis

impacts on SL formation and vice versa. The 9-*cis*/all-*trans*- $\beta$ -carotene isomerization activity of D27 may represent an interesting point for a possible interference with ABA biosynthesis. Moreover, the structural similarity between all-*trans*- $\beta$ -carotene and epoxy-carotenoids also evokes a possible involvement of D27 in ABA biosynthesis (Alder *et al.* 2012). Identification of the isomerase, converting all-*trans*-violaxanthin to 9-*cis*-violaxanthin or 9'-*cis*-neoxanthin, is still the final piece missing for establishment of the overall framework of the ABA biosynthetic pathway in plants. Further analyzes of these genes and the corresponding mutants may help to discover the isomerase (Endo *et al.* 2014).

### **1.7 Aim of the present study**

Tillering, or the production of lateral branches, is an important agronomic trait that determines shoot architecture and grain production in barley. ABA has been shown to be associated with the development of lateral branches or tillers for many years. Strigolactones are recognized as plant hormones since 2008 and well established to mediate adaptive changes in plant architecture, but it has remained elusive whether the SL pathways are conserved in barley. Also little is known about the relationship between ABA and SL and their biosynthetic pathways, and effects of ABA-SL interaction on plant growth and development. Based on the fact that both ABA and SL are derived from the carotenoid pathway, from which they diverge at all-*trans*- $\beta$ -carotene (Al-Babili and Bouwmeester 2015), and D27 is supposed to interfere with ABA biosynthesis (Endo *et al.* 2014), the question arose whether there is a competition between these two pathways which may affect tiller formation in cereals. Therefore, the purpose of the present study was threefold: (a) to examine the ABA-SL interaction mode occurring at the hormone biosynthesis level and the effect of this crosstalk on tiller formation; (b) to examine the roles of *HvD27* in SL and ABA biosynthesis; and (c) to examine the roles of *HvCCD7*, *HvCCD8* and *HvMAX1* in barley plant architecture.

To investigate the ABA-SL crosstalk and its role in tiller formation, *ABA 8'-hydroxylase* RNAi plants were examined in growth-chamber and greenhouse-based phenotyping platforms. These lines were generated in our lab in a previous project and were referred to as LOHi for the *HvLea::HvABA 8'-hydroxylase* RNAi construct. The procedures for transformation of

barley and production of homozygous lines are explained in detail in Seiler *et al.* (2014). Three different homozygous lines LOHi3, LOHi236 and LOHi272 were chosen that show a strong increase in tiller number under control conditions. In this context, three independent experiments were performed for tiller phenotyping of LOHi3/236/272 in growth-chamber and greenhouse conditions. Quantitative real-time PCR (qRT-PCR) was used to quantify the expression levels of genes involved in ABA and SL biosynthesis. To detect and measure hormones, liquid chromatography-tandem mass spectrometry (LC-MS/MS) analysis was carried out. To characterize the *HvD27* function in the SL and ABA biosynthetic pathways, a genetic complementation study was conducted by expressing the *HvD27* gene in a corresponding Arabidopsis mutant and virus-induced gene silencing (VIGS) of *HvD27* was implemented in barley. To examine the roles of *HvCCD7*, *HvCCD8* and *HvMAX1*, a genetic complementation study was conducted by expressing the *HvMAX1* gene in a corresponding Arabidopsis mutant and by employing VIGS for *HvCCD7* and *HvCCD8* in barley.



## 2. Materials and methods

### 2.1 Materials

#### 2.1.1 Plant materials

*Hordeum vulgare* cv. Golden Promise, a two-rowed barley spring cultivar obtained from the Genebank department of the IPK, Gatersleben, Germany, was used as a wild type for comparison to the transgenic lines LOHi3/236/272 generated in this background (Seiler *et al.* 2014). Black Hulless barley plants were used for VIGS experiments. *Arabidopsis thaliana* Columbia (Col-0), *Atd27* mutant (GABI-Kat collection, GK-134E08.01) (Waters *et al.* 2012), *Atccd7* and *Atmax1* mutants (Prof. Dr. Ottoline Leyser lab) (Booker *et al.* 2005) were used for genetic complementation approaches in this study.

#### 2.1.2 Bacterial strains

*Escherichia coli* DH5 $\alpha$ : F-, f80d/*lacZ*\_M15, *recA1*, *endA1*, *gyrA96*, *thi-1*, *hsdR17* (rK<sup>-</sup>, mK<sup>+</sup>), *supE44*, *relA1*, *deoR*, *\_(lacZY AargF)* U169; (Grant *et al.* 1990)

*Agrobacterium tumefaciens*: EHA105 (Chetty *et al.* 2013).

#### 2.1.3 Plasmid and Vectors

pCR4-TOPO	Amp <sup>r</sup> (Invitrogen, Karlsruhe)
pd35S-Nos-AB-M	Amp <sup>r</sup>
p6U10	Spec <sup>r</sup>
BSMV Vectors	Amp <sup>r</sup> (Holzberg <i>et al.</i> 2002)

#### 2.1.4 Primers

The primers for PCR were designed using Primer 3 software (<http://bioinfo.ut.ee/primer3-0.4.0/>), Some RT-PCR and qRT-PCR primers were designed using Primer Express Software v2.0 and others were from previously published primer sets.

All primers were synthesized by Metabion (Germany); for details refer to Table 2.

**Table 2.** Primers used in this study.

Name	Forward primer (5'-3')	Reverse primer (5'-3')
qRT-PCR primers for detection of the RNA level of target genes		
<i>HvABA8'OH-1</i>	GTACAACTCGATGCCGGTG	CGGGCTGAGATGATGTGG
<i>HvABA8'OH-2</i>	GAGATGCTGGTGCTCATC	ACGTCGTCGCTCGATCCAAC
<i>HvABA8'OH-3</i>	TAGTACGTAGTGAGTAATTCCGGA	TGGGAGATTCTTTCAAATTTACAC
<i>HvNCED1</i>	CCAGCACTAATCGATTCC	GAGAGTGGTGATGAGTAA
<i>HvNCED2</i>	CATGGAAAGAGGAAGTTG	GAAGCAAGTGTGAGCTAAC
<i>HvD27</i>	TTTGGACAGCAACCTCTGAAG	CGCGATACATTTCTGTGCTGAA
<i>HvCCD7</i>	GGGAGGATCACGGCTATGTCT	CACCATCAGGTGGCATCTGTCT
<i>HvCCD8</i>	CCACTTCATCAACGCGTACGA	GGAGATTGTGGAGACGGAGGTT
<i>HvMAX1</i>	AAGCTCACCTCATCCACCTCTA	CGATGGAGAAGTGCAGCTTCA
<i>R2*</i>	GATGACTGCAACGCTCACAC	CTCAAAGGAAATAATCAGGCGTC
Primers used for semi-quantitative RT-PCR in VIGS and genetic complementation experiments		
BSMV- $\alpha$	CTTCTTTTGAAGATTCTGTTGG	TCATATGGTTGATGGGCACC
<i>AtACT8</i>	ATGAAGATTAAGGTCGTGGCA	TCCGAGTTTGAAGAGGCTAC
<i>HvD27</i>	ATGGAGGCCACCGCACTT	CTAGCAACTCACACCATAGT
<i>HvMAX1</i>	ATGGAGGGGGCGGGAGCA	TTAGTTGTTCTTTCAAGGACCT
Primers for cloning and vector constructions		
<i>pAtD27</i>	<b>GCACTAGT</b> GTTCTTGAGTGAGAAAAGAG	<b>GCCTCGAGAT</b> CTTTTGTTTTTTTTTTTGG
<i>HvD27</i>	<b>GCTCGAGAT</b> GGAGGCCACCGCACTTGT	<b>ACGCGTGCAC</b> CTAGCAACTCACACCATAGT
<i>HvMAX1</i>	<b>CCTCGAGAT</b> GGAGGGGGCGGGAGCA	<b>GGCAAGCT</b> TTTAGTTGTTCTTTCAAGGAT
<i>HvCCD7</i>	ATGCCGCCCAAGAGGCTGCTGGCG	TCATTCATCTGCCAGAACCCATGGAA
<i>HvCCD8</i>	ATGGCGTCGCTGCCCCATGATGATAGT	TCACTTGTCCCTGGGCACCCAGCAG
VIGS- <i>HvD27-1</i>	<b>CGGGATCC</b> ACGGTCAGAGCACCGTCTT	<b>CCTTAATTA</b> ATGTGTGTCGAGCCTGAAGAT
VIGS- <i>HvD27-2</i>	<b>CGGGATCC</b> GCCAAGTACATCGTCACAA	<b>CCTTAATTA</b> ACGCAGCTCATGTCTTCAAAA
VIGS- <i>HvCCD7-1</i>	<b>CGGGATCC</b> ACAGGATCAGGCTCGACATC	<b>CCTTAATTA</b> ACATCCTGTGGAAATGGAACC
VIGS- <i>HvCCD7-2</i>	<b>CGGGATCC</b> CAGATGTGGTCTGCTGCAC	<b>CCTTAATTA</b> AATTTATCGCAGGGAAATCCG
VIGS- <i>HvCCD8-1</i>	<b>CGGGATCC</b> TGAAGTGGAACGTCACGAAC	<b>CCTTAATTA</b> AACCCGGTCACCGAGAACTAC
VIGS- <i>HvCCD8-2</i>	<b>CGGGATCC</b> TGAAGTGGAACGTCACGAAC	<b>CCTTAATTA</b> AAAGTTCTGGACGCTGATCCC

*R2\**: The housekeeping gene (*serine/threonine protein phosphatase PP2A-4*, catalytic subunit, EST clone HZ44D03) as the reference gene included in each qRT-PCR run. Restriction sites in bold letters. Protective bases in italic letters.

## 2.1.5 Chemicals

Difco, USA

Bacto<sup>®</sup>-Agar, Bacto<sup>®</sup>-Trypton, Yeast extract, Beef extract, Peptone

Duchefa, Belgium	Murashige-Skoog, Hormones
Gibco-BRL, USA	Agarose
Invitrogen	Trizol
Roth, Germany	Acetic acid, Acetone, Ethanol, Chloroform, Formaldehyde, Glycerol, Isoamylalcohol, Isopropanol, Lithium chloride, Glutaraldehyde, Phenol, Ethyl acetate, Acetonitrile, Methanol

### 2.1.6 Enzymes and kits

Qiagen, Hilden, Germany	Plasmid isolation Kit, QIAquick PCR purification Kit, RNA isolation kit, RNase free DNAase set
Stratagene GmbH, Germany	<i>Pfu</i> polymerase, Salmon sperm DNA
Fermentas	GeneRuler™ DNA Ladder Mix, Rapid DNA Ligation Kit, Restriction enzymes
Agilent	RNA nano kit
Applied biosystem, UK	SYBR-GREEN-PCR master mix
Invitrogen	SuperScript III, TA-cloning kit

### 2.1.7 Special instruments

Agilent	Agilent 2100 Bioanalyzer
Applied biosystem, USA	ABI PRISM 7900 HT Sequence Detection System
Peqlab	NanoDrop 1000 Spectrophotometer V3.5.1

### 2.1.8 Media

#### Bacterial media

LB	10 g NaCl, 5 g Tryptone, 5 g Yeast extract for 1 L (pH 7.4) Solidified media contain 1.5% Difco-agar
----	---

YEB 10 g Beef extract, 1 g Yeast extract, 5 g Peptone,  
5 g Sucrose, 1 M MgSO<sub>4</sub> 2 ml; pH 7.0 for 1 L  
Solidified media contain 1.5% Difco-agar

### **Plant growth medium**

Murashige and Skoog medium 4.6 g MS salts, Sucrose 10 g for 1 L  
Solidified media contain 1% Phytoblend  
agar

## **2.2 Methods**

### **2.2.1 Plant growth conditions for Golden Promise and LOHi3/236/272 lines**

For the experimental analyses, wild-type barley (cv. Golden Promise) and homozygous transgenic plants LOHi3/236/272 were cultivated in a greenhouse or growth chamber (phytochamber) (Table 3). For growth in the phytochamber, seeds were sown directly in pots filled with 2 parts of compost, 2 parts of “Substrat 2” (Klasmann) and 1 part of quartz sand. Vernalization was done for a period of 8 weeks from germination under a temperature regime of 11°C day/7°C night and 10 h light. The further growing conditions were divided into four phases with the first three phases extending for 2 weeks each and the last phase lasting till ripening. The conditions during the various phases are as follows: phase 1: 14°C day/9°C night with 12 h light, phase 2: 16°C day/9°C night with 14 h light, phase 3: 20°C day/12°C night with 16 h light, and phase 4: 20°C day/14°C night with 16 h light. The plants were fertilized regularly with plantacote plus (15 g pot<sup>-1</sup>) during vegetative phase and with liquid fertilizer “Hakaphos Rot” (once a week; 2-4%) from the start of spike development. Total tiller number until maturity was counted for all plants every week (n ≥ 20 plants).

**Table 3.** Growth conditions used for the two experiments.

Environmental parameters	Experiment 2	Experiment 1
Experimental site	Greenhouse-IPK	Phytochamber-IPK
Sowing date	28 July 2014	21 Nov. 2012
Spacing (cm)	16	16
Light density ( $\mu\text{mol m}^{-2} \text{s}^{-1}$ )	270~300	350~380
Average daily minimum temperature ( $^{\circ}\text{C}$ )	17	12
Average daily maximum temperature ( $^{\circ}\text{C}$ )	20	20
Humidity (%)	70	70
Water supply (every 2-3 days)	yes	yes

### 2.2.2 Histological analysis

At 2 weeks after germination (WAG) and 3 WAG in phytochamber, whole shoot apical meristems were chemically fixed with 2% glutaraldehyde and 2% formaldehyde in cacodylate buffer (50 mM, pH 7.0, 16 h). Samples were washed in buffer and water (20 min), and dehydrated in a graded ethanol series following by embedding in Spurr's low viscosity resin. Semi-thin (2  $\mu\text{m}$ ) sections were made on a Reichert-Jung Ultracut S (Leica, Vienna, Austria), stained with crystal violet, and examined with a Zeiss Axioimager light microscope (Carl Zeiss, Jena, Germany).

### 2.2.3 RNA isolation from tissues

Total RNA was isolated from plant tissues using the TRIZOL reagent and RNeasy columns. Plant tissue was ground in liquid nitrogen and 100 mg of the homogenized powder was added to 1 ml TRIZOL and incubated for 5 min at room temperature. Samples were centrifuged at 10000 rpm for 10 min and the supernatant was transferred to a new tube. 200  $\mu\text{l}$  of chloroform was added and incubated at room temperature for 2–3 min. Samples were again centrifuged as described above and the aqueous supernatant was transferred to a Qia shredder column (Qiagen) and centrifuged for 30 s at 10000 rpm. 350  $\mu\text{l}$  of RLT buffer (a guanidine-thiocyanate-containing lysis buffer, plus beta-mercaptoethanol 10  $\mu\text{l}/\text{ml}$  of RLT buffer) and 250  $\mu\text{l}$  of absolute ethanol were added to the flow-through and passed through an RNeasy spin column. All the following steps were performed as described in the

manufacturer's protocol (RNeasy Mini Kit-QIAGEN) followed by in-column DNase (DNase I (RNase-free) | NEB) digestion.

#### **2.2.4 Quality check of the RNA using NanoDrop**

RNA concentrations were measured using the NanoDrop photometer (Peqlab) according to the manufacturer's instructions. The purity of the RNA was also determined based on the absorbance value at 230 nm, 260 nm, and 280 nm recorded using the NanoDrop. Nucleic acid absorbs light at a wave length of 260 nm, while organic contaminants like phenols and other aromatic compounds used during the process of RNA extraction absorb light at 230 nm and 280 nm. If the RNA samples were not contaminated with organic compounds or any other impurities then the 260/230 and 260/280 absorbance value should be more than 1.8. RNA quality was also verified on a 1% (w/v) agarose gel to test for the contaminations by DNA and for degraded RNA. The absence of genomic DNA in the RNA samples was confirmed by PCR amplification of intron sequences in RNA samples using primers designed for the intron region.

#### **2.2.5 cDNA synthesis and quality of the cDNA**

The first strand cDNA was synthesized from RNA which was free from any DNA contamination using the SuperScript III reverse transcriptase (Invitrogen GmbH). 2 µg of total RNA, 1 µl of 50 µM oligo (dt-20 mer) primer and 1 µl of 10 mM dNTP mix and water were added to each tube to obtain a total volume of 10 µl and the reaction mixture was incubated at 65°C for 5 minutes, and then rapidly cooled on ice. 10 µl of cDNA master mix consisting of 2 µl of 10 x RT buffer, 4 µl of 25 mM MgCl<sub>2</sub>, 2 µl of 0.1 M DTT, 1 µl of RNaseOUT (40 U/µl) and SuperScript III reverse transcriptase (200 U/µl) was added and incubated at 50°C for 50 minutes. The reaction was terminated by incubating at 85°C for 5 min and chilling on ice. 1 µl of RNase H was added to each reaction tube and incubated at 37°C for 20 minutes to remove the RNA and the synthesized cDNA was stored at -20°C for further use.

To test cDNA yield, qPCR was performed using primers of a reference gene (serine/threonine protein phosphatase PP2A-4, catalytic subunit, EST clone HZ44D03) which was verified to

be stably expressed under all experimental conditions tested. The quality of the cDNA was assessed by using two primer pairs for a reference gene (elongation factor 1a, EST clone HZ42K12) from the 5' and 3' regions. The  $C_T$  value of the 5'-end primer did not exceed that of the 3'-end primer by more than one  $C_T$ , ensuring a uniform synthesis of cDNA.

### **2.2.6 Quantitative real time polymerase chain reaction (qPCR)**

qPCR reaction was carried out with an ABI PRISM 7900 HT Sequence Detection System using Power SYBR Green Mastermix reagent to monitor synthesis of dsDNA. The reaction was carried out in an optical 384-well plate, each reaction well contained 5  $\mu$ l of Power SYBR Green Mastermix reagent, 1  $\mu$ l of cDNA and 200 nM of each gene-specific primer in a final volume of 10  $\mu$ l. The following standard thermal profile was used for all PCR reactions: 50°C for 2 min, 95°C for 10 min, 45 cycles of 95°C for 15 s and 60°C for 1 min. Amplicon dissociation curves, i.e. melting curves, were recorded after the 45<sup>th</sup> cycle by heating from 60°C to 95°C with a ramp speed of 1.9°C per minute. As an internal control for the reference genes initially three genes were checked for their expression pattern in different tissue and it was found that serine/threonine protein phosphatase PP2A-4, catalytic subunit, EST clone HZ44D03 was stably expressed in all different tissues over different developmental stages. The serine/threonine protein phosphatase PP2A-4, catalytic subunit, was used as a reference gene for normalization of the expression level of genes of interest using the comparative  $C_T$  method as described by Schmittgen and Livak (Schmittgen and Livak 2008). All the data were analysed using the SDS2.2.1 software (Applied Biosystems). Expression levels of the gene of interest relative to the reference gene were calculated using the equation  $2^{-\Delta C_T} = 2^{-(C_{T_{GOI}} - C_{T_{RG}})}$  where, GOI = gene of interest, RG = reference gene.

### **2.2.7 Extraction and analysis of ABA**

ABA was extracted from fresh plant materials using ethyl acetate (100%). Isotopically labelled D6-ABA was used as an internal standard and added to each sample during the extraction procedure. Extraction was carried out twice with 1 ml of ethyl acetate at 4°C. The supernatant collected after centrifugation (13.000 g, 10 min, 4°C) was evaporated to dryness

at room temperature using a vacuum concentrator. The dried samples were redissolved in acetonitrile: methanol (1:1) and filtered using 0.8 µm filter (Vivaclear). The filtrate (10 µL) was used for subsequent quantification using LC-MS/MS (Dionex Summit coupled to Varian 1200 L). Chromatogram acquisition and data processing was accomplished with the Varian software, “Work station”. Chromatographic separation was carried out on a C18 column (4 µm, 100 mm; GENESIS; Vydac/USA). MRM and quantification was done using the mass traces 263/153 for ABA and 269/159 for D6-ABA. The validity of the extraction and measurement procedure was verified in recovery experiments (approx. 82-95%). Quantification was based on calibration with known ABA standards and individual recovery rates for the samples, as described in Kong *et al.* (2008).

### **2.2.8 Extraction and analysis of strigolactones**

For the collection of root exudates, 10 germinated seeds of each line were planted in a 3-L plastic pot filled with 1.5 L of silver sand. After 1 week, plants were thinned to 5 plants per pot. Half-strength modified Hoagland’s nutrient solution with corresponding phosphorus concentration ( $\text{KH}_2\text{PO}_4$ , 0.1 mM) was applied to each pot (500 ml at 48-h intervals) as shown in Table 4. The plants were allowed to grow in a phytochamber for 13 weeks under the same growth conditions as used before. In the fourteenth week, phosphorus deficiency ( $\text{KH}_2\text{PO}_4$ , 0.0 mM) was induced to increase strigolactone production. Three litres of phosphorus-deficient nutrient solution (half-strength modified Hoagland’s nutrient solution minus phosphate) were added to the top of each pot and allowed to drain freely through the holes in the bottom of the pot to remove phosphorus from the sand. The plants were kept under phosphorus deficiency for 1 week. In the fifteenth week, the same draining with 3 L of phosphorus-deficient nutrient solution was repeated to remove any accumulated strigolactones. Finally, 48 h later, root exudates were collected in a 1-L plastic bottle by passing nutrient solution without phosphate through each pot. The root exudates were passed through an SPE C18-fast column (500 mg per 3 mL), and the strigolactones were eluted with 6 mL of 100% acetone. For root extracts, 1 g fresh weight of ground root tissue was extracted following the method described by (Jamil *et al.* 2012), and the resulting extracts were evaporated to dryness,



taken up in hexane, loaded on pre-equilibrated Silica gel Grace Pure SPE (200 mg/3 mL) columns, and eluted with 2 mL of hexane:ethyl acetate (1:9) for further purification. The solvent was evaporated, and the residue was redissolved in 200  $\mu$ L of 25% (v/v) acetonitrile in water and filtered through Minisart SRP4 0.45- $\mu$ m filters (Sartorius) before LC-tandem MS (LC-MS/MS) analysis.

SLs were analysed by comparing retention times and mass transitions with SL standards (2'-*epi*-5-deoxystrigol, 5-deoxystrigol and D6-2'-*epi*-5-deoxystrigol) using a Waters Xevo TQ mass spectrometer equipped with an electrospray-ionization source and coupled to a Waters Acquity Ultraperformance LC system using the settings described by (Jamil *et al.* 2012) with some modifications specified in SI Materials and Methods (Cardoso *et al.* 2014). Detection and quantification of strigolactones by Liquid Chromatography-Tandem Mass Spectrometry (LC-MS/MS) and the analyses were performed with three biological replicates.

**Table 4.** Hoagland's nutrient solution.

Hoagland's nutrient solution	
Component	Final concentration
Ca(NO <sub>3</sub> ) <sub>2</sub> •4H <sub>2</sub> O	2 mM
K <sub>2</sub> SO <sub>4</sub>	0.5 mM
MgSO <sub>4</sub> •7H <sub>2</sub> O	0.5 mM
KH <sub>2</sub> PO <sub>4</sub>	0.1 mM
KCl	0.1 mM
H <sub>3</sub> BO <sub>3</sub>	1 $\mu$ M
MnSO <sub>4</sub> •H <sub>2</sub> O	2.5 $\mu$ M
ZnSO <sub>4</sub> •7H <sub>2</sub> O	0.5 $\mu$ M
CuSO <sub>4</sub> •5H <sub>2</sub> O	0.2 $\mu$ M
(NH <sub>4</sub> ) <sub>6</sub> Mo <sub>7</sub> O <sub>24</sub>	0.01 $\mu$ M
Fe-EDTA	100 $\mu$ M

### 2.2.9 Basic cloning methods and sequencing

The basic molecular cloning methods such as polymerase chain reaction, DNA electrophoresis and enzymatic digestion and ligation were performed according to standard protocols described by Chong 2001 (Chong 2001). DNA fragments were isolated and purified

from agarose gel by QIAquick gel extraction kit. Plasmid extractions were done using Qiagen Plasmid kits according to the protocol as prescribed by the manufactures. The sequences were confirmed by sequencing at LGC Genomics (Germany).

### 2.2.10 Phylogenetic analyses

Amino acid sequence alignments were performed using the ClustalW module in the MEGA (Molecular Evolutionary Genetics Analysis) 6.0 program (Tamura *et al.* 2013). Neighbor-joining trees and bootstrap analyses were also conducted using MEGA 6.0, and the following parameters were selected: model, p-distance; bootstrap, 1000 replicates; and gap/missing data, pairwise deletion. Protein sequences utilized in this analysis as well as NCBI accession numbers and data sources are listed in Table 5.

**Table 5.** List of protein sequences used in the phylogenetic analysis.

D27 and D27-like protein sequences			
Sequence ID	Species	Genbank ID	Name
1	<i>Oryza sativa</i>	254946546	OsD27
2	<i>Oryza sativa</i>	218186055	
3	<i>Zea mays</i>	226501302	
4	<i>Sorghum bicolor</i>	242068981	
5	<i>Vitis vinifera</i>	270235937	
6	<i>Arabidopsis thaliana</i>	18379048	AtD27
7	<i>Populus trichocarpa</i>	224062291	
8	<i>Medicago truncatula</i>	357462337	
9	<i>Medicago truncatula</i>	361064616	MtD27
10	<i>Hordeum vulgare</i>	326492644	HvD27
11	<i>Vitis vinifera</i>	225426574	
12	<i>Populus trichocarpa</i>	224057988	
13	<i>Arabidopsis thaliana</i>	18408106	
14	<i>Sorghum bicolor</i>	242080297	
15	<i>Oryza sativa</i>	115474501	
16	<i>Hordeum vulgare</i>	326495048	
17	<i>Zea mays</i>	195609902	
18	<i>Sorghum bicolor</i>	242089393	
19	<i>Vitis vinifera</i>	225437593	
20	<i>Zea mays</i>	224036007	
21	<i>Arabidopsis thaliana</i>	22328234	
22	<i>Oryza sativa</i>	115461907	
23	<i>Oryza sativa</i>	218196032	

CCD7 and CCD8 protein sequences			
Sequence ID	Species	Genbank ID or Locus	Name
1	<i>Hordeum vulgare</i>	<i>MLOC_55474.1</i>	HvCCD7
2	<i>Brachypodium distachyon</i>	357168137	
3	<i>Oryza sativa</i>	115459782	OsCCD7
4	<i>Zea mays</i>	308081144	
5	<i>Setaria italica</i>	514803094	
6	<i>Petunia x hybrida</i>	261863854	
7	<i>Nicotiana tabacum</i>	732554089	
8	<i>Solanum lycopersicum</i>	350535122	
9	<i>Chrysanthemum x morifolium</i>	938149454	
10	<i>Artemisia annua</i>	284055816	
11	<i>Lotus japonicus</i>	306450597	
12	<i>Citrus sinensis</i>	568825583	
13	<i>Orobanche ramosa</i>	350605181	
14	<i>Medicago truncatula</i>	357504533	
15	<i>Actinidia chinensis</i>	310896479	
16	<i>Glycine max</i>	359807642	
17	<i>Arabidopsis thaliana</i>	240254651	AtCCD7
18	<i>Jatropha curcas</i>	831204067	
19	<i>Hordeum vulgare</i>	<i>MLOC_66551.1</i>	HvCCD8
20	<i>Oryza sativa</i>	297597606	OsCCD8
21	<i>Oryza sativa</i>	115437714	
22	<i>Zea mays</i>	308081194	
23	<i>Vitis vinifera</i>	225429936	
24	<i>Solanum lycopersicum</i>	928192545	
25	<i>Citrus sinensis</i>	568844508	
26	<i>Petunia x hybrida</i>	57116144	
27	<i>Medicago truncatula</i>	357466651	
28	<i>Nicotiana tabacum</i>	515019305	
29	<i>Pisum sativum</i>	45504725	
30	<i>Glycine soja</i>	734366735	
31	<i>Cucumis melo</i>	661902861	
32	<i>Arabidopsis thaliana</i>	30689501	AtCCD8
MAX1 protein sequences			
Sequence ID	Species	Genbank ID	Name
1	<i>Hordeum vulgare</i>	326492025	HvMAX1
2	<i>Hordeum vulgare</i>	326530386	
3	<i>Oryza sativa</i>	475653170	
4	<i>Oryza sativa</i>	475653168	
5	<i>Oryza sativa</i>	937902656	
6	<i>Oryza sativa</i>	937923359	
7	<i>Oryza sativa</i>	937897916	

8	<i>Zea mays</i>	413926093	
9	<i>Sorghum bicolor</i>	241933382	
10	<i>Setaria italica</i>	944263874	
11	<i>Brachypodium distachyon</i>	944088318	
12	<i>Brachypodium distachyon</i>	944082596	
13	<i>Zea mays</i>	226493876	
14	<i>Arabidopsis thaliana</i>	30683024	AtMAX1
15	<i>Vitis vinifera</i>	296081643	
16	<i>Medicago truncatula</i>	357465755	
17	<i>Zea mays</i>	237908823	
18	<i>Setaria italica</i>	944242277	

### 2.2.11 Vector constructions of *pAtD27::HvD27* and *35S::HvMAX1*

The *AtD27* promoter was cloned from Arabidopsis genomic DNA and ligated into the pCR™2.1-TOPO® vector from the TOPO TA cloning® system (Invitrogen). Using the *SpeI* and *XhoI* sites present at both ends of the promoter, the sequence was further cloned into *pd35S-Nos-AB-M* vector (Figure 4). The cloning and orientation of the promoter was confirmed by digestion and sequencing; the vector was named as *pAtD27-Nos-AB-M*.

For sub-cloning *HvD27* under control of the *AtD27* promoter, the sequence was amplified from barley leaf cDNA using gene-specific primers and the PCR product was purified and cloned into the Topo-TA vector. The cloning was confirmed by sequencing. The *HvD27* Topo clone was further amplified with gene-specific primers having *XhoI* and *Sall* sites. The purified PCR product digested with *XhoI* and *Sall* was ligated to linearized *pAtD27-Nos-AB-M* to obtain a *pAtD27::HvD27-Nos-AB-M* vector. The *pAtD27::HvD27-Nos-AB-M* was then subcloned into p6U10 binary vector for plant transformation (Figure 4). This was achieved by releasing the whole cassette (*AtD27* promoter::*HvD27* gene: Nos terminator) using *Sfi* digestion that is compatible between both vectors. The obtained positive clones were sequenced to verify the orientation of the cassette in p6U10 vector.

For the vector construction of *35S::HvMAX1*, *HvMAX1* was amplified from barley leaf cDNA using gene-specific primers and the PCR product was purified and cloned into the Topo-TA

vector. The cloning was confirmed by sequencing. The *HvMAX1* Topo clone was further amplified with gene-specific primers having *XhoI* and *HindIII* sites. The purified PCR product was digested with *XhoI* and *HindIII* and ligated to linearized *pd35S-Nos-AB-M* to obtain a *pd35S::HvMAX1-Nos-AB-M* vector. The *pd35S::HvMAX1-Nos-AB-M* was then subcloned into the p6U10 binary vector for plant transformation (Figure 4).

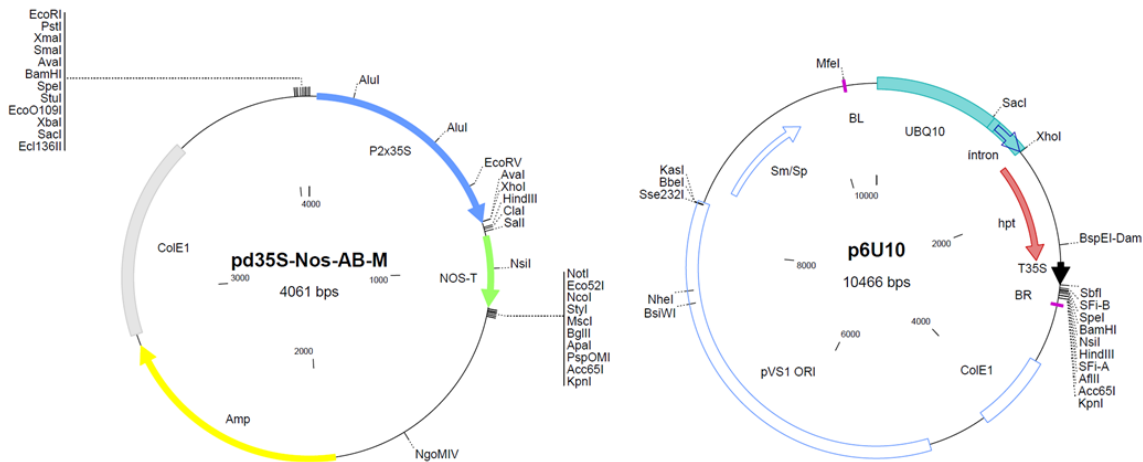


**Figure 4.** The plasmid maps of *pd35S-Nos-AB-M* and p6U10.

### 2.2.12 Stable transformation of Arabidopsis and generation of transgenic plants

Arabidopsis plants were grown in growth rooms under long-day conditions (16 h light/8 h dark) at 22°C. *Agrobacterium*-mediated transformation was performed using the floral dipping method as previously described (Clough and Bent 1998). Seeds collected from the transformed plants were sterilized with 2% sodium hypochlorite for 15 min and plated on Murashige and Skoog (MS) medium containing 50 µg ml<sup>-1</sup> hygromycin to inhibit *Agrobacterium* growth. The resistant transformants were transplanted to soil 2 weeks later. Transgenic Arabidopsis plants were grown in growth rooms under long-day conditions.

### 2.2.13 Genomic DNA extraction

Genomic DNA was extracted following the protocol described by Pallotta *et al.* (2000). Leaf tissue (100-200 mg) was finely ground in liquid nitrogen and incubated with 800 µl of

extraction buffer (100 mM Tris-HCl, 10 mM EDTA, 100 mM NaCl and 1% N-lauryl sarkosin, pH8) for 5 min at room temperature with intermittent vortexing and then 800  $\mu$ l phenol/chloroform/isoamylalcohol (25:24:1) mix was added before the sample was vortexed for 2 min at RT. The sample was centrifuged at 5000 rpm for 3 min (RT). The obtained supernatant (700  $\mu$ l) was transferred to a fresh Eppendorf tube and incubated on ice for 15 min after addition of 1 volume of isopropanol (700  $\mu$ l) and 1/10th volume of 3 M sodium acetate, pH 5.2 (70  $\mu$ l). DNA was precipitated by centrifugation of samples at 13000 rpm for 10 min (4°C). The DNA pellet was washed in 70% ethanol by re-suspending the pellet and centrifuging the samples at 7500 rpm for 10 min (4°C). The pellet was air dried to remove any traces of alcohol and then re-suspended in water or TE buffer (100  $\mu$ l). The DNA was freed of RNA by adding 2  $\mu$ l of RNase (40  $\mu$ g/ml) and incubating for 30 min at 37°C. DNA was then quantified using Nanodrop.

#### **2.2.14 Plant growth conditions for VIGS experiments**

Black Hulless plants used for VIGS experiments were grown in a controlled environmental climate chamber at 20–25°C with a 16/8 h light/dark photoperiod until the two leaf-stage, then inoculated with BSMV, kept for two weeks and transferred to a phytochamber until evaluation in laboratories of the biological safety level 2 (Pathogen-Stress Genomics lab, IPK).

#### **2.2.15 Vector constructions of VIGS-*HvD27*, VIGS-*HvCCD7* and VIGS-*HvCCD8***

The genome of BSMV consists of three RNA fragments,  $\alpha$ ,  $\beta$ , and  $\gamma$ . The constructs used in this study based on BSMV RNAs were described by Holzberg *et al.* (2002). A 336 bp and 306 bp sequence of *HvD27* was amplified using Thermo Scientific *Pfu* DNA polymerase with gene-specific primers harbouring *BamHI* and *PacI* restriction sites, respectively, at their extremities (Table 2), and then directionally cloned in antisense orientation into the *BamHI*- and *PacI*- digested BSMV- $\gamma$ -MCS multiple cloning site to generate the constructs VIGS-*HvD27*-1 and VIGS-*HvD27*-2, respectively. A 295 bp and 306 bp sequence of *HvCCD7* was amplified using Thermo Scientific *Pfu* DNA polymerase with gene-specific primers

harbouring *BamHI* and *PacI* restriction sites, respectively, at their extremities (Table 2), and then directionally cloned in antisense orientation into the *BamHI*- and *PacI*- digested BSMV- $\gamma$ -MCS multiple cloning site to generate the constructs VIGS-*HvCCD7-1* and VIGS-*HvCCD7-2*, respectively. A 202 bp and 338 bp sequence of *HvCCD8* was amplified using Thermo Scientific *Pfu* DNA polymerase with gene-specific primers harbouring *BamHI* and *PacI* restriction sites, respectively, at their extremities (Table 2), and then directionally cloned in antisense orientation into the *BamHI*- and *PacI*- digested BSMV- $\gamma$ -MCS multiple cloning site to generate the constructs VIGS-*HvCCD8-1* and VIGS-*HvCCD8-2*, respectively.

#### **2.2.16 *In vitro* transcription and BSMV inoculation**

The plasmids corresponding to the three components of BSMV were linearized with *MluI* ( $\alpha$  and  $\gamma$  components) or *SpeI* ( $\beta$  component) and used as templates for *in vitro* transcription using the AmpliCap-Max™ T7 High Yield Message Maker Kit (CELLSCRIPT™), following the manufacturers protocol. The three viral RNA components were mixed in a 1:1:1 ratio and 4.5  $\mu$ l of combined transcripts were mixed with 10  $\mu$ l of FES buffer (77 mM glycine, 60 mM  $K_2HPO_4$ , 22 mM  $Na_4P_2O_7 \cdot 10H_2O$ , and 1% w/v bentonite) and applied with gentle strokes to Carborundum-dusted leaves of barley 7 days post sowing. Unless stated otherwise, all barley plants were cv. Black Hullless grown in 12-cm pots filled with soil (Pindstrup Mix 2, Ryomgaard, Denmark), in either the growth chamber or a phytochamber at 20°C with 16 h of light and 8 h of darkness. Growth chamber light intensities did not exceed 1200  $\mu$ mol  $m^{-2} s^{-1}$  and were between 240 and 380  $\mu$ mol  $m^{-2} s^{-1}$  in the phytochamber of the biological safety level 2 (Pathogen-Stress Genomics lab, IPK).

#### **2.2.17 Statistical analysis**

Values derived from several biological replicates were used to calculate means and standard deviations, and statistical significance was assessed using the Student's *t*-test and one-way ANOVA across genotypes with Tukey's multiple comparison test ( $P < 0.05$ ). These calculations were performed using Genstat, 17<sup>th</sup> edition (VSN International Ltd., Hemel Hempstead, UK). Letters a, b, c and d represent statistical differences across means and across genotypes.

### 3. Results

#### 3.1 Silencing *HvABA 8'-hydroxylase* gene provokes a late-tillering phenotype

Previous studies demonstrated that abscisic acid functions in many plant biological processes such as plant stress tolerance, germination, seed development, lateral root development, and bud development (Yao and Finlayson 2015). To determine whether the *HvABA 8'-hydroxylase* gene is involved in the regulation of tiller formation in barley, an RNA interference (RNAi) approach was carried out to repress the endogenous *HvABA 8'-hydroxylase* gene and thereby modulate the ABA content in transgenic barley lines. The expression of the RNAi construct was controlled by the barley *late embryogenesis abundant (Lea)* B19.3 gene promoter. This promoter shows high activity not only during embryo development in seeds but also in shoot and root tissues ([www.geneinvestigator.com](http://www.geneinvestigator.com); Zimmermann *et al.* 2004) (Figure 5). The *ABA 8'-hydroxylase* RNAi lines have been obtained in our lab in a previous project and were named by LOHi, standing for the *HvLea::HvABA 8'-hydroxylase* RNAi construct (Seiler *et al.* 2014). The selected fragment intended for post-transcriptional gene silencing was based on a rather conserved region of *HvABA 8'-hydroxylase 1*, so it was likely that all three *HvABA 8'-hydroxylase 1/2/3* genes will be suppressed. Among the total 103 independent primary transformants obtained, T1 transgenic plants (n = 9) harboring a single copy of transgene were screened and finally 5 different transgenic homozygous lines were obtained in the T2 generation. Three homozygous lines LOHi3, LOHi236 and LOHi272 were chosen for further analysis of tiller development. Given that the RNAi-mediated gene silencing in LOHi236 and LOHi272 exerted a strong influence on tiller formation when plants were grown in a growth chamber, the subsequent investigations mainly focussed on these two lines.



Dataset: 28 anatomical parts (sample selection: HV\_AFFY\_BARLEY1-1)  
1 probe (gene selection: HV-1)

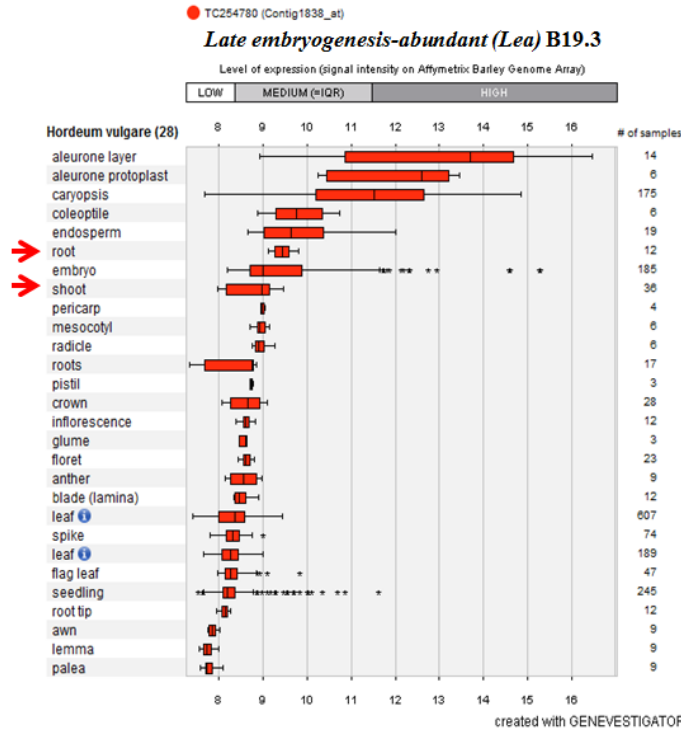


**Figure 5.** The expression levels of *late embryogenesis-abundant (Lea) B19.3* in barley tissues. Expression data was taken from Genevestigator ([www.genevestigator.com](http://www.genevestigator.com); Zimmermann *et al.* 2004).

*Hordeum vulgare* cv. Golden Promise, a two-rowed barley spring cultivar obtained from the Genebank at IPK Gatersleben, Germany, was used as reference line along with the *ABA 8'-hydroxylase* RNAi lines transformed in this background. The wild type and *HvABA 8'-hydroxylase* RNAi lines (LOHi236 and LOHi272) were grown in a growth chamber and tiller number was analysed from 7 weeks after germination (WAG) to 18 WAG. Interestingly, there is a small increase in expression of *LeaB19.3* around the time of inflorescence emergence (Genevestigator) (Figure 6), when the RNAi effect might be expected to become stronger and affect the late-tillering development in LOHi lines.

Dataset: 7 developmental stages (sample selection: HV\_AFFY\_BARLEY1-0)  
 1 probe (gene selection: HV-0)

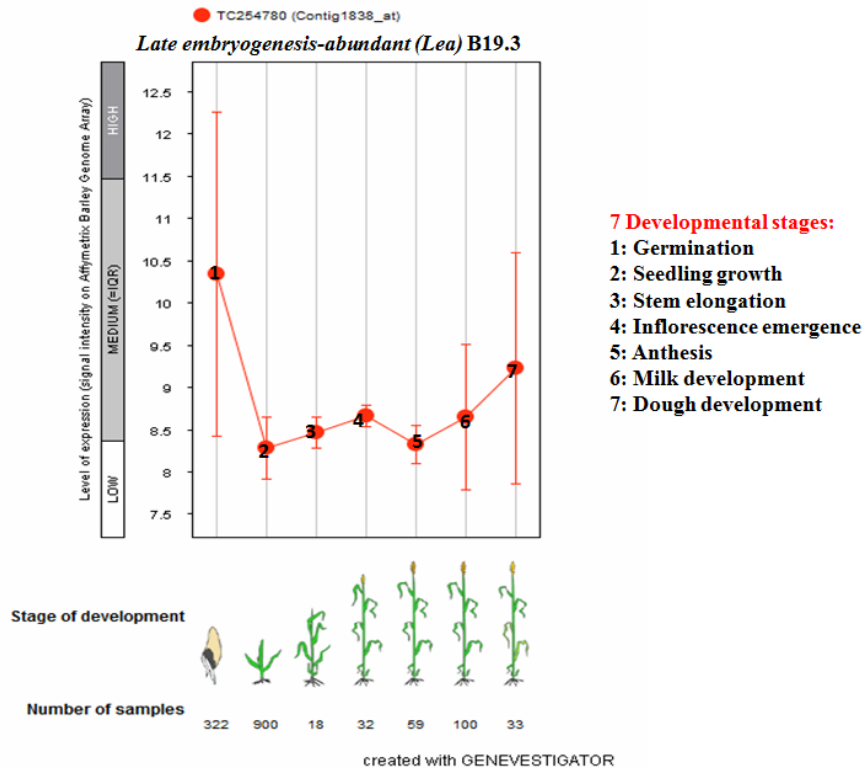


**Figure 6.** The expression levels of *late embryogenesis-abundant (Lea) B19.3* in the life cycle of barley. Expression data was taken from Genevestigator ([www.genevestigator.com](http://www.genevestigator.com); Zimmermann *et al.* 2004).

During the vegetative stage, the total tiller number per plant in LOHi236 and LOHi272 lines was the same as that of wild-type plants. However, at 14 WAG around the time of inflorescence emergence, the frequency of tiller outgrowth was elevated in LOHi236 and LOHi272 lines and by 8.03% or 14.7% higher in LOHi236 or LOHi272, respectively than in the wild type. This effect became stronger over time (Figure 7).

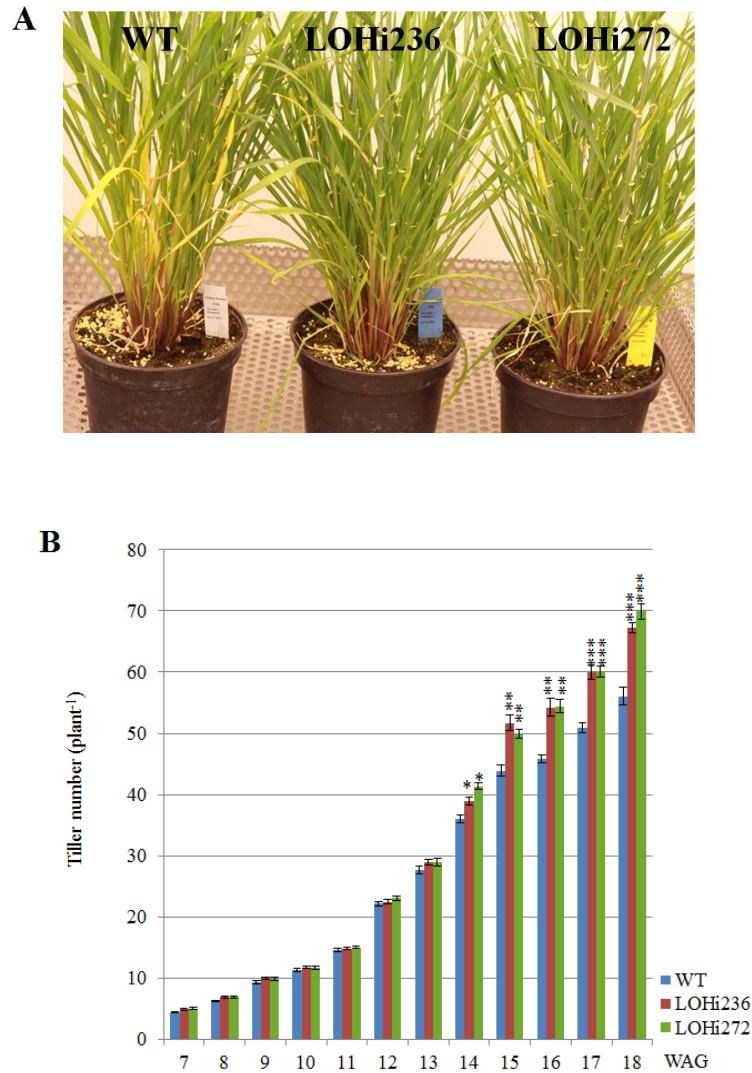


**Figure 7.** Phenotypic evaluation of tiller number in phytochamber. (A) The tillering phenotype in wild type (Golden Promise) and *HvABA 8'-hydroxylase* RNAi lines (LOHi236, LOHi272) at 16 WAG. WAG: Weeks after Germination. (B) Total tiller number per plant in transgenic lines LOHi236, LOHi272, compared with wild-type plants from 7 WAG to 18 WAG. Values represent means  $\pm$  SE of 20 plants. Significant differences as determined by Student's *t*-test are indicated by asterisks, \*,  $P < 0.05$ , \*\*,  $P < 0.01$ , \*\*\*,  $P < 0.001$ .

A similar experiment was carried out in the greenhouse and the phenotype of increased tillering in LOHi236/272 lines was also observed there (Figure 8). The increase in tiller number of LOH236/272 was observed starting from 12 WAG, which was two weeks earlier than in the phytochamber. This difference in tiller development could result from different growth conditions used in these two experiments, such as sowing date, light density or temperature (Table 3).

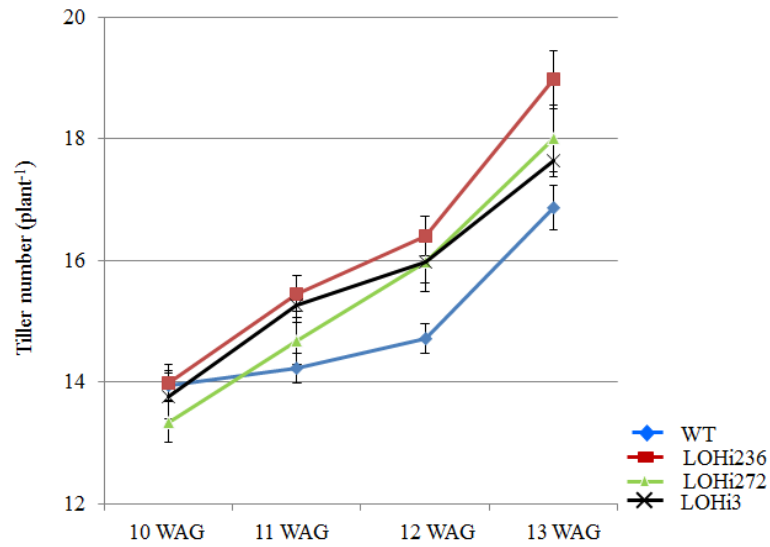
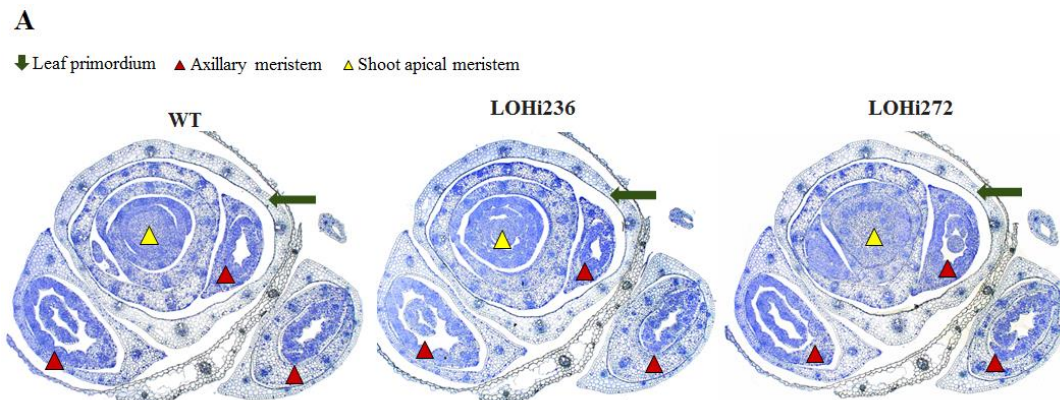


**Figure 8.** Phenotypic evaluation of tiller number under greenhouse conditions. The total tiller number per plant in transgenic lines LOHi236, LOHi272 was compared that in wild-type plants from 10 WAG to 13 WAG (WAG: Weeks after Germination). Values represent means  $\pm$  SE of 15 plants.

The number of tillers increased in particular at later developmental stages (Figure 7 and 8). The reason for this late increase in tiller number may be due to enhanced axillary meristem formation or a differential regulation of axillary bud outgrowth. In order to verify the first possibility, axillary meristem formation was investigated by taking meristem sections from an early developmental stage (3 WAG) for microscopic examination. No difference was found in the number of axillary meristems between LOHi lines and wild-type plants (Figure 9A). Moreover, there was also no difference in the developmental stages, as indicated in Figure 9B.



**B**

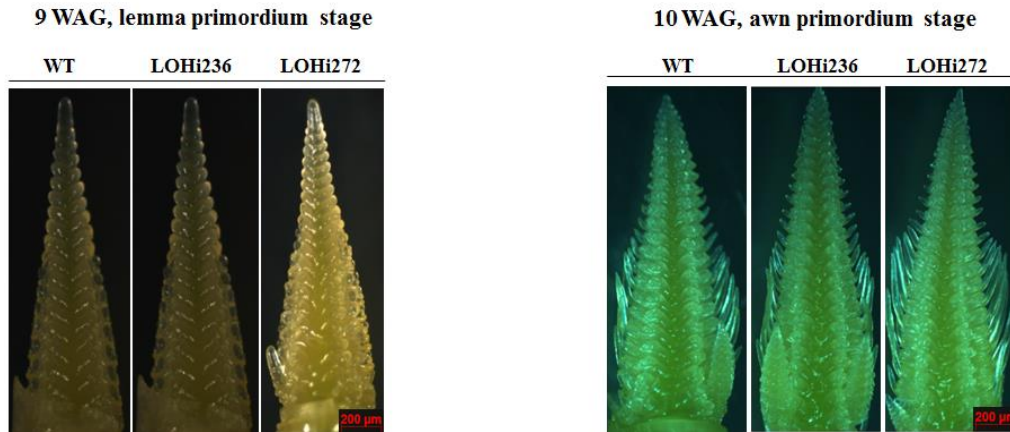


**Figure 9.** Development of axillary meristem and shoot apical meristem in wild-type and LOHi antisense lines. (A) Transverse section of the shoot apical meristem (SAM) at 3 WAG. Green arrowheads indicate leaf primordia; Red arrows point to axillary meristems; Yellow arrows show SAMs,  $n = 9$ . (B) Views of the apices at lemma primordium stage or awn primordium stage, at 9 WAG, or 10 WAG, respectively. WAG: Weeks after Germination, Bars: 200  $\mu\text{m}$ .

### 3.2 ABA accumulation in stem bases and roots of LOHi lines

#### 3.2.1 Expression analysis of ABA biosynthesis and degradation genes

To better understand the dynamics between ABA biosynthesis and degradation and to assess whether the altered late-tillering phenotype in LOHi236 and LOHi272 correlates with the extent of *HvABA 8'-hydroxylase* gene silencing, quantitative real-time (qRT) PCR was performed to detect and quantify the expression levels of ABA biosynthesis (*HvNCED1/2*) and degradation (*HvABA 8'-hydroxylase1/2/3*) genes. Additionally, in an early attempt to determine whether RNAi activity is responsible for the cleavage of *HvABA 8'-hydroxylase* gene, gene expression analysis by qRT-PCR was employed to quantify the expression patterns of *HvABA 8'-hydroxylase 1/2/3*. For example, at 10 WAG, much higher expression levels were found for *HvABA 8'-hydroxylase 1* and *HvABA 8'-hydroxylase 3* than for *HvABA 8'-hydroxylase 2* in root, stem base, leaf and axillary bud tissues, indicating that the latter gene product makes no significant contribution to ABA degradation (Figure 10). Thus, qRT-PCR data are subsequently only shown for *HvABA 8'-hydroxylase 1* and 3.

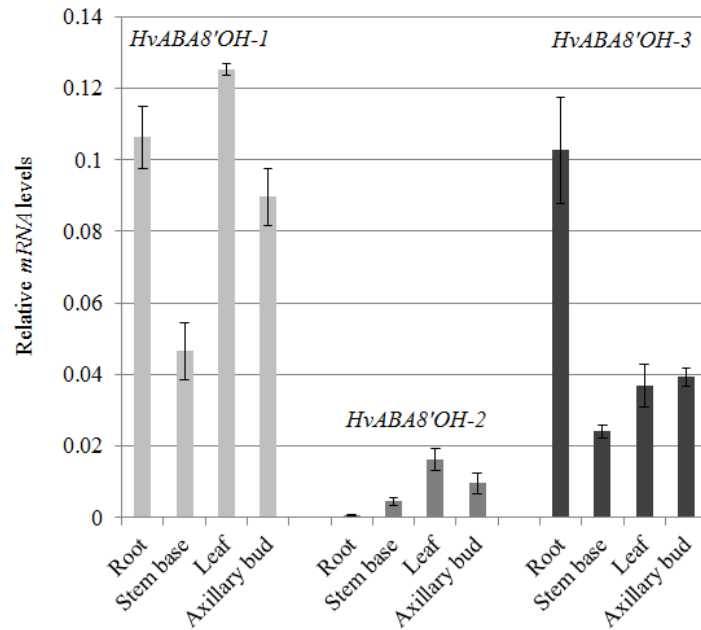


**Figure 10.** Expression levels of the genes *HvABA 8'-hydroxylase 1, 2 and 3* in the root, stem base, leaf and axillary bud at 10 WAG in wild-type (WT) plants. The graph shows mean values  $\pm$  SE of qRT-PCR experiments from three biologically independent samples. *Serine/threonine protein phosphatase PP2A-4* was used as a reference gene.

In the RNAi lines LOHi236 and LOHi272 grown in the phytochamber, relative mRNA levels of *HvABA 8'-hydroxylase 1/3* in stem bases were not modified relative to wild type at earlier time point 12 WAG. However, a significant reduction in *HvABA 8'-hydroxylase 1/3* transcript levels in stem bases was observed mainly at 14 WAG. Moreover, *HvABA 8'-hydroxylase 1/3* transcript levels were not significantly changed in LOHi236 and LOHi272 relative to wild type at 15 WAG. There, the silencing effect of *HvABA 8'-hydroxylase* was weaker than at 14 WAG (Figure 11A). At the same time, transcript levels of *HvNCED1* and *HvNCED2*, encoding 9-*cis*-epoxycarotenoid dioxygenase, a key enzyme of the ABA biosynthesis pathway were sharply down-regulated in LOHi236, compared to a weaker down-regulation in LOHi272. The down-regulation of *HvNCED1* and *HvNCED2* expression levels might have resulted from a negative feedback regulatory loop to balance the ABA homeostasis (Figure 11B).

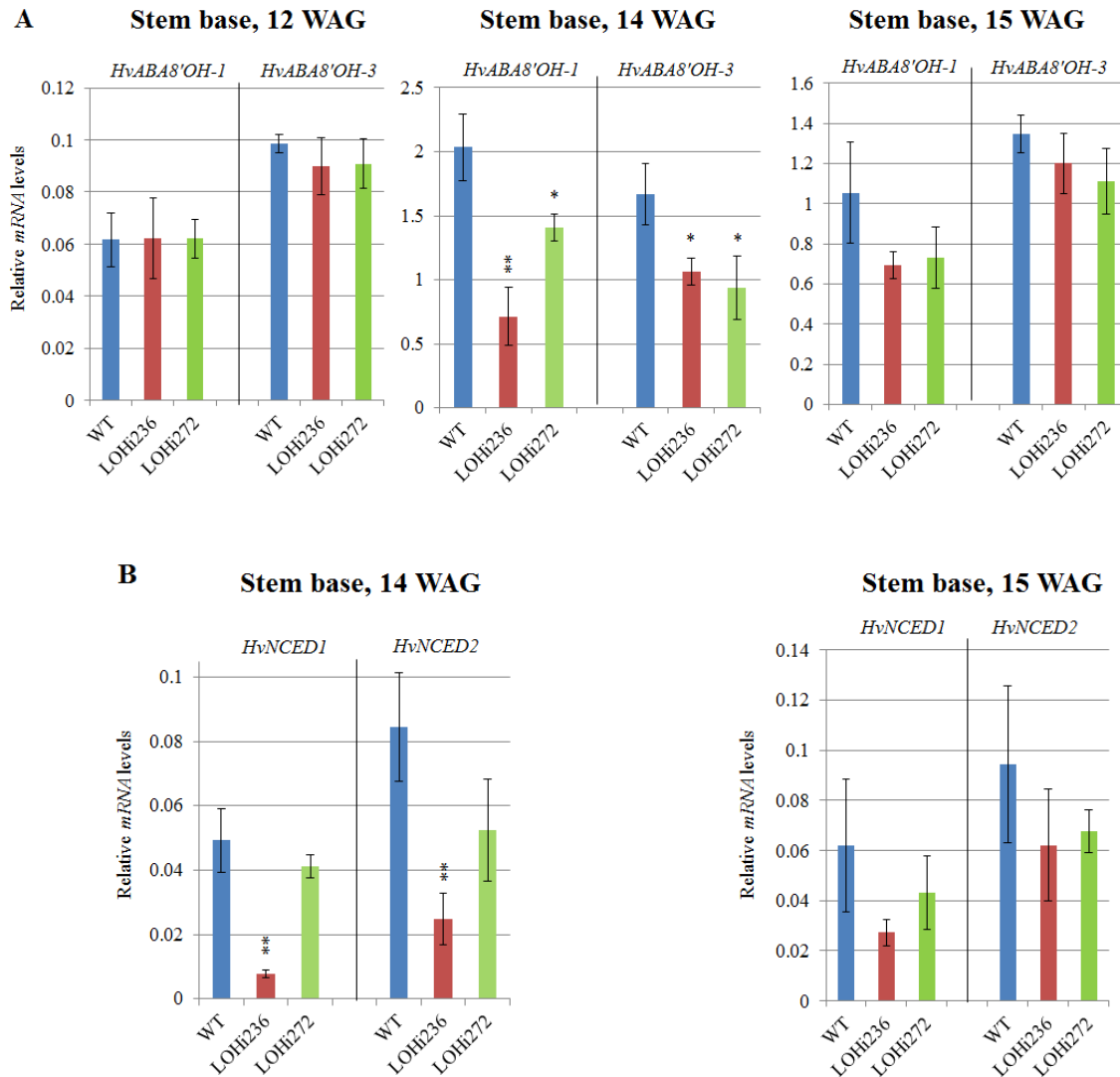


**Figure 11.** Expression levels of the genes *HvABA 8'-hydroxylase 1, 3* and *HvNCED1, 2* in the stem base at 12 WAG, 14 WAG and 15 WAG in wild-type (WT) plants and transgenic lines LOHi236/272. The graphs show mean values  $\pm$  SE of qRT-PCR experiments from three biologically independent samples. *Serine/threonine protein phosphatase PP2A-4* was used as a reference gene. Significant differences as determined by Student's *t*-test are indicated by asterisks, \*,  $P < 0.05$ , \*\*,  $P < 0.01$ .

Transcript levels of genes associated with ABA degradation were also quantified in roots using qRT-PCR, and there the trend was similar as in the stem base (Figure 12A). Therefore, the reason leading to the increased late-tillering phenotype in LOHi lines, which was more apparent after 14 WAG, might be due to a temporal-spatial interaction between ABA and other plant hormones involved in regulating tiller development. This may be triggered by the transient silencing of *HvABA 8'-hydroxylase 1/3*. To confirm this phenotype, the expression

levels of *HvABA 8'-hydroxylase 1/3* were further analyzed in axillary buds, showing that there was no significant alteration in LOHi lines relative to WT plants from 12 WAG to 15 WAG (Figure 12B).

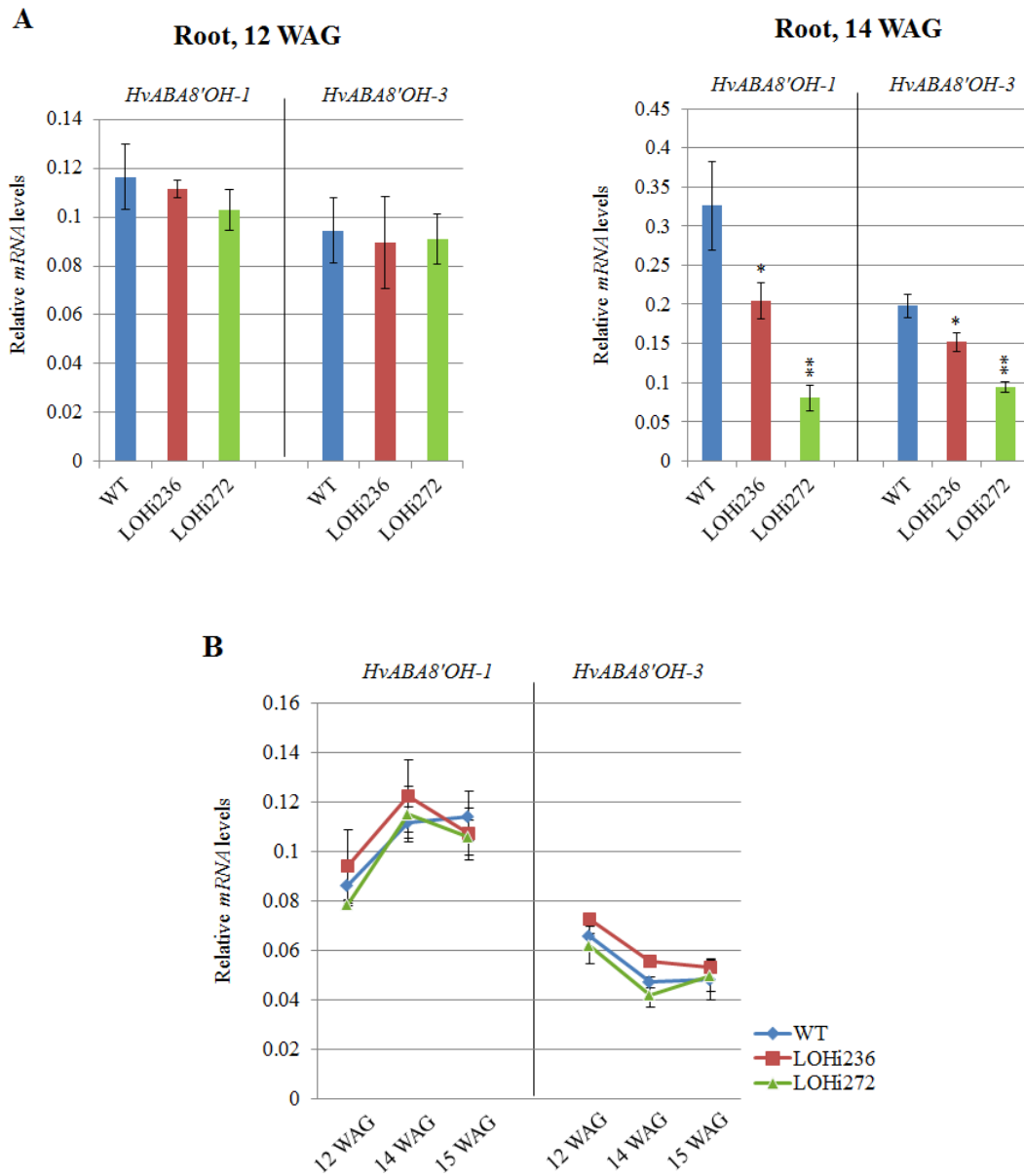


**Figure 12.** Expression levels of the genes *HvABA 8'-hydroxylase 1* and *3* in the root and axillary bud at 12 WAG, 14 WAG and 15 WAG in wild-type (WT) plants and transgenic lines LOHi236/272. The graphs show mean values  $\pm$  SE from three experiments each consisting of three independent biological replicates. *PP2A-4* was used as a reference gene. Significant of differences according to Student's *t*-test are indicated by asterisks, \*,  $P < 0.05$ , \*\*,  $P < 0.01$ .



### 3.2.2 ABA levels in wild type and LOHi antisense lines

Based on the dynamics of ABA biosynthesis and degradation genes from 12 WAG to 15 WAG and *LeaB19.3* expression patterns in tissues, ABA concentrations were measured in the stem bases and roots of the wild-type plants and transgenic lines LOHi236 and LOHi272 in collaboration with Dr. Kai Eggert and Dr. Mohammad-Reza Hajirezaei (MPE Group, IPK). Liquid chromatography-tandem mass spectrometry (LC–MS/MS) showed that there was no difference in abscisic acid concentration between LOHi lines and wild-type plants at 12 WAG (Figure 13A). This was in agreement with similar transcript levels of *HvABA 8'-hydroxylase 1/3* at 12 WAG (Figure 11A). However, ABA levels in the stem bases were by 73% higher in LOHi236 and by 67% higher in LOHi272 compared to the wild type at 14 WAG (Figure 13B). In agreement with a stronger silencing of *HvABA 8'-hydroxylase 1/3* in LOHi236, the ABA level in LOHi236 stem bases was higher than that in LOHi272. In roots, higher levels of ABA in LOHi lines than in the wild-type were also observed at 14 WAG relative to 12 WAG (Figure 13C and 13D). The differences in ABA levels at 14 WAG between wild-type and LOHi antisense lines suggested that ABA accumulation in the stem bases may have been linked to the tillering phenotype.

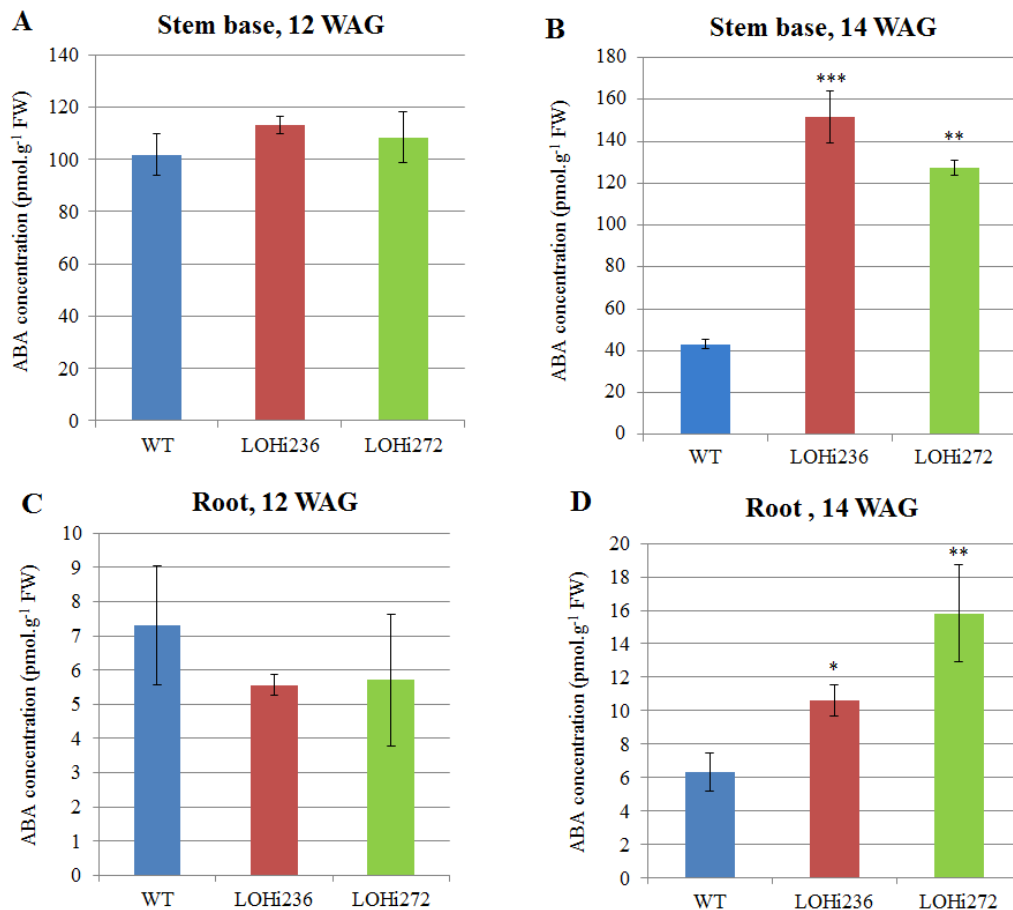


**Figure 13.** ABA concentration in the stem base and root at 12 WAG and 14 WAG in wild-type (WT) plants and LOHi antisense lines. Bars represent the average  $\pm$  SE of three independent replicates. The concentration of ABA is indicated as pmol.g<sup>-1</sup> FW. FW: Fresh Weight. Significant differences as determined by Student's *t*-test are indicated by asterisks, \*,  $P < 0.05$ , \*\*,  $P < 0.01$ , \*\*\*,  $P < 0.001$ .

### 3.3 Investigations on strigolactone biosynthesis in wild-type plants and *ABA 8'-hydroxylase* antisense lines

#### 3.3.1 LC-MS/MS analysis and quantification of strigolactones

Recently, the importance of an interconnection between ABA and SL biosynthesis has received more attention. Although SLs have been detected in a variety of plant species, there is no report for barley. Thus, first the identity of SLs had to be explored in barley before quantities could be compared between wild-type plants and transgenic lines. 5-deoxystrigol was found to be distributed widely in the plant kingdom and detected in root from both monocots (Awad *et al.* 2006) and dicots (Yoneyama *et al.* 2007).

To explore the identity of SLs and assess whether the late-tillering phenotype of LOHi236 and LOHi272 resulted from a decrease in the production of SLs, Multiple-Reaction Monitoring Liquid Chromatography Mass Spectrometry (MRM-LC-MS/MS) was performed in collaboration with Prof. Dr. Harro J. Bouwmeester (Laboratory of Plant Physiology, Wageningen University, Netherlands). For the analysis of SLs, barley exudates were collected and compared to retention times (RT) and mass transitions of available SL standard substances (Figure 14A). In the MRM-LC-MS/MS chromatograms, two intense peaks were detected in the different MRM channels. 5-deoxystrigol was detected at a retention time (RT) 7.95 min in the MRM channel  $m/z$  331.2>234.15, D6-5-deoxystrigol was detected at RT 7.92 min and  $m/z$  337.16>97.017, and one weak peak of 2'-*epi*-5-deoxystrigol was detected at RT 7.88 and  $m/z$  331.2>234.0. The chromatogram of crude root exudates from barley revealed an intense peak in the channel  $m/z$  331.2>216.15 at RT 7.95 min, which matched the standard of 5-deoxystrigol (Figure 14A).

To improve the conditions for SL detection, barley plants were precultured hydroponically and subjected to P starvation as P deficiency has been shown to enhance SL exudation by roots (Al-Babili and Bouwmeester 2015). A strong quantitative variation in SL production was observed between the wild-type plants and LOHi lines. The major SL 5-deoxystrigol purified was significantly ( $P<0.01$ ) lower in root exudates of LOHi236 and LOHi272 compared with the wild type at 14 WAG (Figure 14B). Other SLs including 2'-*epi*-orobanchol and sorgomol were also detected in barley root exudates, but their concentrations were too low for accurate quantification. Moreover, the peak areas obtained with MRM-LC-MS/MS for 5-deoxystrigol from root extracts of barley at 14 WAG became very weak with that of the standard, therefore this data was not available. Taken together, these results indicated that the exudation of 5-deoxystrigol was lower in LOHi236 and LOHi272 than in wild-type plants, which coincided with their late-tillering phenotype.

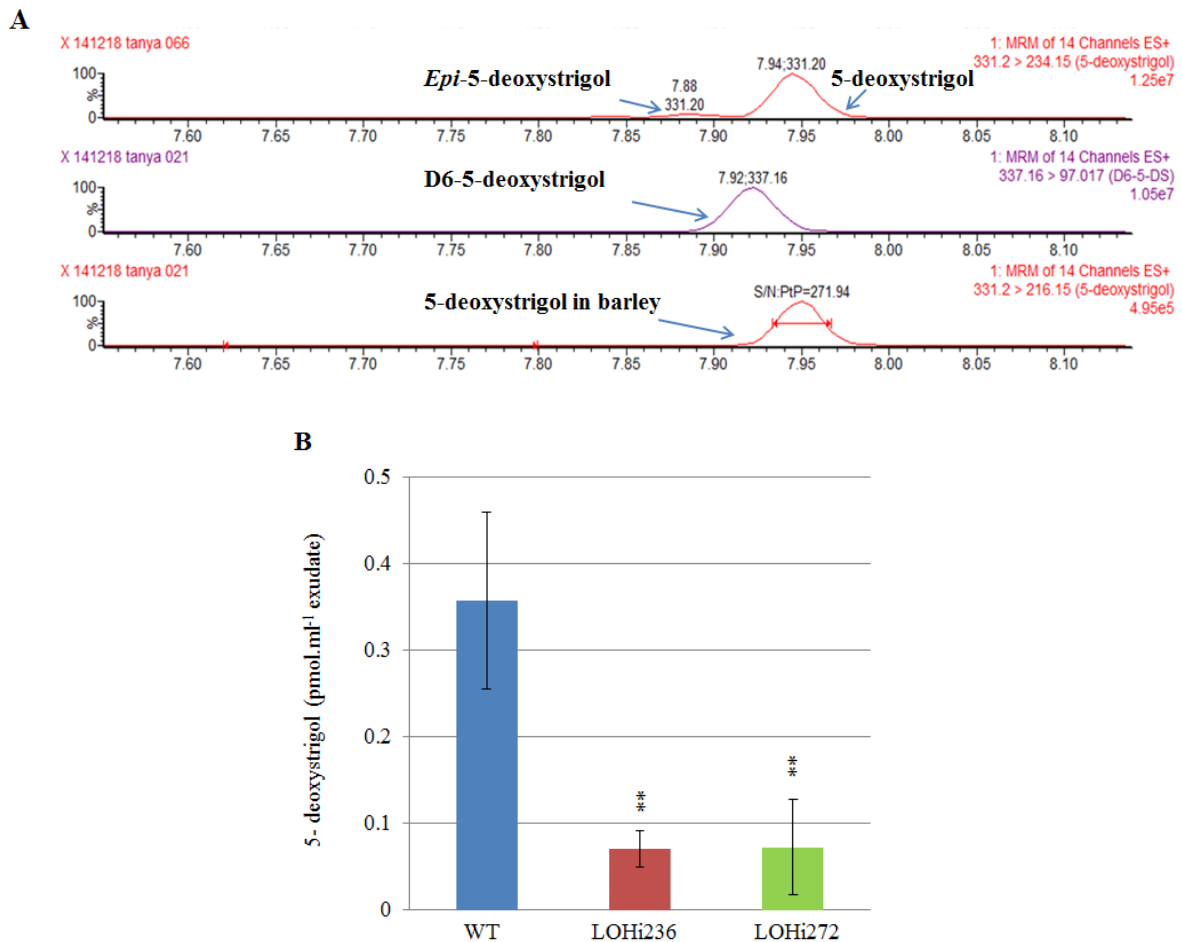


**Figure 14.** MRM-LC-MS/MS analysis of strigolactone concentrations in barley root exudates. (A) Transition 331.2>234.15 for authentic 5-deoxystrigol, transition 337.16>97.017 for authentic D6-5-deoxystrigol, transition 331.2>234.0 for *ent-2'-epi-5-deoxystrigol*. (B) The concentrations of 5-deoxystrigol in root exudates of LOHi (LOHi236 and LOHi272) and wild-type plants after 7 days of phosphate starvation at 14 WAG. Bars represent the means  $\pm$  SE of five independent replicates. Significant differences as determined by Student's *t*-test are indicated by asterisks, \*\*,  $P < 0.01$ .

### 3.3.2 Identification of putative strigolactone biosynthesis pathway genes in barley

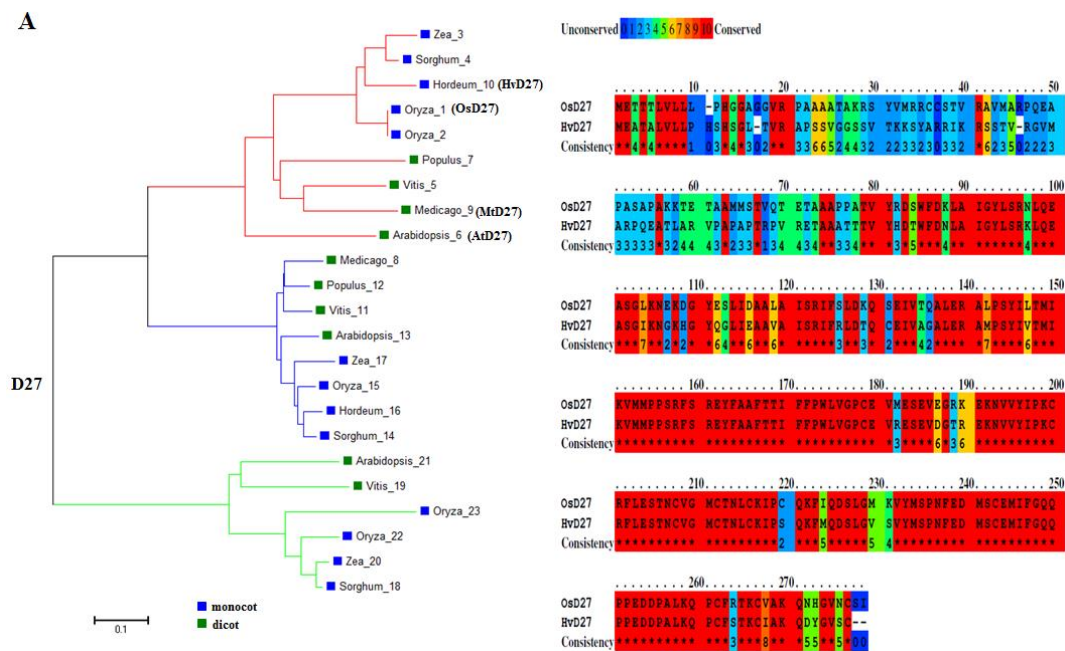
An open question was whether the dramatic change in SL hormone levels was related with the regulation of genes involved in SL biosynthesis in LOHi236/272 lines. So far, however, there have been no corresponding reports on SL-related genes in barley. In order to identify the most relevant genes for SL biosynthesis in barley, a phylogenetic analysis was conducted for orthologous gene sequences based on a comparison of SL biosynthesis genes from different plant species and sequences from the barley genome (Figure 15).

It has been described that *DWARF27* (*D27*), *MORE AXILLARY GROWTH3* (*MAX3*), *MORE AXILLARY GROWTH4* (*MAX4*) and *MORE AXILLARY GROWTH1* (*MAX1*) are genes involved in the SL biosynthetic pathway in the model plant *Arabidopsis* (Brewer *et al.* 2013). Moreover, *OsD27* has been identified as a novel iron-containing protein participating in the biosynthesis of SLs in rice (Lin *et al.* 2009). To identify orthologous genes from barley, amino acid sequences of *Arabidopsis* or rice proteins were used as templates to perform protein homology search in the fully-sequenced barley genome (<http://webblast.ipk-gatersleben.de/barley/index.php>). The barley genome encodes two proteins with superficial similarity to rice *OsD27* (Lin *et al.* 2009). In order to identify the likely ortholog of *OsD27*, a phylogenetic analysis of D27-like proteins in dicots and monocots was performed (Table 5). The red-marked branch indicates that the group contains *OsD27*, its ortholog in *Medicago truncatula* (Liu *et al.* 2011), an *Arabidopsis* D27 (*AtD27*) protein encoded by *At1g03055* (Waters *et al.* 2012), and a barley D27 protein encoded by AK358967 (NCBI number). Notably, another barley protein with similarity to *OsD27*, encoded by AK354401 (NCBI number), could be assigned unambiguously to another sub-branch indicated in blue (Figure 15A). Thus, it was concluded that AK358967, subsequently designated as *HvD27*, is the likely barley ortholog of *OsD27*. The *HvD27* protein shared about 71% identity with *OsD27* at the amino acid level. Nevertheless, the presence of other D27-like proteins in the barley genome might be indicative of potential genetic redundancy.

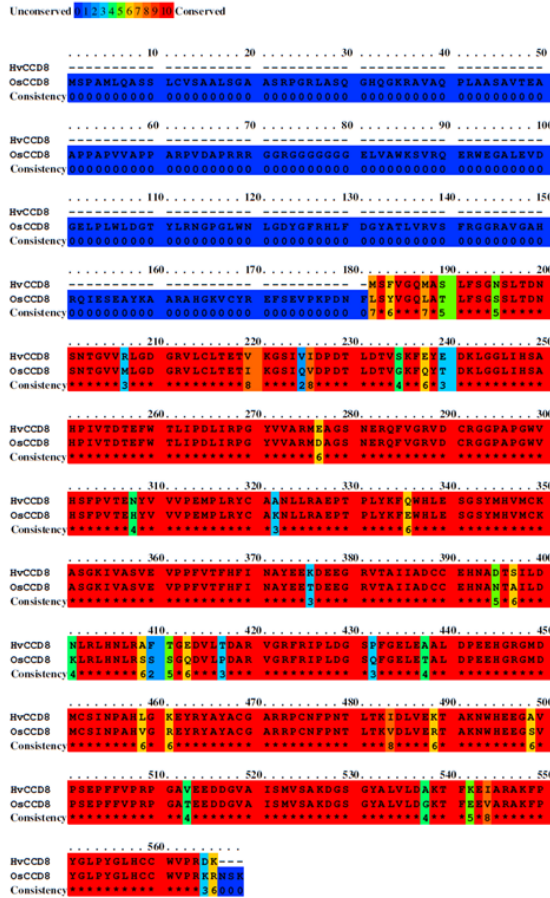
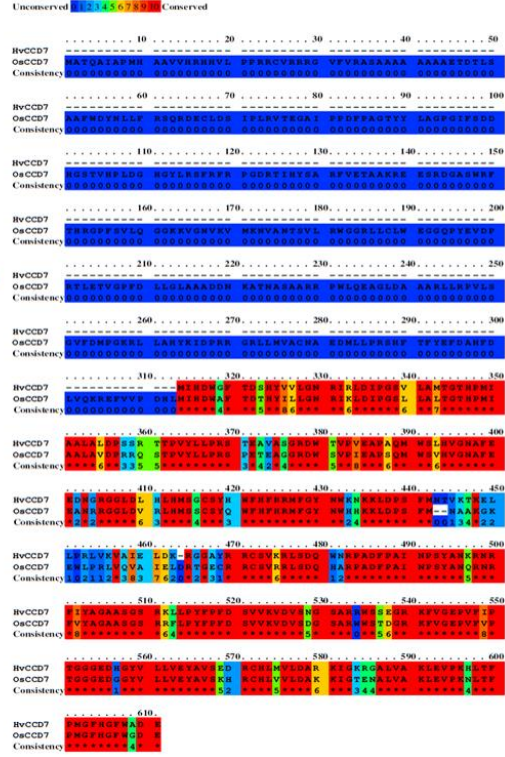
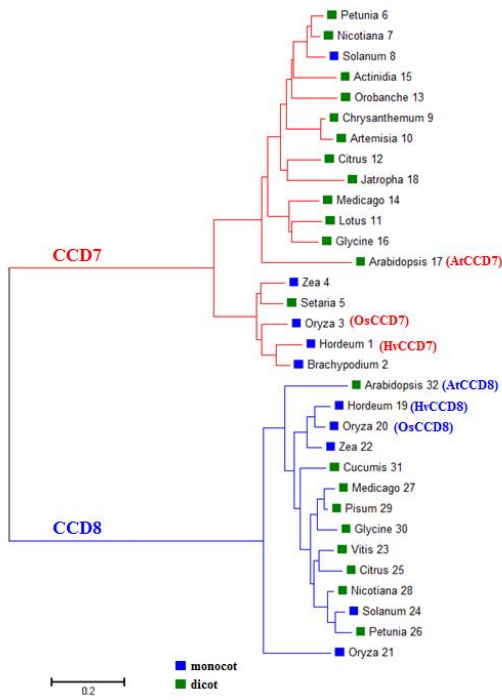
The amino acid sequences of *Arabidopsis thaliana* *CCD7* and *CCD8* (*AtCCD7* and *AtCCD8*; NCBI numbers 130064.4 and 119434.3, respectively) were used as reference sequences to search for orthologous sequences in barley. By using the NCBI website (<http://blast.ncbi.nlm.nih.gov/Blast.cgi?PAGE=Proteins>), BLASTP was performed. A total of 11 model species were selected for sequence analyses of their *CCD7* and *CCD8* genes, including ten monocotyledonous and twenty-one dicotyledons species (Table 5). The *CCD7* and *CCD8* genes were identified according to their E-values in the BLASTP program and synteny to other *CCDs*. Since amino acid sequences are more conserved than nucleotide sequences, a phylogenetic tree based on amino acid sequences divided the *CCD7* and *CCD8* proteins into two distinct groups. Proteins of the cluster marked in red showed that

Arabidopsis MAX3 (AtCCD7) has only one close sequence homologue in barley encoded by locus MLOC\_55474.1, which was designated as HvCCD7. The branch marked in blue indicated that Arabidopsis MAX4 (AtCCD8) has also only one close sequence homologue in barley encoded by locus MLOC\_66551.1, which was designated as HvCCD8 (Figure 15B). The partial protein sequences of HvCCD7 and HvCCD8 shared higher identity 80% with D17 (CCD7) and 90% with D10 (CCD8), respectively.

Relationships among the target gene ortholog sets were examined in arbitrarily rooted neighbour-joining phylogenies of protein sequences (Table 5). Comparison among sequences from monocot and dicot plants identified at least two separate clades of MAX1, although the second clade was only represented in a limited number of species. In this case, a likely barley MAX1 protein encoded by AK367034 (NCBI number) and named as HvMAX1, appeared as a close homologue to Arabidopsis MAX1 (AtMAX1) (Figure 15C). HvMAX1 had 57% sequence identity with AtMAX1. These phylogenetic relationships among SL biosynthesis pathway genes in barley provided the baseline information for their subsequent functional characterization.



B



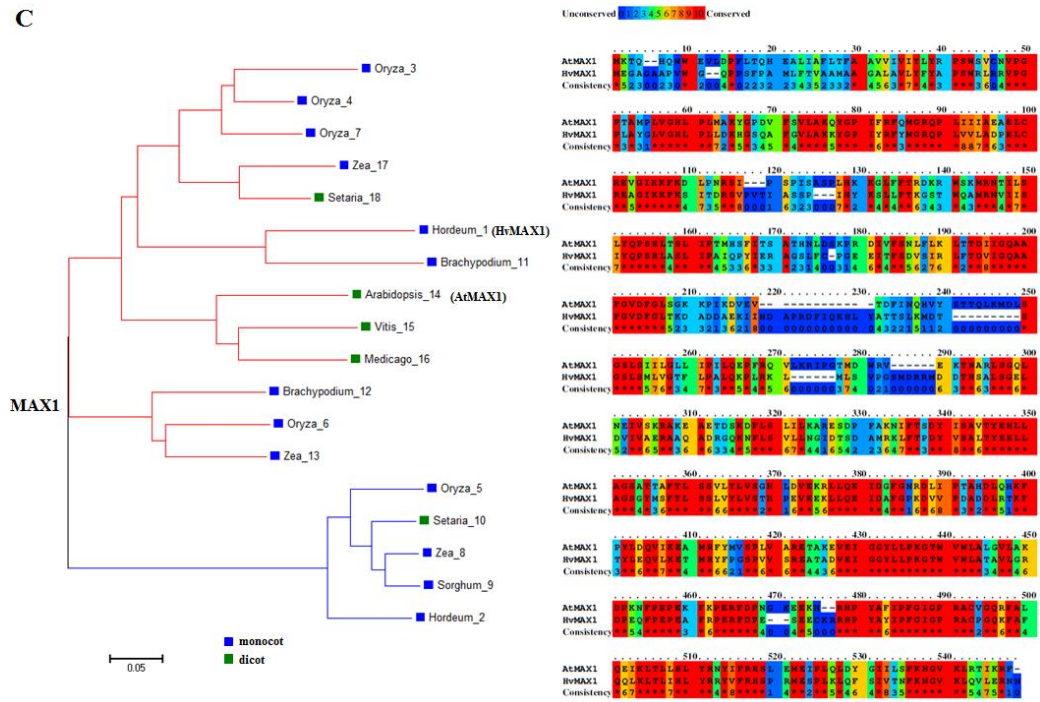


**Figure 15.** Phylogenetic trees and alignments of amino acid sequences of proteins in the strigolactone biosynthesis pathway. Phylogenetic tree of A) D27, B) CCD7/8 and C) MAX1 orthologs from different plant species. Sequence alignments were performed using the ClustalW module in the MEGA (Molecular Evolutionary Genetics Analysis) 6.0 program (Tamura *et al.* 2013). Neighbor-joining trees and bootstrap analyses were conducted using MEGA 6.0. Different colors in branches denote different phylogenetic groups. Squares of different colors represent proteins from monocot and dicot species. Protein sequences utilized in this analysis as well as NCBI accession numbers and data sources are listed in Table 5.

Subsequently, real-time PCR was used to examine the expression patterns of *HvD27*, *HvCCD7*, *HvCCD8* and *HvMAX1* across various tissues and organs. As expected, the transcript abundance of each gene was most abundant in the root. In stem base, the transcript levels of *HvD27*, *HvCCD7* and *HvCCD8* were also relatively high. Interestingly, the highest expression level of *HvD27* was observed in the leaves, while the highest expression of *HvMAX1* was in the roots. These data suggested that SLs are mainly synthesized in barley roots and stem tissues (Figure 16).



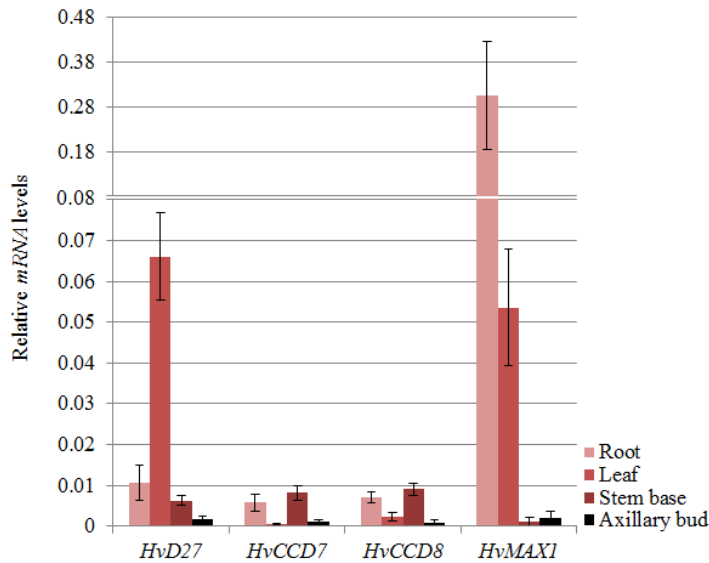
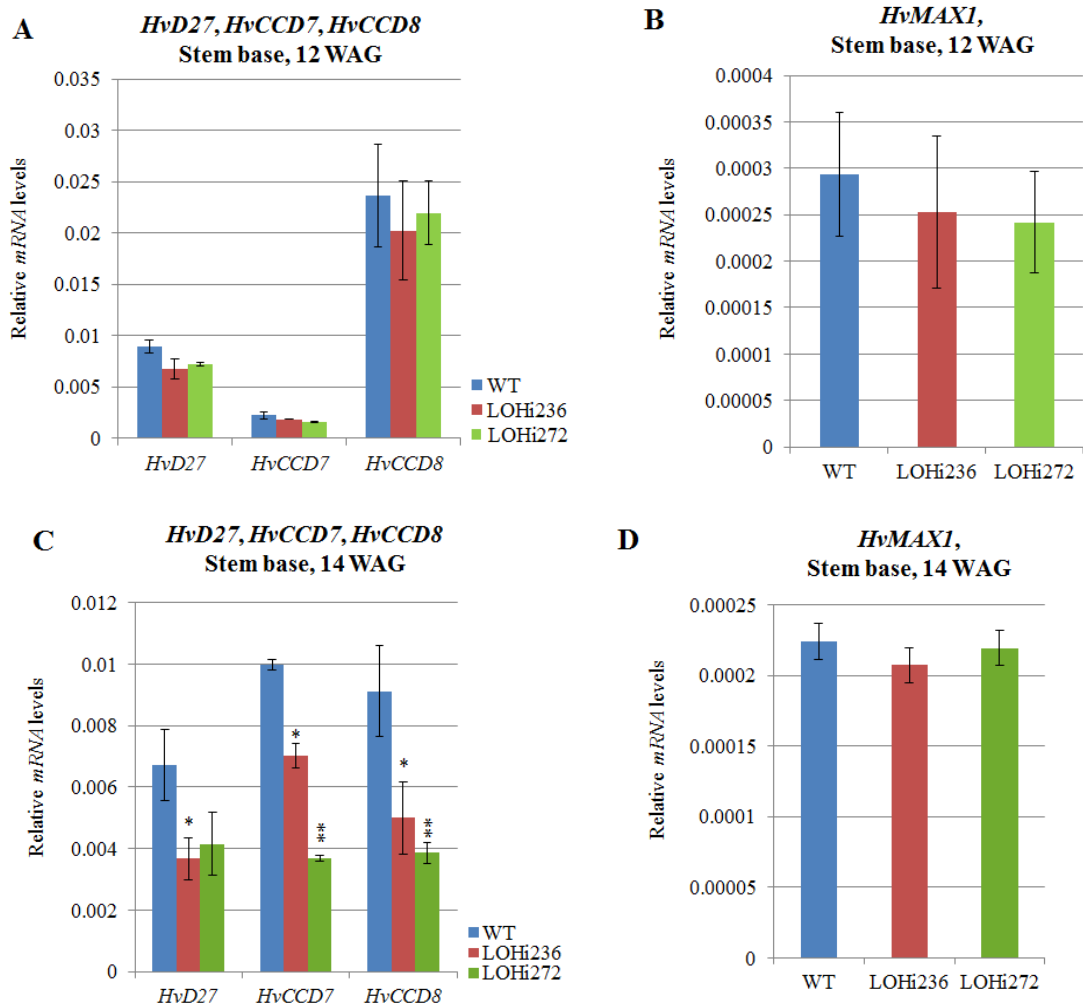


**Figure 16.** Expression of genes from the strigolactone biosynthesis pathway across various tissues and organs in barley wild-type plants. The graph shows mean values  $\pm$  SE of the relative gene expression from three biologically independent samples. *Serine/threonine protein phosphatase PP2A-4* was used as a reference gene.

### 3.3.3 Gene expression analysis of putative strigolactone biosynthesis genes

Quantitative real-time PCR was used to investigate the expression of putative SL biosynthetic pathway genes in LOHi236, LOHi272 lines, which showed an increase in tiller number. A list of genes studied in the present work putatively involved in SLs biosynthesis and the primer sequences used for qRT-PCR are provided in Table 2.

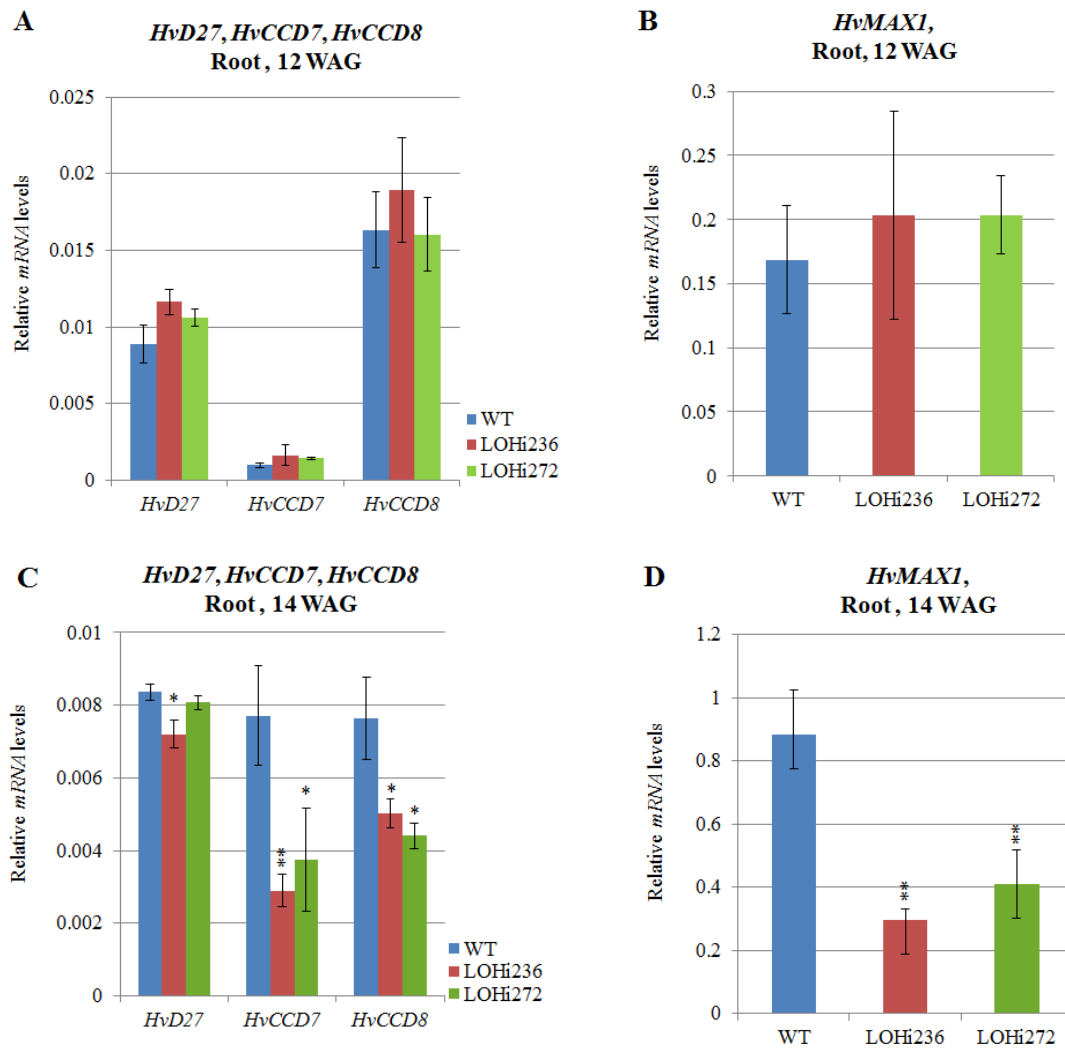
Expression of putative SL biosynthetic pathway genes in stem bases at 12 WAG was similar between LOHi lines and wild-type plants (Figure 17A and 17B). However, at 14 WAG, compared to the wild type Golden Promise transcript levels of *HvCCD7* and *HvCCD8* were clearly reduced in stem base tissues of LOHi236 and LOHi272, whereas the expression level of *HvMAX1* was not different. The relative transcript levels of *HvD27* in stem bases showed a clear reduction only in LOHi236, but not in LOHi272, which coincided with the relatively stronger extent of *HvABA 8'-hydroxylase* gene silencing (Figure 17C and 17D).



**Figure 17.** Transcript levels of genes from the strigolactone biosynthetic pathway in stem bases of wild-type plants and LOHi antisense at 12 WAG and 14 WAG. The graphs show mean values  $\pm$  SE of the relative gene expression from three biologically independent samples. *Serine/threonine protein phosphatase PP2A-4* was used as a reference gene. Significant differences as determined by Student's *t*-test are indicated by asterisks, \*,  $P < 0.05$ , \*\*,  $P < 0.01$ .

In the roots of LOHi lines and wild-type plants, expression levels of the putative SL biosynthetic pathway genes *HvD27*, *HvCCD7*, *HvCCD8* and *HvMAX1* were also similar at 12 WAG (Figure 18A and 18B). However, at 14 WAG, transcript levels of *HvCCD7* and *HvCCD8* were clearly decreased in roots of LOHi236 and LOHi272. Also the expression level of *HvMAX1* was lower in the LOHi antisense lines, while it was not affected in stem base. The relative transcript levels of *HvD27* in roots showed a clear reduction only in

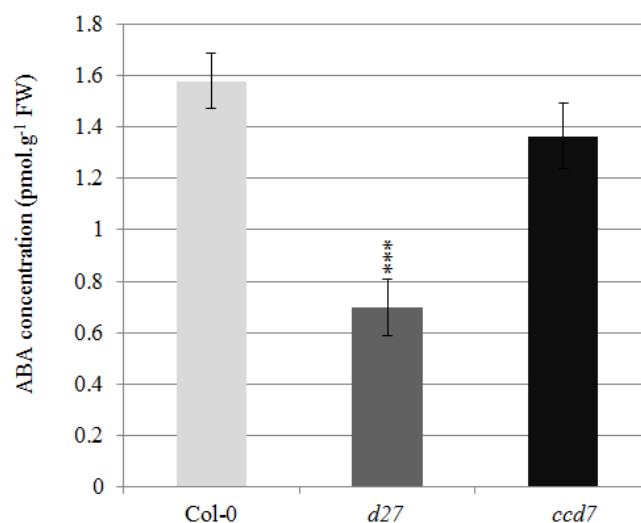
LOHi236, but not in LOHi272, which could also be the result of the relatively stronger silencing effect of *HvABA 8'-hydroxylase* genes (Figure 18C and 18D).



**Figure 18.** Transcript levels of genes from the strigolactone biosynthetic pathway in roots of wild-type plants and LOHi antisense lines at 12 WAG and 14 WAG. The graphs show mean values  $\pm$  SE of the relative gene expression from three biologically independent samples. *Serine/threonine protein phosphatase PP2A-4* was used as a reference gene. Significant differences as determined by Student's *t*-test are indicated by asterisks, \*,  $P < 0.05$ , \*\*,  $P < 0.01$ .

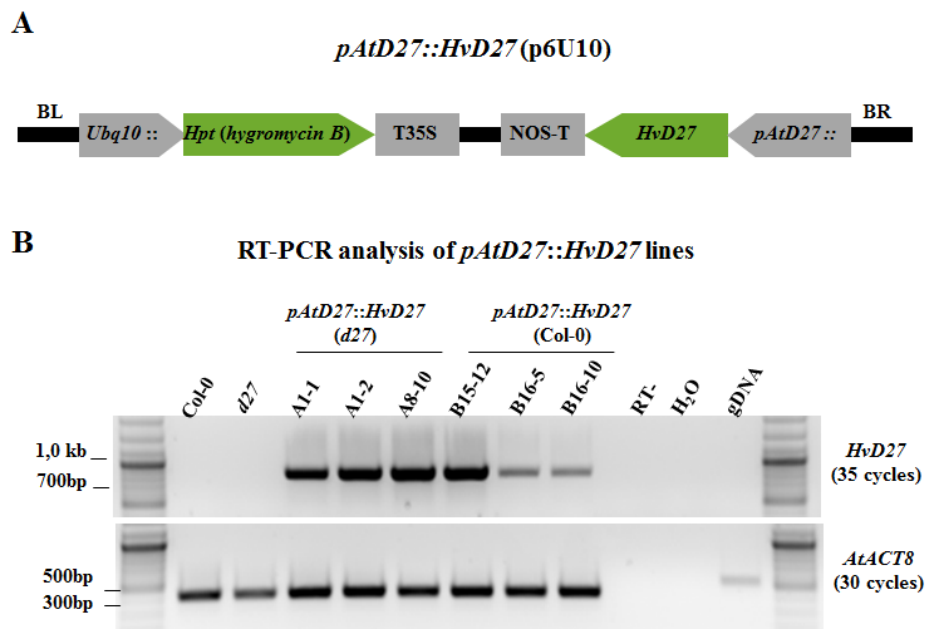
Recently, Alder *et al.* (2012) found that the rice strigolactone biosynthetic enzyme D27 showed isomerase activity converting all-*trans*- $\beta$ -carotene into 9-*cis*- $\beta$ -carotene and that the conversion was reversible. The structural similarity between all-*trans*- $\beta$ -carotene and epoxy-carotenoids evokes the possible involvement of D27 in ABA biosynthesis. This notion

prompted the search for a *Hvd27* mutant that fails to activate the SL pathway, but such a mutant is not available. Therefore, the Arabidopsis *d27* mutant (Waters *et al.* 2012) was considered most suitable for verifying whether HvD27 is involved in ABA biosynthesis and for characterizing the *HvD27* gene function through a genetic complementation approach. As previously reported, the *Atd27* mutant carries a T-DNA insertion residing in the fifth exon of the *At1g03055* locus. The *Atd27* homozygous line was first confirmed by genomic PCR using the primers as indicated in Waters *et al.* 2012. Importantly, the *Atd27* mutant plants exhibited a substantial increase in axillary rosette branches relative to wild-type Columbia (Col-0) plants under the growth conditions used in this study. ABA levels were also measured in two-week-old Col-0, *Atd27*, and *Atccd7* mutant plants (Booker *et al.* 2004) to use these values for comparison to barley. Interestingly, the *Atd27* mutant seedlings showed lower ABA concentrations than those of Col-0, but there was no significant difference to the *Atccd7* mutant (Figure 19). This indicated that AtD27 not only plays a role in the SL biosynthesis but also interferes with the ABA biosynthetic pathway.



**Figure 19.** ABA concentrations in two-week-old Arabidopsis seedlings of Col-0, *Atd27* and *Atccd7*. Seeds were grown on 1/2 Murashige and Skoog (MS) medium for two weeks. Bars represent means  $\pm$  SE of six independent biological replicates. Significant differences according to Student's *t*-test are indicated by asterisks, \*\*\*,  $P < 0.001$ .

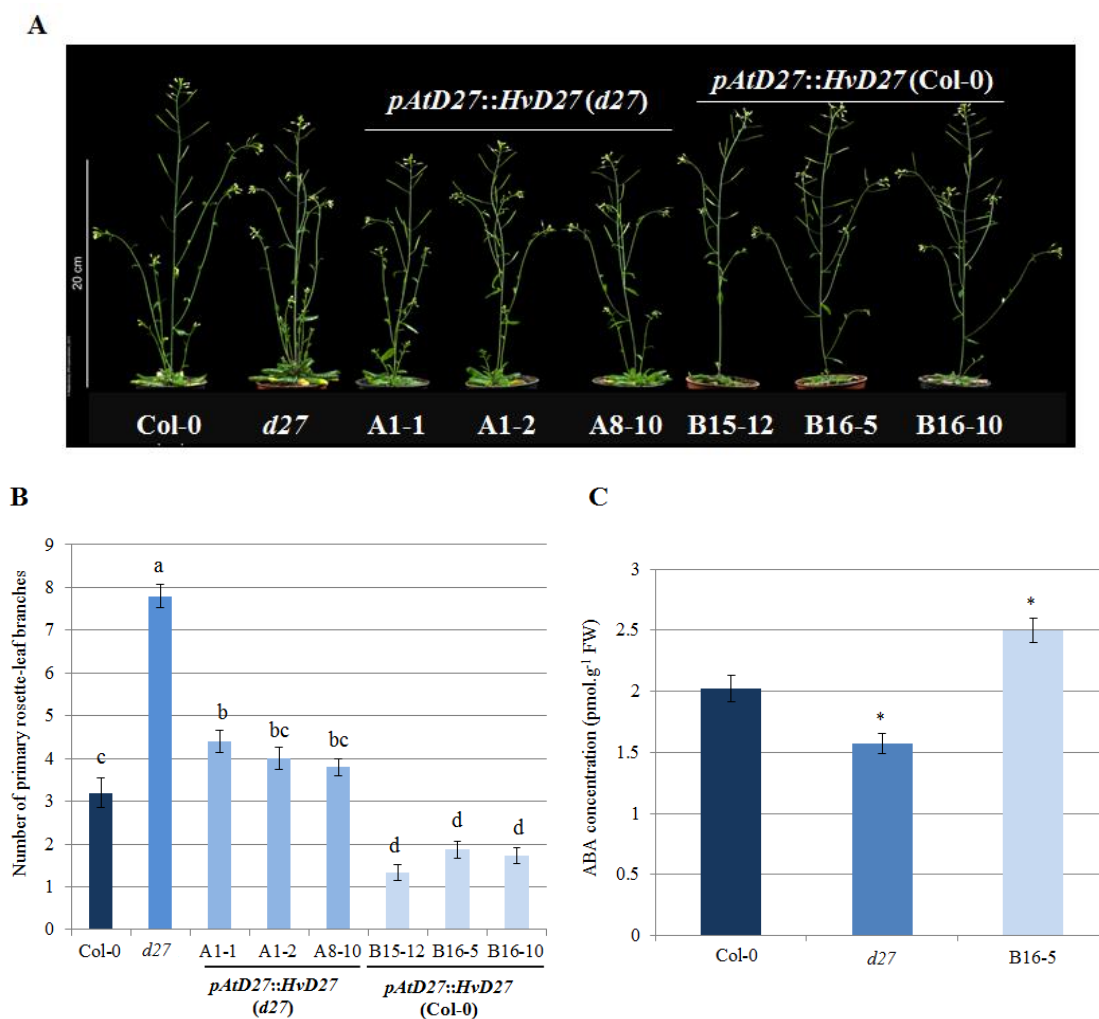
In order to test whether the *HvD27* gene may take over the same function in SL biosynthesis and shoot branching as *AtD27*, a genetic complementation study was conducted by expressing the *HvD27* gene in the Arabidopsis *d27* mutant (Waters *et al.* 2012). For complementation, the full-length ORF of *HvD27* (AK358967) was placed under the control of the *AtD27* promoter, then the combined fragment was cloned into the binary plant expression vector p6U10 for expression in the *AtD27* mutant and the Col-0 reference line using Agrobacterium-mediated transformation (Figure 20A). The RT-PCR analysis indicated that the *HvD27* transgene was successfully expressed in several of the transgenic lines with *d27* or wild-type background (Figure 20B).



**Figure 20.** (A) The vector map of *pAtD27::HvD27* used for transformation of the Arabidopsis *d27* mutant. (B) RT-PCR analysis for verification of the *pAtD27::HvD27* construct in transgenic lines.

The *pAtD27::HvD27* transgenic lines in the T3 generation were homozygous plants carrying a single T-DNA insertion. The number of primary rosette-leaf branches was counted and compared to that of Col-0 and *Atd27* mutants, which were grown side-by-side with the transgenic lines under identical conditions. The number of primary rosette-leaf branches in the transgenic lines A1-1, A1-2 and A8-10 was largely reverted to a similar number as in Col-0, whereas additional axillary branching was completely blocked in the transgenic lines B15-12,

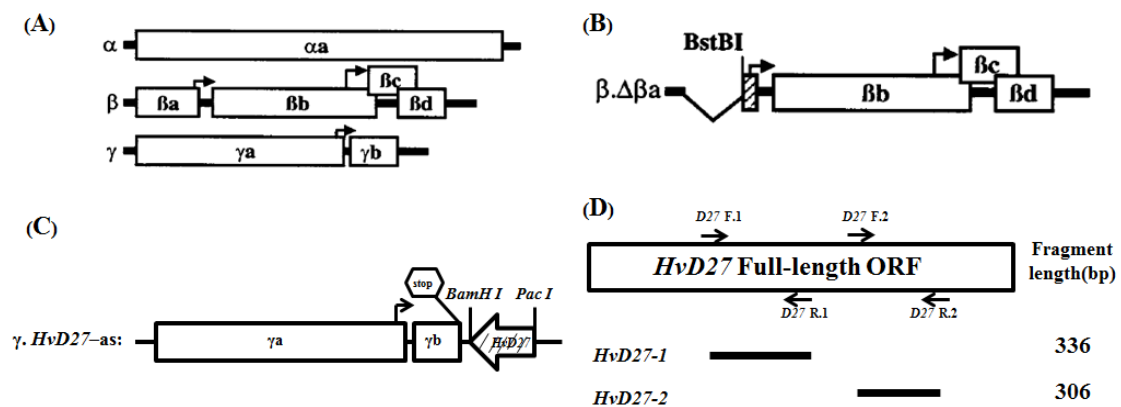
B16-5 and B16-10. Under these growth conditions, Col-0 produced about three primary rosette-leaf branches, whereas *Atd27* mutants produced about eight primary rosette-leaf branches. In the *Atd27* background, *HvD27* expression conferred three to four primary rosette-leaf branches while in the Col-0 background *HvD27* expression led to an almost complete suppression of primary rosette-leaf branching (Figure 21A and 21B). These results indicated that *HvD27* was able to complement or partially complement the shoot branching phenotype of the Arabidopsis *Atd27* mutant. When ABA concentrations were analyzed in leaves, higher ABA levels were measured in the line B16-5 with suppressed shoot branching than in Col-0, indicating that *HvD27* might also be associated with ABA biosynthesis (Figure 21C). This suggested that *HvD27* plays a dual role in SL and ABA biosynthesis.



**Figure 21.** Genetic complementation of the *Arabidopsis d27* mutant with the *Hordeum vulgare D27* gene and ABA measurements. (A) Axillary branching phenotypes. (B) Number of primary rosette-leaf branches. Shown are average numbers of primary rosette-leaf branches from at least 15 individual plants  $\pm$  SE. Different letters indicate significant differences (Tukey,  $p < 0.05$ ). (C) ABA concentrations in leaves of Col-0, the *AtD27* mutant and the transgenic line B16-5 expressing a *pAtD27::HvD27* construct in the Col-0 background. Significant differences as determined by Student's *t*-test are indicated by asterisks, \*,  $P < 0.05$ .

### 3.4 Functional characterization of the *HvD27* gene by virus-induced gene silencing in barley

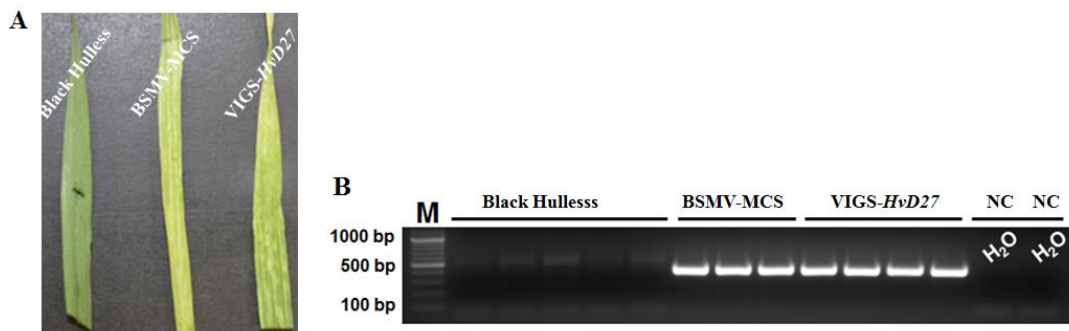
Gene silencing by vectors derived from the barley stripe mosaic virus (BSMV) is used efficiently to study gene functions in barley (Pacak *et al.* 2010). To further explore the role of *HvD27* in tiller development, a virus-induced gene silencing (VIGS) approach was implemented. To start with BSMV-mediated VIGS in barley, fragments of two different lengths (336 bp and 306 bp) of the *HvD27* coding sequence were inserted into the multiple cloning site of BSMV- $\gamma$  to generate the vectors VIGS-*HvD27*-1 and VIGS-*HvD27*-2 (Figure 22).



**Figure 22.** Genomic organization of barley stripe mosaic virus (BSMV). (A) Genomic RNA  $\alpha$ ,  $\beta$ ,  $\gamma$  of BSMV, strain ND-18. (B) Genomic organization of a coat-protein deletion mutant of BSMV RNA  $\beta$ . (C) Genomic organization of BSMV RNA  $\gamma$  modified to express antisense *HvD27* fragments. Open boxes indicate ORFs. Subgenomic promoters are indicated by arrows. The orientation of the *HvD27* insert is indicated by an arrow-shaped box. The positions of selected restriction enzyme sites are indicated. (D) Size and position of barley *HvD27* cDNA fragments amplified by PCR relative to the *HvD27* ORF. The positions of the PCR primers are indicated by arrows.

Seeds of the barley “Black Hulless” were germinated, and 9 days after germination the second leaf was mechanically inoculated with a mixture of RNA transcribed from clones of BSMV- $\alpha$ , - $\beta$  and VIGS-*HvD27*-1 or VIGS-*HvD27*-2. As a negative control, plants were infected with BSMV- $\alpha$ , - $\beta$  and BSMV- $\gamma$ -MCS. Plants inoculated with BSMV displayed mosaic-type necrosis and curling symptoms from 9 to 11 days post inoculation (dpi) (Figure 23A). 21 dpi the third leaf was harvested for analysis. Only plants showing virus symptoms at the time of harvest were included in the analysis, and all virus-infected plants growing together in one growth chamber were treated as one sample. The presence of viral DNA in the harvested plant leaves was confirmed by RT-PCR (Figure 23B).

The transcript levels of *HvD27* were determined by qRT-PCR and showed significantly lower *HvD27* mRNA levels in plants inoculated with VIGS-*HvD27*-1 or VIGS-*HvD27*-2 (Figure 23C). Interestingly, BSMV-inoculated plants produced fewer tillers than non-inoculated Black Hulless reference plants. However, the VIGS-*HvD27* silenced plants exhibited a higher tiller number than BSMV-inoculated plants (Figure 23D and 23E), which could be ascribed to the significant down-regulation of *HvD27*.





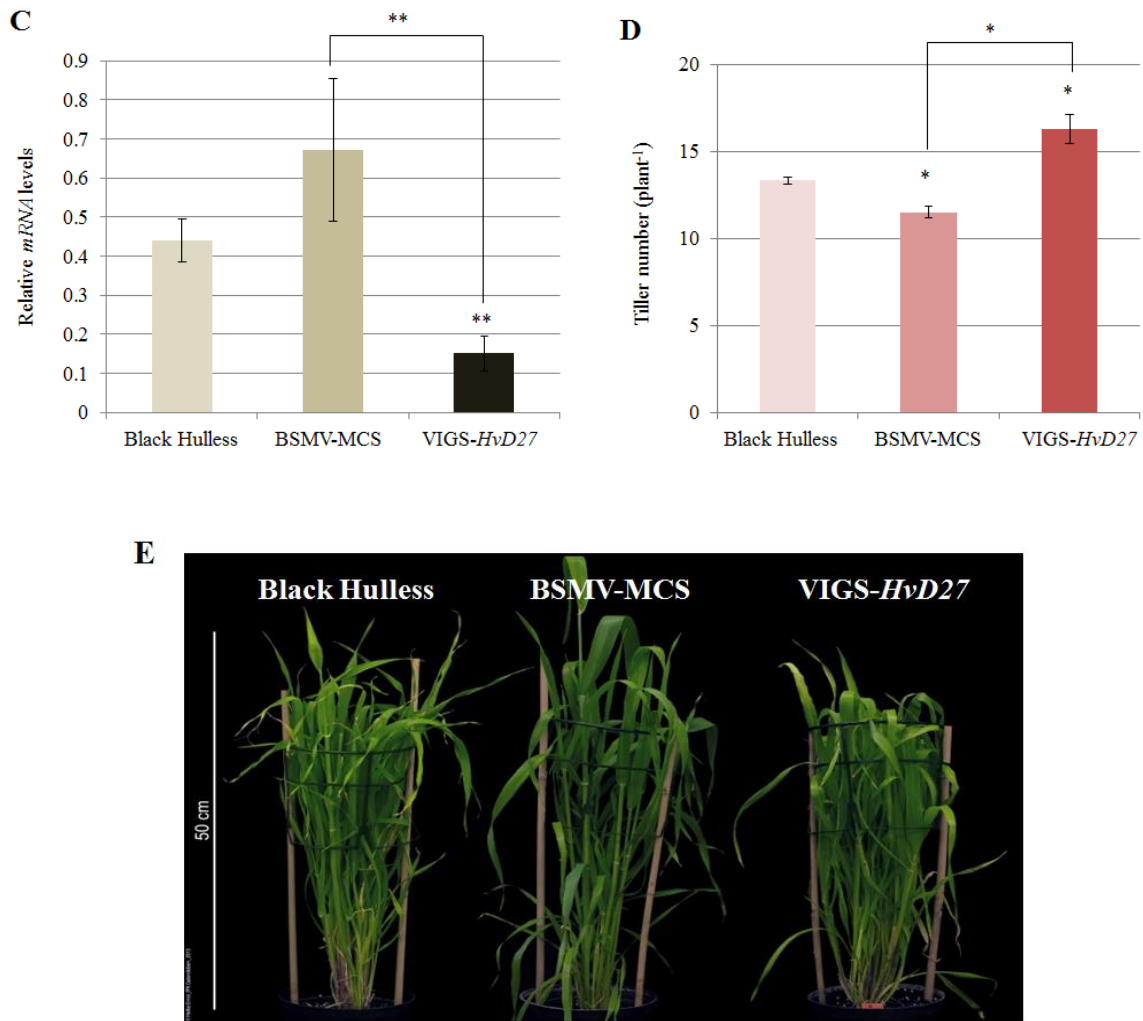


**Figure 23.** Virus-induced gene silencing (VIGS) of *HvD27* in barley. (A) Barley leaves infected with BSMV-MCS, VIGS-*HvD27*-1, or VIGS-*HvD27*-2 at 14 days post inoculation (dpi). (B) RT-PCR analysis showing the presence of a BSMV $\alpha$  construct in barley leaves. (C) *HvD27* expression levels in leaf tissue as determined by qRT-PCR. *Serine/threonine protein phosphatase PP2A-4* was used as a reference gene. Bars represent means from three independent samples  $\pm$  SD. (D) Total tiller number per plant. Values represent means  $\pm$  SE of 12 plants. (E) The tillering phenotype of BSMV-MCS and VIGS-*HvD27* silenced plants and the reference Black Hulless. Significant differences according to Student's *t*-test are indicated by asterisks \*,  $P < 0.05$ , \*\*,  $P < 0.01$ .

The VIGS approach is not a stable transformation approach but works transiently. Therefore, the experiment was repeated three times. The tillering phenotypes of BSMV-MCS or VIGS-*HvD27* silenced plants and of Black Hulless were observed, and the total tiller number per plant was counted at 14 dpi and 21 dpi in the second (Figure 24A-D) and third VIGS experiment (Figure 24E-H), respectively. The VIGS-*HvD27* silenced plants represented a

higher tiller number than BSMV-inoculated plants (Figure 24). For subsequent analysis, only the data of one representative experiment was shown.

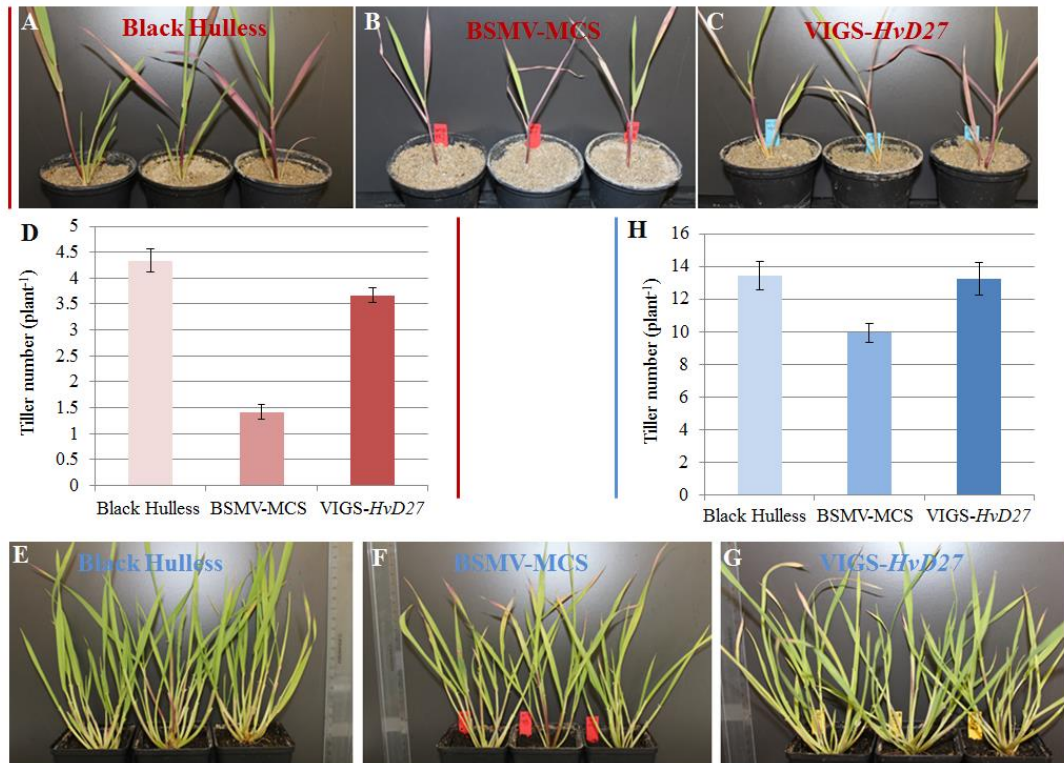


**Figure 24.** Virus-induced gene silencing of *HvD27* in barley. (A-C) Tillering phenotype of BSMV-MCS or VIGS-*HvD27* silenced plants and of the reference line Black Hulless and (D) total tiller number per plant at 14 dpi in the second VIGS experiment. (E-G) Tillering phenotype of BSMV-MCS or VIGS-*HvD27* silenced plants and of the reference line Black Hulless and (H) total tiller number per plant at 21 dpi in the third VIGS experiment. Shown are three independent replicates for each construct. Bars represent means  $\pm$  SE from 12 independent replicates.

The spikelet can be seen as a single unit of cereal inflorescence. Inflorescence architecture of barley bears one to three single-flowered spikelets at each rachis internode. Black Hulless used in this study is a six-rowed barley variety and produces a central spikelet and two lateral spikelets. When the spike morphology was compared between Black Hulless, BSMV-MCS and VIGS-*HvD27*, It became obvious that BSMV-inoculated plants generated the same central and lateral spikelets as non-inoculated Black Hulless reference plants, although the central or lateral spikelet infertility was slightly higher. Interestingly, the VIGS-*HvD27* silenced plants produced additional spikelets while BSMV-inoculated plants did not. The

additional spikelets emerging at rachis internodes were frequently fertile and developed grains (Figure 25).

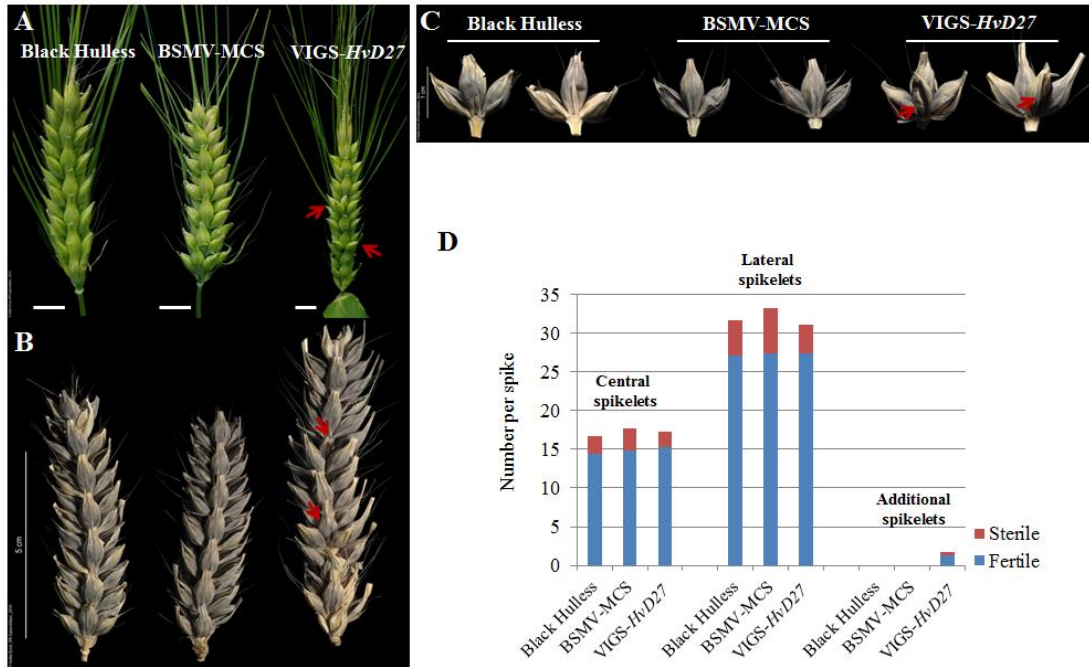


**Figure 25.** Virus-induced gene silencing of *HvD27* in barley. (A and B) Spike phenotype of BSMV-MCS, VIGS-*HvD27* silenced plants and the reference line Black Hulless at late milk or ripening stage, respectively. Bars = 1 cm. (C) Spikelet formation at one rachis internode. Red arrows mark additional spikelets. (D) Spike structures produced by BSMV-MCS, VIGS-*HvD27* silenced plants and the reference Black Hulless. Total number of fertile or sterile central spikelets, lateral spikelets and additional spikelets. Data were recorded from nine plants with on average two spikes per plant.

### 3.5 Functional characterization of the *HvCCD7* gene by virus-induced gene silencing in barley

To examine the role of *HvCCD7* in regulating barley plant architecture, another virus-induced gene silencing (VIGS) approach was performed. To start with BSMV-mediated VIGS in barley, fragments of two different lengths (295 bp and 306 bp) of the *HvCCD7* coding sequence were inserted into the multiple cloning site of BSMV- $\gamma$  to generate the vectors VIGS-*HvCCD7*-1 and VIGS-*HvCCD7*-2 (Figure 26).

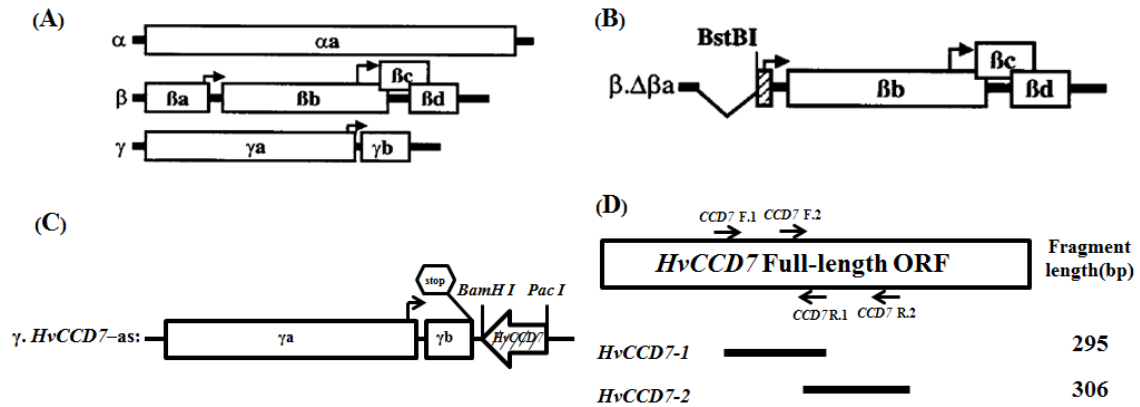


**Figure 26.** Genomic organization of barley stripe mosaic virus (BSMV). (A) Genomic RNA  $\alpha$ ,  $\beta$ ,  $\gamma$  of BSMV, strain ND-18. (B) Genomic organization of a coat-protein deletion mutant of BSMV RNA  $\beta$ . (C) Genomic organization of BSMV RNA  $\gamma$  modified to express antisense *HvCCD7* fragments. Open boxes indicate ORFs. Subgenomic promoters are indicated by arrows. The orientation of the *HvCCD7* insert is indicated by an arrow-shaped box. The positions of selected restriction enzyme sites are indicated. (D) Size and position of barley *HvCCD7* cDNA fragments amplified by PCR relative to the *HvCCD7* ORF. The positions of the PCR primers are indicated by arrows.

Black Hulless seeds were germinated, and 9 days after germination the second leaf was mechanically inoculated with a mixture of RNA transcribed from clones of BSMV- $\alpha$ , - $\beta$  and VIGS-*HvCCD7-1* or VIGS-*HvCCD7-2*. As negative control, plants were infected with BSMV- $\alpha$ , - $\beta$  and BSMV- $\gamma$ -MCS. 21 dpi the third leaf was harvested for analysis. Only plants showing symptoms of viral infection at the time of harvest were included in the analysis, and all virus-infected plants growing together in one growth chamber were treated as one sample.

Interestingly, BSMV-inoculated plants produced fewer tillers than non-inoculated Black Hulless reference plants. However, the VIGS-*HvCCD7* silenced plants exhibited a higher tiller number than BSMV-inoculated plants (Figure 27A and 27B), which could result from the significant down-regulation of *HvCCD7*. Subsequently, the transcript levels of *HvCCD7* were quantified and showed significantly lower *HvCCD7* mRNA levels in plants inoculated with VIGS-*HvCCD7-1* or VIGS-*HvCCD7-2* (Figure 27C).

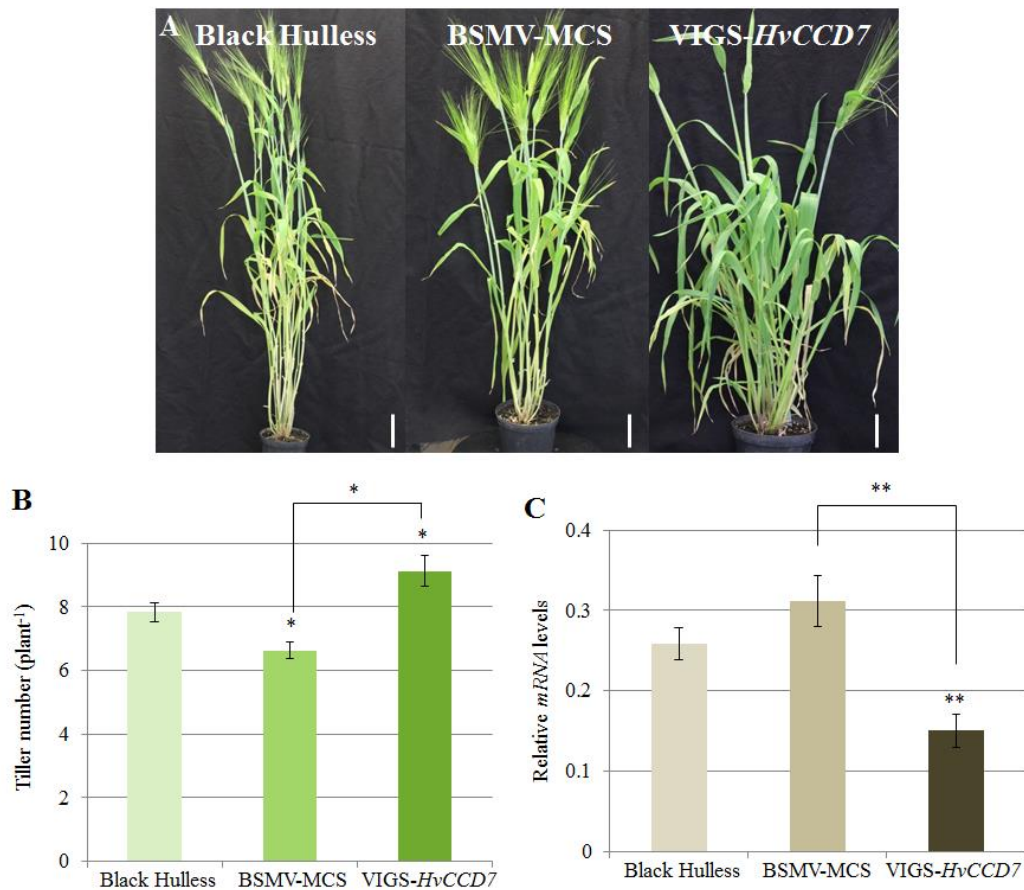


**Figure 27.** Virus-induced gene silencing (VIGS) of *HvCCD7* in barley. (A) The tillering phenotype of BSMV-MCS and VIGS-*HvCCD7* silenced plants and the reference Black Hulless. Bars = 10 cm. (B) Total tiller number per plant. Values represent means  $\pm$  SE of 12 plants. (C) *HvCCD7* expression levels in leaf tissue as determined by qRT-PCR. *Serine/threonine protein phosphatase PP2A-4* was used as a reference gene. Bars represent means from three independent samples  $\pm$  SD. Significant differences according to Student's *t*-test are indicated by asterisks \*,  $P < 0.05$ , \*\*,  $P < 0.01$ .

By the same way, the spike architecture was analyzed between Black Hulless, BSMV-MCS and VIGS-*HvCCD7*. BSMV-inoculated plants produced the same central and lateral spikelets as non-inoculated Black Hulless reference plants, although the central or lateral spikelet sterility was slightly higher. However, the VIGS-*HvCCD7* silenced plants produced additional spikelets in contrast to BSMV-inoculated plants. The additional spikelets emerging at rachis internodes were frequently fertile and developed grains (Figure 28).

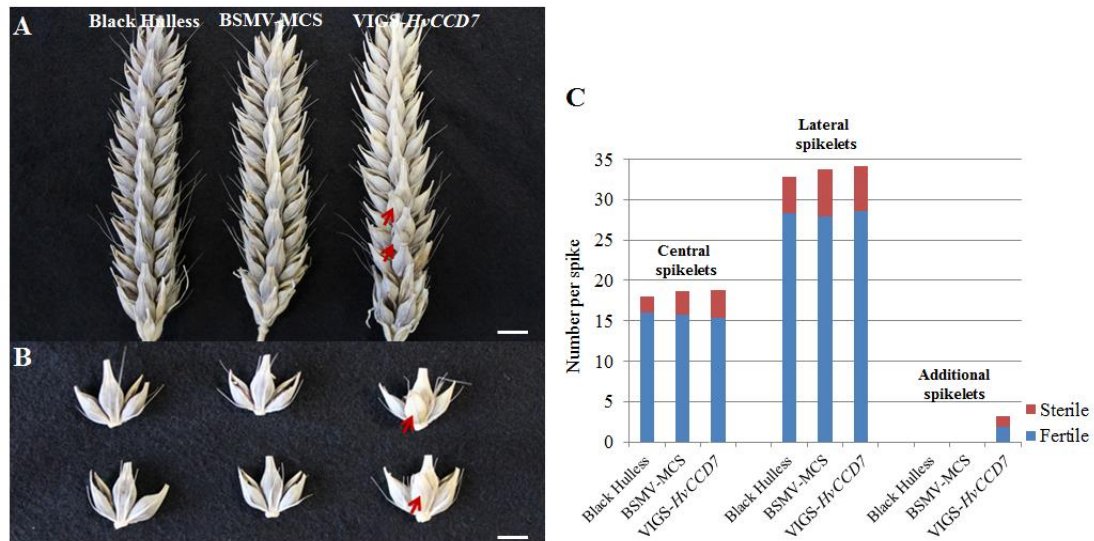


**Figure 28.** Virus-induced gene silencing of *HvCCD7* in barley. (A) Spike phenotype of BSMV-MCS, VIGS-*HvCCD7* silenced plants and the reference Black Hulless at ripening stage. (B) Spikelet formation at one rachis internode. Red arrows mark additional spikelets. (C) Spike structures produced by BSMV-MCS, VIGS-*HvCCD7* silenced plants and the reference Black Hulless. Total number of fertile or sterile central spikelets, lateral spikelets and additional spikelets. Data were recorded from nine plants with on average two spikes per plant. Bars = 1 cm.

### 3.6 Functional characterization of the *HvCCD8* gene by virus-induced gene silencing in barley

To further investigate the role of *HvCCD8* in regulating barley plant architecture, a third virus-induced gene silencing (VIGS) approach was performed. To start with BSMV-mediated VIGS in barley, fragments of two different lengths (202 bp and 338 bp) of the *HvCCD8* coding sequence were inserted into the multiple cloning site of BSMV- $\gamma$  to generate the vectors VIGS-*HvCCD8*-1 and VIGS-*HvCCD8*-2 (Figure 29).

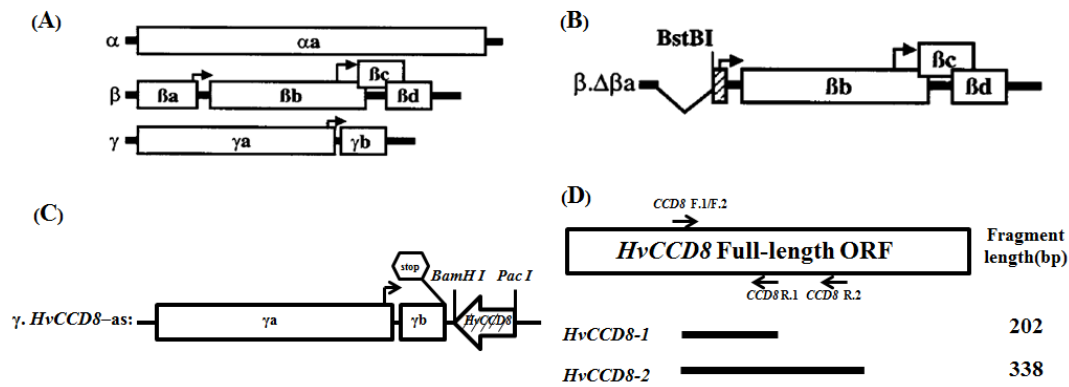


**Figure 29.** Genomic organization of barley stripe mosaic virus (BSMV). (A) Genomic RNA  $\alpha$ ,  $\beta$ ,  $\gamma$  of BSMV, strain ND-18. (B) Genomic organization of a coat-protein deletion mutant of BSMV RNA  $\beta$ . (C) Genomic organization of BSMV RNA  $\gamma$  modified to express antisense *HvCCD8* fragments. Open boxes indicate ORFs. Subgenomic promoters are indicated by arrows. The orientation of the *HvCCD8* insert is indicated by an arrow-shaped box. The positions of selected restriction enzyme sites are indicated. (D) Size and position of barley *HvCCD8* cDNA fragments amplified by PCR relative to the *HvCCD8* ORF. The positions of the PCR primers are indicated by arrows.

Black Hulless seeds were germinated, and 9 days after germination the second leaf was mechanically inoculated with a mixture of RNA transcribed from clones of BSMV- $\alpha$ , - $\beta$  and VIGS-*HvCCD8*-1 or VIGS-*HvCCD8*-2. As negative control, plants were infected with BSMV- $\alpha$ , - $\beta$  and BSMV- $\gamma$ -MCS. 21 dpi the third leaf was harvested for analysis. Only plants showing symptoms of viral infection at the time of harvest were included in the analysis. All virus-infected plants growing together in one growth chamber were treated as one sample.

BSMV-inoculated plants produced fewer tillers than non-inoculated Black Hulless reference plants. However, the VIGS-*HvCCD8* silenced plants exhibited a higher tiller number than BSMV-inoculated plants (Figure 30A and 30B), which could result from the significant down-regulation of *HvCCD8*. Subsequently, the transcript levels of *HvCCD8* were quantified by qRT-PCR and showed significantly lower *HvCCD8* mRNA levels in plants inoculated with VIGS-*HvCCD8*-1 or VIGS-*HvCCD8*-2 (Figure 30C).

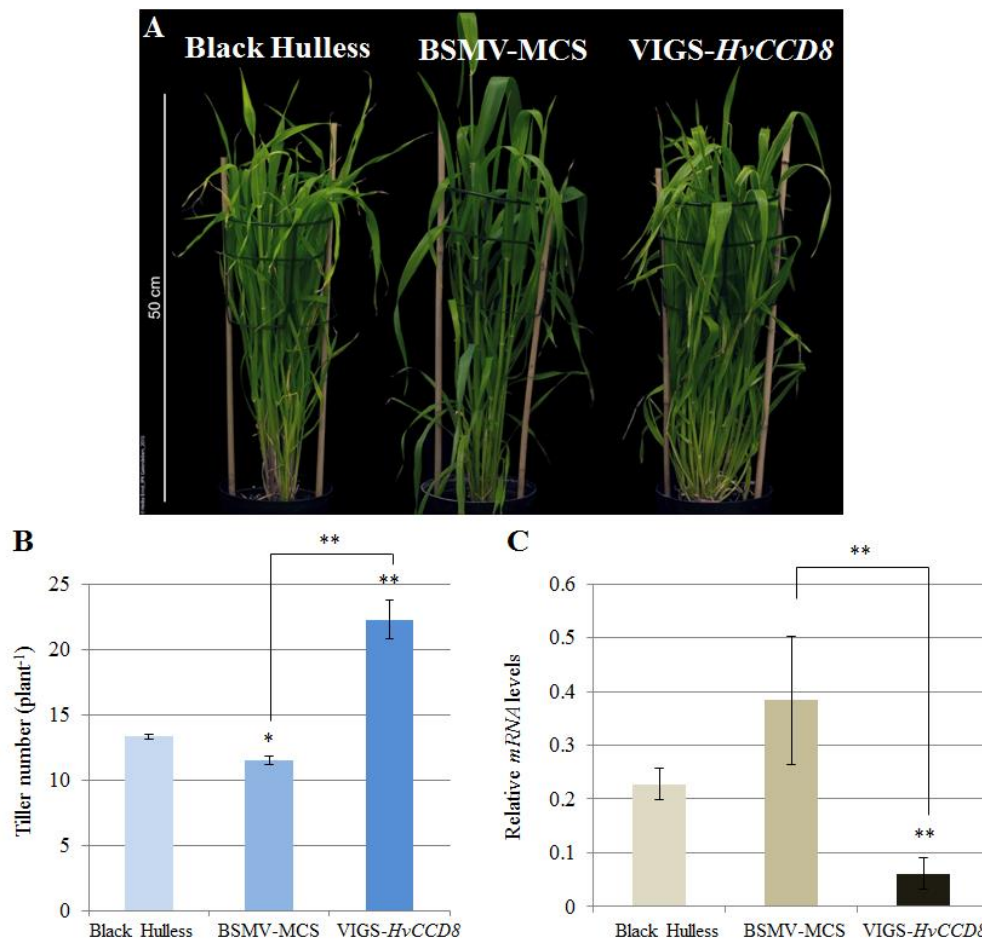


**Figure 30.** Virus-induced gene silencing (VIGS) of *HvCCD8* in barley. (A) The tillering phenotype of BSMV-MCS and VIGS-*HvCCD8* silenced plants and the reference Black Hulless. (B) Total tiller number per plant. Values represent means  $\pm$  SE of 12 plants. (C) *HvCCD8* expression levels in leaf tissue as determined by qRT-PCR. *Serine/threonine protein phosphatase PP2A-4* was used as a reference gene. Bars represent means from three independent samples  $\pm$  SD. Significant differences according to Student's *t*-test are indicated by asterisks \*,  $P < 0.05$ , \*\*,  $P < 0.01$ .

At the same time, the spike architecture was compared between Black Hulless, BSMV-MCS and VIGS-*HvCCD8*. BSMV-inoculated plants also produced central and lateral spikelets to a similar extent as non-inoculated Black Hulless reference plants, although the central or lateral spikelet infertility was slightly higher. However, the VIGS-*HvCCD8* silenced plants produced additional spikelets in contrast to BSMV-inoculated plants. The additional spikelets emerging at rachis internodes were also frequently fertile and developed grains (Figure 31).



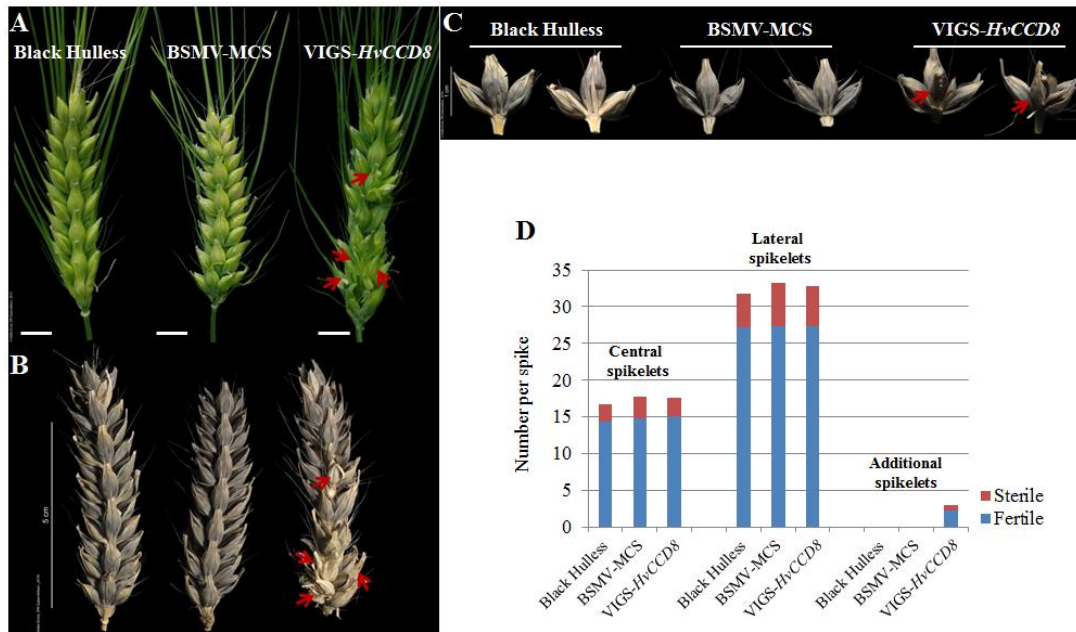


**Figure 31.** Virus-induced gene silencing of *HvCCD8* in barley. (A and B) Spike phenotype of BSMV-MCS, VIGS-*HvCCD8*-silenced plants and the reference Black Hulless at late milk or ripening stage, respectively. Bars = 1 cm. (C) Spikelet formation at one rachis internode. Red arrows mark additional spikelets. (D) Spike structures produced by BSMV-MCS, VIGS-*HvCCD8* silenced plants and the reference Black Hulless. Total number of fertile or sterile central spikelets, lateral spikelets and additional spikelets. Data were recorded from nine plants with on average two spikes per plant.

### 3.7 Functional characterization of the *HvMAX1* gene by a genetic complementation approach

In the end, to test whether *HvMAX1* functions in shoot branching, similar as *AtMAX1* does in Arabidopsis, a genetic complementation study was conducted by expressing the *HvMAX1* gene in Arabidopsis homozygous *max1* mutant obtained from Prof. Dr. Ottoline Leyser (Sainsbury Laboratory, Cambridge University). For complementation, the full-length ORF of *HvMAX1* (AK367034) was placed under the control of CaMV 35S promoter, then the combined fragment was subcloned into the binary plant expression vector p6U10 for expression in the *Atmax1* mutant or the Col-0 reference line using Agrobacterium-mediated transformation (Figure 32A). The RT-PCR analysis indicated that the *HvMAX1* transgene was successfully integrated in the transgenic lines (Figure 32B).

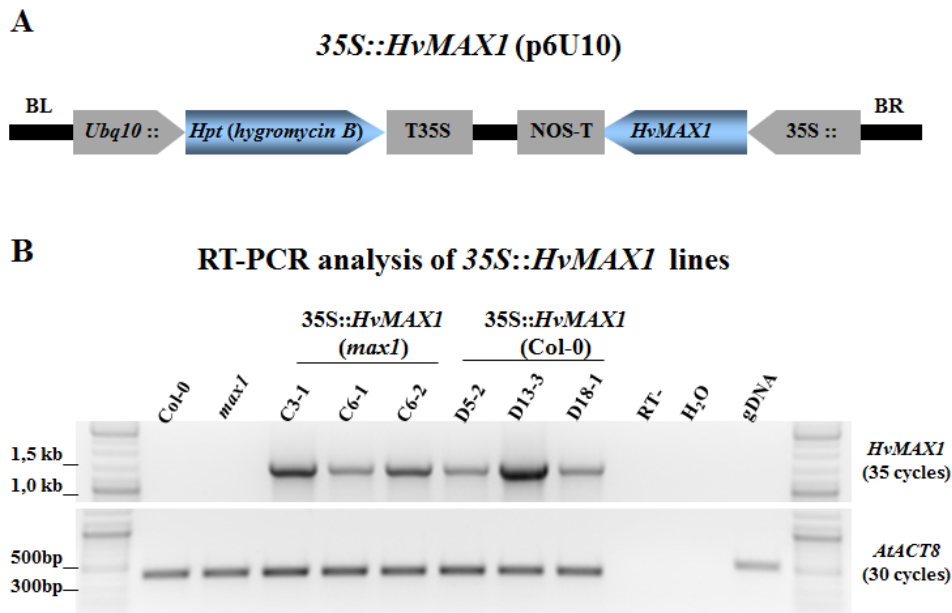


**Figure 32.** (A) The vector map of 35S::*HvMAX1* used for transformation of the Arabidopsis *max1* mutant. (B) RT-PCR analysis for verification of the 35S::*HvMAX1* construct in transgenic lines.

The 35S::*HvMAX1* lines in the T3 generation were homozygous, carrying a single T-DNA insertion. The number of primary rosette-leaf branches was counted and compared to that of Col-0 and *Atmax1* mutants, which were grown side-by-side with the transgenic lines under identical conditions. The number of primary rosette-leaf branches in the transgenic lines C3-1, C6-1 and C6-2 was largely reverted to a similar number as in Col-0, whereas additional axillary branching was completely blocked in the transgenic lines D5-2, D13-3 and D18-1. Under these growth conditions, Col-0 produced about three primary rosette-leaf branches, whereas *Atmax1* mutants produced about twelve primary rosette-leaf branches. In the *Atmax1* background, *HvMAX1* expression could lead to three to four primary rosette-leaf branches while in the Col-0 background *HvMAX1* expression could lead to an almost complete suppression of primary rosette-leaf branching (Figure 33). These results indicated that *HvMAX1* was able to complement or partially complement the shoot branching phenotype of the Arabidopsis *Atmax1* mutant.

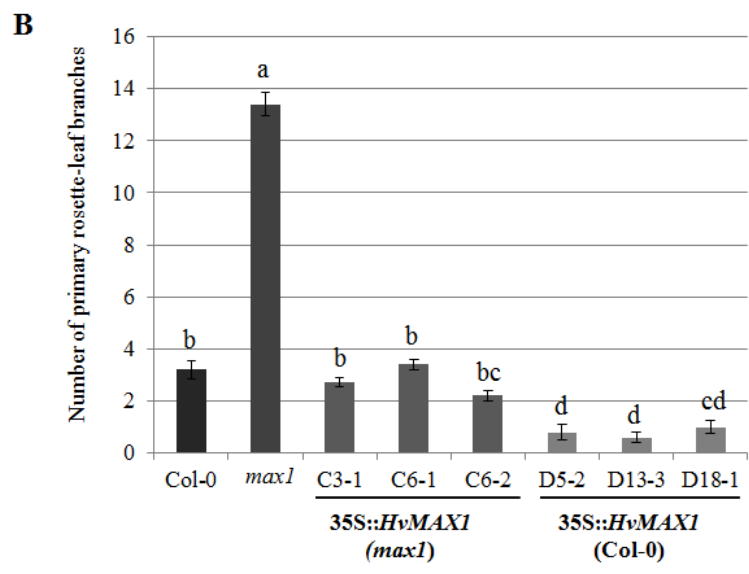
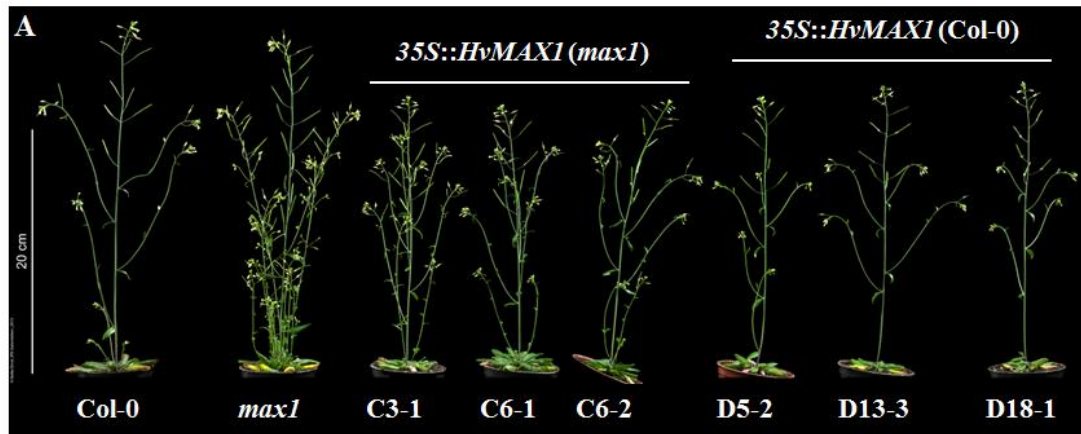


**Figure 33.** Genetic complementation of the *Arabidopsis max1* mutant with the *Hordeum vulgare MAX1* gene. (A) Axillary branching phenotypes. (B) Number of primary rosette-leaf branches. Shown are average numbers of primary rosette-leaf branches from at least 15 individual plants  $\pm$  SE. Different letters indicate significant differences (Tukey,  $p < 0.05$ ).

## 4. Discussion

### 4.1 The signaling role of strigolactones in barley shoot architecture

Strigolactones are a recently identified class of plant hormones that play a key role in regulating plant architecture. Studies on branching mutants in *Arabidopsis*, pea, rice and petunia have identified several genes involved in SL biosynthesis or signaling (Al-Babili and Bouwmeester 2015). However, it has still remained elusive whether the same SL pathway is conserved in barley. Firstly, to explore the molecular identity of SLs in barley (*Hordeum vulgare* cv. Golden Promise), major SLs produced by barley root exudates were purified and their stereochemical structures were identified by comparison with optically pure synthetic standards on the basis of their retention times and mass fragmentations using MRM-LC-MS/MS. The major SL purified from root exudates of barley plants was 5-deoxystrigol (Figure 14A), which is distributed widely in the plant kingdom and detected in roots of both monocots (Awad *et al.* 2006) and dicots (Yoneyama *et al.* 2007). In addition to 5-deoxystrigol, 2'-*epi*-orobanchol and sorgomol were detected by LC-MS/MS, belonging to orobanchol-type and strigol-type SLs, respectively. Based on MS signal intensities these SLs occurred in relatively low levels, which is likely the reason why they have not been purified in barley. In rice (*Oryza sativa* L. cv. Nipponbare) plants, the major SLs produced were orobanchol, orobanchyl acetate, and *ent*-2'-*epi*-5-deoxystrigol. In addition to these SLs, 7-oxoorobanchyl acetate and three putative methoxy-5-deoxystrigol isomers were detected by LC-MS/MS (Xie *et al.* 2010). It is intriguing to note that rice plants produced only orobanchol-type SLs, derived from *ent*-2'-*epi*-5-deoxystrigol, while both orobanchol-type and strigol-type SLs, derived from 5-deoxystrigol were detected in barley plants. The study of the genetic variation in SL production and tillering in rice indicated that root exudates of rice cultivars contained large amounts of the SLs orobanchol, 2'-*epi*-5-deoxystrigol including three methoxy-5-deoxystrigol isomers, which were associated with a smaller number of tillers (Jamil *et al.* 2012). In line with this coincidence, the major identified SL 5-deoxystrigol was significantly ( $P < 0.01$ ) lower in root exudates of LOHi236 and LOHi272 compared with the wild type at 14 WAG (Figure 14B), which may thus be causally related to the late-tillering

phenotype of LOHi236/272 lines. Although the main structure of SLs is rather similar, their A- and B-ring decoration and stereochemistry can vary substantially (Figure 3). It is obvious that different functional groups and stereochemical differences will lead to different biological activities (Yoneyama *et al.* 2009). Definitely, a more detailed investigation of barley SLs should enable a deeper understanding of their biological relevance in the future.

To isolate and characterize SL biosynthesis genes in barley, sequence homologues of four founding members of the SL biosynthesis pathway in rice and Arabidopsis were identified. Phylogenetic analysis confirmed the identification of barley homologues to four founding members, namely *HvD27*, *HvCCD7*, *HvCCD8* and *HvMAX1* (Figure 15). Using the barley genome database, full-length coding sequences of *HvD27* (AK358967) and *HvMAX1* (AK367034) could be obtained, since only a partial coding sequence was available for *HvCCD7* (MLOC\_55474.1) and *HvCCD8* (MLOC\_66551.1). While the *HvD27* gene will be discussed in more detail below, the partial protein sequences of *HvCCD7* and *HvCCD8* shared highest identity (80%) with D17 (CCD7) and (90%) with D10 (CCD8), respectively (Figure 15B). *HvMAX1* had 57% sequence identity with *AtMAX1* (Figure 15C). Gene expression analysis indicated that these barley SL biosynthesis homologous genes are differentially expressed across various tissues and organs. The transcript abundance of each of these genes was highest in the root. In the stem base, the transcript levels of *HvD27*, *HvCCD7* and *HvCCD8* were also relatively high. The expression analysis also indicated that *HvD27* and *HvMAX1* were highly expressed in leaves and roots, respectively (Figure 16). It remains unclear whether differences in expression level or pattern of barley SL biosynthesis genes may result in differences in their physiological function. Nevertheless, these results are consistent with the view that roots represent one of the major sites for SL biosynthesis in planta (Al-Babili and Bouwmeester 2015). This has been demonstrated in a grafting experiment, in which grafting wild-type Arabidopsis root stocks to *max1*, *max3*, or *max4* scions restored the wild-type branching pattern in the mutant shoots (Booker *et al.* 2005).

In addition to SL biosynthesis pathway genes, several other genes are involved in SL signaling such as *D14*, *MAX2* and *D53* (Al-Babili and Bouwmeester 2015). It would be

helpful to identify sequence homologs of each of those genes in barley and conduct genetic complementation studies similar to what has been described in this study in order to better understand how the SL pathway operates in barley. A preliminary analysis indicated that the sequence homologue of AtD14 (encoded by At3G03990) is present in the genome of barley. A protein encoded by AK363454 showed about 72% similarity with AtD14 at the amino acid level (Appendix C.1). A preliminary analysis indicated that the sequence homologue of AtMAX2 (encoded by AT2G42620) is also present in the genome of barley. A protein encoded by MLOC\_4044.5 showed about 59% similarity with AtMAX2 at the amino acid level (Appendix C.2). A preliminary analysis indicated that sequence homologue of AtD53 (encoded by AT1G07200) is also present in the genome of barley. A protein encoded by locus AK372211 showed about 29% similarity with AtD53 at the amino acid level (Appendix C.3). In order to fully assign these genes to the SL pathway in barley, further complementation and gene expression studies need to be conducted as well as physiological studies with the corresponding mutants or lines with modulated expression of these genes.

In addition to *HvD27*, the present work also included cloning of the *MAX1* gene from *Hordeum vulgare* cv. Golden Promise including its further characterization by functional complementation of the *max1* mutation in Arabidopsis. The *MAX1* gene encodes a carlactone oxidase which catalyzes one of the late steps in the SL biosynthesis pathway (Figure 2). Compared to the tissue-dependent expression of *HvMAX1*, the major sites of *AtMAX1* transcription were characterized in more detail and found to be in vascular-associated tissues throughout the plant, such as the vascular cylinder in roots, the cambial region in inflorescence stems, axillary regions of leaves and flowers (Booker *et al.* 2005). The Arabidopsis *max1* mutant showed increased branching relative to wild-type plants (Figure 33), and analogous phenotypes have been identified in pea, petunia, and rice mutants. In the complementation test, *HvMAX1* was able to completely rescue the shoot branching phenotype of the Arabidopsis *max1* mutant. Consistently, overexpression of *HvMAX1* completely suppressed the secondary shoot branching (Figure 33). These results suggested that *HvMAX1* has a conserved function, similar to *AtMAX1*, and is involved in SL biosynthesis and regulation of tillering in barley.

Virus-Induced Gene Silencing (VIGS) is a powerful tool for endogenous gene silencing in barley plants and based on the exploitation of recombinant viruses, harboring sequences that induce gene silencing. The Barley Stripe Mosaic Virus (BSMV) - based VIGS system is an efficient and rapid RNAi approach that is routinely applied in functional genomics studies of cereals (Bruun-Rasmussen *et al.* 2007). Therefore, the roles of *HvD27*, *HvCCD7* and *HvCCD8* in plant architecture were further characterized by employing virus-induced gene silencing. The complete or partial coding sequence of each target gene was subjected to an in silico analysis using the si-Fi (siRNA Finder; <http://labtools.ipk-gatersleben.de/>) software to select sequences of 200-340 nucleotides that were predicted to produce a large number of silencing-effective siRNAs. The likelihood of off-target silencing by the introduced sequence in other genomic was also evaluated using si-Fi. Whenever possible, two preferably non-overlapping regions were selected for each target gene. The subsequent observation of the same phenotype induced by each of the two independent VIGS constructs was taken as a reliable indication that the phenotype was due to a specific silencing of the target gene. As expected, the VIGS-*HvD27* silenced, VIGS-*HvCCD7* silenced or VIGS-*HvCCD8* silenced plants exhibited a higher tiller number than BSMV-inoculated plants (Figure 23E, 27A and 30A). The tillering phenotypes of these VIGS-silenced plants were similar to phenotypes of known SL-related mutants in rice, pea and Arabidopsis that all showed enhanced shoot branching (Arite *et al.* 2007, Booker *et al.* 2004, Drummond *et al.* 2009, Johnson *et al.* 2006, Simons *et al.* 2007, Sorefan *et al.* 2003, Wen *et al.* 2016, Zheng *et al.* 2016, Zou *et al.* 2006). While a large body of evidence has been collected for the importance of SLs in modifying shoot branching in various plant species, little is known about the function of SLs during reproductive development. A recent study suggested that SLs signaling regulates ear architecture and kernel size in maize (Jiahn *et al.* 2012). Intriguingly, the VIGS-*HvD27* silenced, VIGS-*HvCCD7* silenced or VIGS-*HvCCD8* silenced plants not only showed increased tillering but also produced additional spikelets and influenced spikelet fertility (Figure 25, 28 and 31). Therefore, it will be important in future to explore the mechanisms by which SLs coordinate plant traits during vegetative and reproductive development, and whether there is a SL-dependent, regulatory link between tiller formation, spikelet determination and row-type in barley.

In monocots and dicots, two proteins, the leucine-rich-repeat F-box protein MAX2 in *Arabidopsis* and the  $\alpha/\beta$ -fold hydrolase D14 in rice, have been shown to be required for the SL response (Seto and Yamaguchi 2014). MAX2 acts as a recognition subunit in a SKP1-CUL1-F-box-protein (SCF)-type ubiquitin ligase complex and is believed to target proteins for proteasomal degradation (Stirnberg *et al.* 2007). The petunia D14 ortholog DAD2 can bind and hydrolyze the SL analog GR24, and this hydrolytic activity is a prerequisite for the protein-protein interaction of the DAD2-GR24 complex with PhMAX2 (Hamiaux *et al.* 2012). The effect of this interaction was recently elucidated in rice with the discovery of a new high-tillering rice mutant, *d53* (Jiang *et al.* 2013). The D53 protein is degraded through the D3 (rice MAX2 ortholog)-dependent proteasome pathway upon binding of GR24 to D14, and thus likely represents a repressor of SL downstream signaling (Jiang *et al.* 2013). It has been found that SLs can upregulate a common target in the bud, *TEOSINTE BRANCHED 1* (*TBI*), encoding a TCP transcription factor and homolog of the *Arabidopsis thaliana* gene *BRANCHED 1* (*BRC1*) gene known to inhibit shoot branching (Brewer *et al.* 2009, Dun *et al.* 2012, Ferguson and Beveridge 2009). In barley, a homolog of *TBI*, *Intermedium-c* (*Int-c*) was found to increase the formation of lateral spikelets. In addition, the *int-c* mutant has an increased tiller number at early developmental stages (Ramsay *et al.* 2011). Interestingly, the gene underlying the *Vrs1* locus encodes a HD-ZIP transcription factor, which is expressed in lateral spikelet primordia of the developing spike. *Vrs1* suppresses lateral spikelet fertility resulting in the two-rowed spike phenotype (Komatsuda *et al.* 2007). Similar to the *vrs1* mutant, the *vrs4* mutant shows complete fertility of central and lateral spikelets and the spikes produce additional florets. *Vrs4* encodes a homolog of maize *RAMOSA2* (*RA2*), a gene involved in the control of branching of the female inflorescence (Koppolu *et al.* 2013). No tillering phenotype was observed in *vrs1* mutants suggesting that *vrs1* does not directly affect the initiation and outgrowth of axillary buds. Mutants of *vrs4* show a similar trend, with no reduction in tiller number until the plants reach full maturity. In line with this, *Vrs4* was reported to act upstream of *Vrs1* in the same pathway, suggesting that this signaling cascade does not directly influence shoot branching (Liller *et al.* 2015). Taken together, a putative model has been set up to summarize the architectural roles of SL signaling in barley. In this putative model, SLs regulate axillary bud formation and outgrowth via the downstream target



gene *INT-C* during the early vegetative phase of plant development in barley. During the reproductive phase, SLs control spikelet branching and fertility via the downstream target gene *Vrs4*. In future, an interesting research focus will be to study further mechanisms and target pathways of SL signaling using genetic, biochemical and functional genomics approaches in barley.

#### **4.2 The $\beta$ -carotene isomerase DWARF27 links abscisic acid with the strigolactones biosynthesis**

Firstly, the rice enzyme D27 was identified and characterized as an iron-containing enzyme involved in SL biosynthesis, based on low SL levels of the corresponding mutant (Lin *et al.* 2009). Using purified enzyme, it has been shown that OsD27 exerts the isomerase activity required to catalyze the isomerization in both directions, i.e. forming 9-*cis*- $\beta$ -carotene from all-*trans*- $\beta$ -carotene and vice versa (Alder *et al.* 2012). In the biosynthesis pathway of SLs, the position of D27 upstream of other known SL biosynthesis enzymes, i.e. CCD7, CCD8 and MAX1, was confirmed in Arabidopsis by studies on the corresponding mutants (Waters *et al.* 2012). The 9-*cis*/all-*trans* isomerase activity of D27 raised the question whether this enzyme is also involved in ABA biosynthesis, by providing the precursor 9-*cis*-violaxanthin or 9'-*cis*-neoxanthin from the corresponding all-*trans* isomers (Figure 34). Indeed, the *Atd27* mutant showed lower ABA concentration relative to Col-0 (Figure 19). This indicated that *AtD27* can interfere with ABA biosynthesis in Arabidopsis. To examine the roles of *HvD27* in SL and ABA biosynthesis, a phylogenetic analysis of D27-like proteins in the barley genome was initiated to identify AK358967, which was subsequently named by *HvD27* as it is the most likely ortholog of OsD27. The *HvD27* protein shares about 71% identity with OsD27 at the amino acid level (Figure 15A). The *OsD27* expression level was high in axillary buds and young panicles, lower in shoot bases and culms, and even lower in roots, sheaths and leaves (Lin *et al.* 2009). In comparison, the highest expression level of *HvD27* was observed in the leaves, while expression was lower in roots and stem bases and in particular in axillary buds (Figure 16).

In rice, the phenotype of the *d27* mutant was weaker than the ones of *d17*-(CCD7) and

*d10*-mutants (CCD8) (Ishikawa *et al.* 2005), demonstrating that the OsD27 isomerase activity can be partially compensated by non-enzymatic carotenoid isomerization or by other enzymes (Waters *et al.* 2012). The enhanced shoot branching of *Atd27* was relatively lower than *Atmax1*, *Atmax3* (CCD7) and *Atmax4* (CCD8) (Waters *et al.* 2012). In this present study, *Atd27* produced about eight primary rosette-leaf branches, whereas *Atmax1* mutants produced about fourteen primary rosette-leaf branches (Figure 21A and 33A). In agreement with these observations, VIGS-*HvD27* silenced plants exhibited a higher tiller number, i.e. 15% more tillers than BSMV-inoculated control plants (Figure 23E), whereas VIGS-*HvCCD8* silenced plants increased the tiller number by 60% compared to BSMV-inoculated plants (Figure 30A). Further genetic complementation experiment demonstrated that the *HvD27* gene was able to rescue or partially rescue the shoot branching phenotype of the Arabidopsis *d27* mutant, while in the Col-0 background *HvD27* overexpression led to an almost complete suppression of primary rosette-leaf branching (Figure 21A and 21B). These findings allowed concluding that *HvD27* is involved in SL biosynthesis and in the regulation of tillering in barley.

The study on the substrate specificity of the rice SL biosynthesis enzyme DWARF27 in carotenoid-accumulating *E. coli* strains and in in-vitro assays performed with the heterologously expressed and purified enzyme revealed that OsD27 does not directly provide the ABA precursors 9-*cis*-violaxanthin or 9'-*cis*-neoxanthin. This was based on the incapability of OsD27 to convert xanthophylls like zeaxanthin, violaxanthin and neoxanthin (Bruno and Al-Babili 2016). However, it may be speculated that 9-*cis*- $\beta$ -carotene produced by D27 requires a series of hydroxylation and epoxidation reactions to be converted into 9-*cis*-violaxanthin, for instance, via a 9-*cis*-route similar to the established all-*trans*-pathway that leads from all-*trans*- $\beta$ -carotene to all-*trans*-violaxanthin (Figure 34). This speculation is based on the observation that modulating the *HvD27* activity in Arabidopsis leads to changes in ABA levels (Figure 21C). Ongoing studies focus on the analysis of carotenoid components in the *Atd27* mutant and in the line B16-5 overexpressing *HvD27* and on the role of *HvD27* in abiotic stress responses.

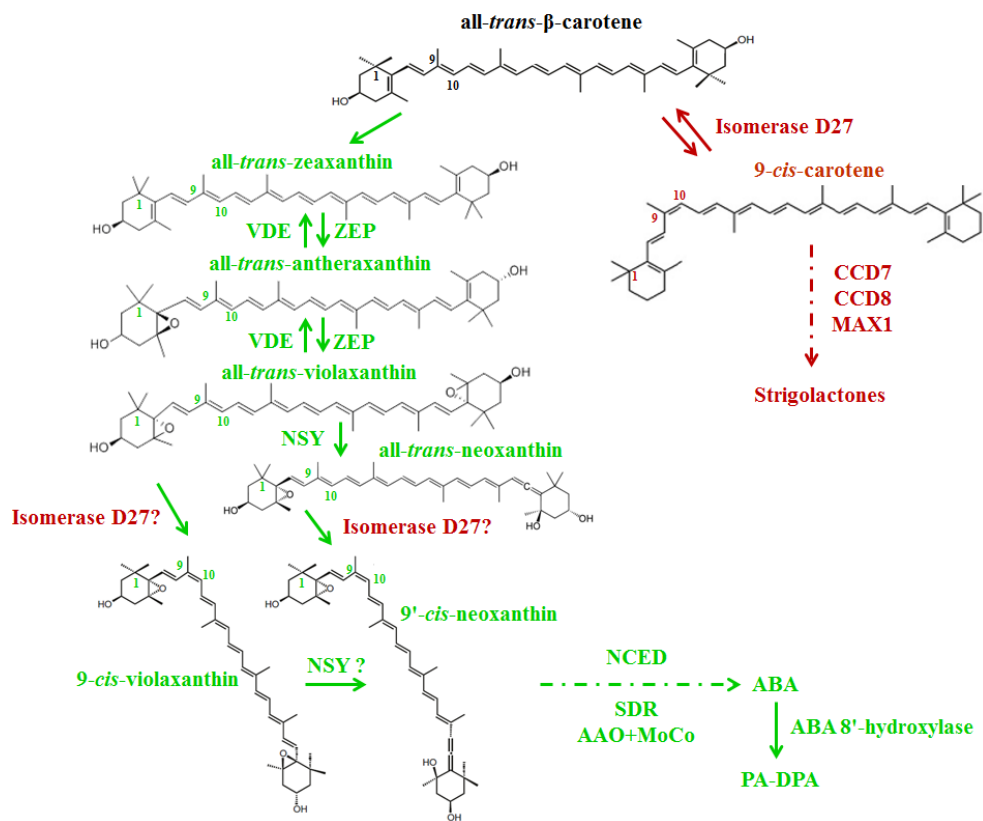


**Figure 34.** Abscisic acid and strigolactone biosynthetic pathways. *Solid arrows* indicate one-step modification of an intermediate and *dashed arrows* represent multistep modifications of an intermediate. Enzyme names are given in **bold**. Abbreviations: ZEP zeaxanthin epoxidase, VDE violaxanthin de-epoxidase, NSY neoxanthin synthase, NCED 9-cis-epoxycarotenoid dioxygenase, SDR short-chain dehydrogenase/reductase, AAO ABA aldehyde oxidase, MoCo molybdenum cofactor synthase, D27 dwarf 27, CCD7/8 carotenoid cleavage dioxygenase 7/8, MAX1 more axillary growth1.

### 4.3 Crosstalk between the biosynthetic pathways of ABA and strigolactones

Abscisic acid is a phytohormone with critical functions in many plant biological processes such as plant stress tolerance, germination, seed development, lateral root development, and bud development (Yao and Finlayson 2015). Recently, strigolactones (SLs) have been considered a novel class of plant hormones with endogenous signaling functions especially in plant architecture (Al-Babili and Bouwmeester 2015). Considering the biological importance of SLs and their biosynthetic origin, Lopez-Raez *et al.* (2010) firstly investigated the relationship between ABA and SL in tomato by studying the correlation between ABA and SL in different tomato mutants that were defective in ABA biosynthesis in combination with

the application of specific inhibitors for NCEDs and CCDs, which are enzymes involved in the biosynthesis of ABA and SLs, respectively. Their results showed that ABA is involved in the regulation of SLs, but the mode of action remained elusive. The first purpose of the present study was therefore to examine the mode of interaction between ABA and SLs taking place at the biosynthesis level of these hormones and the effect of this crosstalk on tiller formation in barley. To address the first question, three different transgenic lines, namely LOHi3/236/272, were analyzed, because in these lines expression of *HvABA 8'-hydroxylase* genes was downregulated by RNAi-mediated gene silencing (Seiler *et al.* 2014). Interestingly, these transgenic lines (LOHi3/236/272) showed an increase in tiller number at a relatively late developmental stage, i.e. 14 weeks after germination (WAG) when grown in the growth chamber (Figure 7) or 12 WAG when grown in the greenhouse (Figure 8). Even though the different environmental conditions acting in the growth chamber and in the greenhouse (Table 3) probably had an impact on plant development, the robustness of this late-tillering phenotype in the LOHi3/236/272 lines was dependent on the introduced transgene and thus offered the possibility to investigate the interaction between ABA and SL.

The LOHi3/236/272 lines have been generated in our lab in a previous project and were referred to as LOHi, standing for the *HvLea::HvABA 8'-hydroxylase* RNAi construct that was used for transformation (Seiler *et al.* 2014). An RNA interference approach was carried out to decrease the endogenous *HvABA 8'-hydroxylase* gene expression and thereby alter the ABA status in transgenic barley lines. In barley, the *ABA 8'-hydroxylase* gene family (CYP707A) includes the three members *HvABA 8'-hydroxylase 1/2/3* (Seiler *et al.* 2014), whose transcript levels decreased significantly in stem bases and roots at 14 WAG (Figure 11A and 12A). ABA 8'-hydroxylation is a key step in the major ABA catabolic route in several plant species (Nambara and Marion-Poll 2005). In agreement with a stronger silencing of *HvABA 8'-hydroxylase 1/3* in stem bases and roots at 14 WAG in LOHi236/272 lines, the ABA concentrations in LOHi236/272 stem bases and roots were higher than in wild-type plants (Figure 13B and 13D). Based on these data, it was concluded that silencing *HvABA 8'-hydroxylase* leads to ABA accumulation in stem bases and roots of LOHi lines, which provokes a late-tillering phenotype.

The association of ABA with axillary bud development has already been considered in several studies. ABA levels in dormant axillary buds of different plant species have been observed to decrease after decapitation (Gocal *et al.* 1991, Knox and Wareing 1984, Mader *et al.* 2003) or fruit removal, a treatment that also promoted bud outgrowth (Tamas *et al.* 1979). Another study showed that increased expression of ABA-associated genes in Arabidopsis buds under light with a high R: FR ratio resulted in a general reduction in branch number (González-Grandío *et al.* 2013). Recently, it has been clearly demonstrated that ABA acts as a negative regulator of axillary bud growth in Arabidopsis plants, in which elevated ABA levels were associated with bud dormancy (Yao and Finlayson 2015). To examine the ABA status in axillary buds and to confirm the late-tillering phenotype in LOHi236/272 lines (Figures 7 and 8), the transcript levels of *HvABA 8'-hydroxylase 1/3* were also analyzed in axillary buds. However, there was no significant difference between LOHi lines and WT plants at 12 WAG or 15 WAG (Figure 12B), although in these samples gene expression was more variable due to the bulking of axillary buds with the different length. Therefore, the envisaged investigation of the ABA-SL crosstalk in this study needs to be considered in an organ-specific manner. With regard to the relatively stable promoter activity of *LeaB19.3* during the course of plant development (Figure 6), it is not yet clear why the late-tillering phenotype appeared not before 12 or 14 WAG (Figures 7 and 8). Moreover, considering that strigolactones are mostly synthesized in the root with little synthesis in the shoot (Al-Babili and Bouwmeester 2015) it remains also to be addressed whether the cross-talk between ABA and SL observed here really took place in the stem base.

The possibility that SL biosynthesis is regulated by ABA was also studied by the application of exogenous ABA to Arabidopsis plants, leading to a decrease in the transcript levels of the SL biosynthesis genes *CCD7* and *CCD8* (Ha *et al.* 2014). In agreement with this observation, the major SL 5-deoxystrigol was significantly ( $P < 0.01$ ) lower in root exudates of LOHi236 and LOHi272 compared with the wild type at 14 WAG (Figure 14B). This correlated with a clear reduction in the relative transcript levels of *HvCCD7* and *HvCCD8* in roots of LOHi236/272 lines (Figure 18C) and coincided with the late-tillering phenotype in LOHi236/272 lines. Despite this agreement between the present and previous studies, results

from experiments with exogenous ABA application may be misleading as suggested from a study on drought stress-induced ABA using luciferase-expressing ABA-reporter plants. Exposure of *Arabidopsis* seedlings to exogenous ABA resulted in a uniform pattern of reporter gene expression, whereas reporter gene expression in response to drought stress was predominantly confined to the vasculature and stomata (Christmann *et al.* 2005). Nevertheless, the present thesis is the first report on SL production in response to genetically altered ABA metabolism, allowing to consider the LOHi236/272 lines as suitable plant material to address the question how increased levels of endogenous ABA regulate SL production. Furthermore, ABA plays an important role in integrating various stress signals to modulate downstream stress responses (Tuteja 2007). Strigolactones are proposed to be responsive to environmental cues. Two reports pointed to the involvement of SL in drought tolerance using SL-deficient *Arabidopsis* mutants, but the positive regulatory role of SLs in plant responses to drought was controversial (Bu *et al.* 2014, Ha *et al.* 2014). Still, the picture is far from being complete, because SLs were not quantified under stress in either work. The relationship between ABA and SL pathways was also investigated in *Lotus japonicus* under abiotic stress. This study indicated that in *Lotus* shoots under drought stress conditions there is an elevated level of ABA, while the SL flowing acropetally decrease (Liu *et al.* 2015). Nevertheless, all of these results in this study suggested that the crosstalk between the biosynthetic pathways of ABA and SL could affect the tiller formation in LOHi lines (Figure 35).

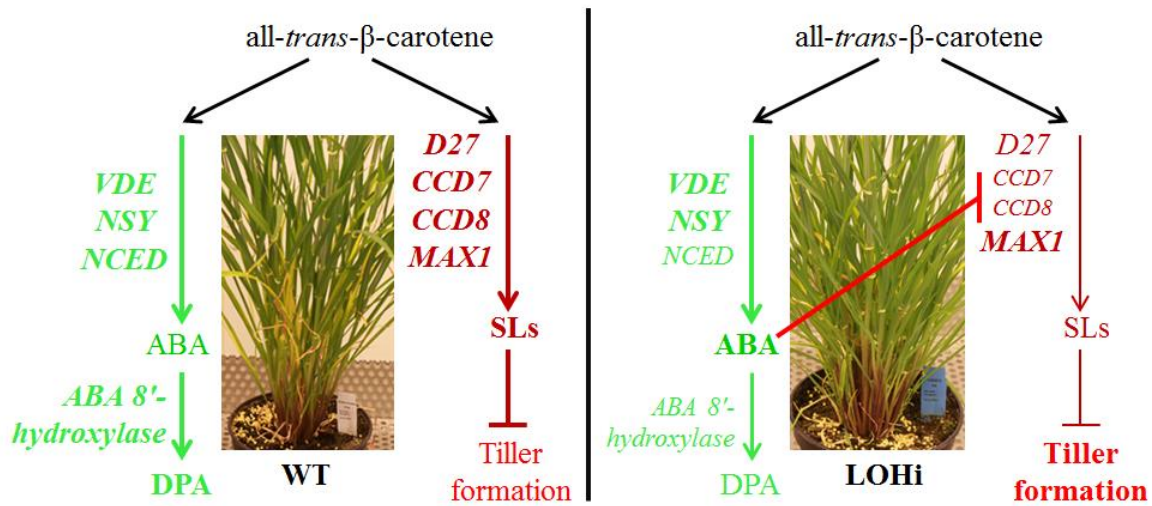


**Figure 35.** Schematic working model of the regulatory interaction between ABA and SL in tiller formation. The wild-type plants maintain hormonal homeostasis between ABA and SL, while high endogenous ABA level triggered by a transient silencing of the *ABA 8'-hydroxylase* gene represses SL biosynthesis mainly via down-regulation of *CCD7/8*, which results in low SL production, subsequently releases the inhibition of SL and finally causes a high late-tillering phenotype in LOHi lines.

## 5. Summary

Strigolactones (SLs) are considered a novel class of plant hormones acting in endogenous signaling to restrict axillary bud growth in plants. Likewise, abscisic acid (ABA) has been shown to regulate the development of lateral buds, branches and tillers. However, little is known about the crosstalk between ABA and SLs, and the effect of such interaction on tiller formation in barley. Therefore, it was the goal of the present thesis to examine the mode of interaction between ABA and SLs and the effect of this interaction on tiller formation in barley.

As a prerequisite for expression analysis of genes involved in SL biosynthesis, genomic sequences of the barley orthologs for *D27*, *CCD7*, *CCD8* and *MAX1* were identified. *D27* and *MAX1* were functionally characterized by heterologous expression in corresponding *Arabidopsis* mutants, in which they partially rescued their shoot branching phenotypes. Furthermore, virus-induced gene silencing was employed to show that *HvD27*-silenced, *HvCCD7*-silenced and *HvCCD8*-silenced plants not only showed increased tillering but also produced more additional spikelets and influenced the spikelet fertility.

To investigate cross-talk between ABA and SLs, transgenic barley lines were employed, in which the gene *HvABA 8'-hydroxylase* was silenced. This gene encodes an enzyme catalyzing the hydrolysis and thus the catabolism of ABA. The two corresponding transgenic lines LOHi236 and 272 continued tillering during the reproductive phase, resulting in enhanced tiller numbers. LC-MS/MS analysis of root and stem base tissues confirmed higher ABA levels in the two transgenic lines due to the downregulation of the two isoforms *HvABA 8'-hydroxylase 1* and *3*. In addition, concentrations of the SL 5-deoxystrigol, which could only be quantified in root exudates, were lower. Gene expression analysis further confirmed that the accumulation of ABA in the transgenic lines led to a repression of SL biosynthesis genes, in particular of *HvCCD7* and *HvCCD8*, probably as a result of a feed-back regulation by elevated ABA levels. However, the de-regulation of gene expression was only seen at 14



weeks after germination, i.e. when plants had entered booting stage, which was most likely due to the developmental regulation of the promoter activity driving the transgene.

Taken together, these results indicate that enhanced levels of endogenous ABA can decrease SL production, which triggers enhanced tillering. Thereby, this study provides first genetic evidence for a direct cross-talk between these two phytohormone classes that takes place at the level of their biosynthesis.

**Keywords:** strigolactones, abscisic acid, cross-talk, barley, tiller, ABA 8'-hydroxylase, 5-deoxystrigol

## 6. Zusammenfassung

Strigolactones (SLs) repräsentieren eine neue Klasse von Pflanzenhormonen, die über endogene Signalwege das Austreiben axillärer Seitentriebe unterdrücken. Ebenso kann Abscissinsäure (ABA) die Entwicklung von Seitenknospen und Seitentrieben beeinflussen. Bisher ist jedoch wenig über die Interaktion zwischen ABA und SLs bekannt und die Wirkung einer solchen Interaktion auf die Seitentriebbildung in Gerste. Daher war es das Ziel der vorliegenden Arbeit die Art der Interaktion zwischen ABA und SLs sowie die Wirkung dieser Interaktion auf die Seitentriebbildung in Gerste zu untersuchen.

Als Voraussetzung für die Expressionsanalyse von Genen in der SL-Biosynthese, wurden in der Gerste orthologe, genomische Sequenzen für D27, CCD7, CCD8 und MAX1 identifiziert. D27 und MAX1 wurden durch heterologe Expression in entsprechenden Arabidopsis-Mutanten funktionell charakterisiert, in denen sie teilweise die Bildung axillärer Seitentriebe wiederherstellten. Des Weiteren wurde „Virus-induced gene silencing“ eingesetzt, um zu zeigen, dass *HvD27*-reprimierte, *HvCCD7*-reprimierte und *HvCCD8*-reprimierte Pflanzen nicht nur einer verstärkte Bestockung zeigten, sondern auch zusätzliche Ährchen bildeten und die Ährchenfruchtbarkeit beeinflussten.

Um die Interaktion zwischen ABA und SLs zu untersuchen, wurden transgene Gerstenlinien verwendet, in denen das Gen *HvABA-8'-Hydroxylase* reprimiert wurde. Dieses Gen kodiert für ein Enzym, das die Hydrolyse und somit den Katabolismus von ABA katalysiert. Die beiden transgenen Linien LOHi236 und LOHi272 zeigten eine verstärkte Bestockung während der generativen Wachstumsphase, was zu einer erhöhten Anzahl von Seitentrieben führte. LC-MS-/MS-Analysen von Wurzel- und Stängelgewebe bestätigten erhöhte ABA-Konzentrationen, welche durch ein geringeres Expressionsniveau der Isoformen *HvABA-8'-Hydroxylase 1* und *3* bedingt waren. Zudem war die Konzentration des SL 5-Deoxystrigol, das nur in Wurzelexsudaten quantifiziert werden konnte, geringer. Genexpressionsanalysen zeigten weiterhin, dass die Akkumulation von ABA in den transgenen Linien zu einer Repression von Genen aus der Biosynthese von SL führte, insbesondere von

*HvCCD7* und *HvCCD8*, wahrscheinlich als Ergebnis einer Rückkopplung durch erhöhte ABA-Konzentrationen. Allerdings wurde die De-Regulierung der Genexpression nur ab der 14. Woche nach der Keimung beobachtet, d.h. als die Pflanzen im Schossen waren. Dies war höchstwahrscheinlich durch die entwicklungsabhängige Regulation des Promoters bedingt, der das Transgen kontrollierte.

Zusammengenommen zeigen diese Ergebnisse, dass erhöhte endogene Gehalte an ABA die Biosynthese von SL verringern können, wodurch die Bestockung angeregt wird. Damit liefert diese Studie den ersten genetischen Hinweis für eine direkte Interaktion zwischen diesen beiden Phytohormonklassen, die auf der Ebene ihrer Biosynthese stattfindet.

**Schlüsselwörter:** strigolactones, abscissinsäure, interaktion, gerste, pinne, ABA 8'-hydroxylase, 5-deoxystrigol

## 7. References

- Agusti, J. and Greb, T.** (2013) Going with the wind--adaptive dynamics of plant secondary meristems. *Mechanisms of development*, **130**, 34-44.
- Al-Babili, S. and Bouwmeester, H.J.** (2015) Strigolactones, a novel carotenoid-derived plant hormone. *Annual review of plant biology*, **66**, 161-186.
- Alder, A., Jamil, M., Marzorati, M., Bruno, M., Vermathen, M., Bigler, P., Ghisla, S., Bouwmeester, H., Beyer, P. and Al-Babili, S.** (2012) The path from beta-carotene to carlactone, a strigolactone-like plant hormone. *Science*, **335**, 1348-1351.
- Arend, M., Schnitzler, J.P., Ehling, B., Hansch, R., Lange, T., Rennenberg, H., Himmelbach, A., Grill, E. and Fromm, J.** (2009) Expression of the Arabidopsis mutant ABI1 gene alters abscisic acid sensitivity, stomatal development, and growth morphology in gray poplars. *Plant Physiol*, **151**, 2110-2119.
- Arite, T., Iwata, H., Ohshima, K., Maekawa, M., Nakajima, M., Kojima, M., Sakakibara, H. and Kyojuka, J.** (2007) DWARF10, an RMS1/MAX4/DAD1 ortholog, controls lateral bud outgrowth in rice. *The Plant journal : for cell and molecular biology*, **51**, 1019-1029.
- Audran, C., Liotenberg, S., Gonneau, M., North, H., Frey, A., Tap-Waksman, K., Vartanian, N. and Marion-Poll, A.** (2001) Localisation and expression of zeaxanthin epoxidase mRNA in Arabidopsis in response to drought stress and during seed development. *Aust J Plant Physiol*, **28**, 1161-1173.
- Awad, A.A., Sato, D., Kusumoto, D., Kamioka, H., Takeuchi, Y. and Yoneyama, K.** (2006) Characterization of strigolactones, germination stimulants for the root parasitic plants *Striga* and *Orobanche*, produced by maize, millet and sorghum. *Plant Growth Regul*, **48**, 221-227.
- Babb, S. and Muehlbauer, G.J.** (2003) Genetic and morphological characterization of the barley unicum2 (cul2) mutant. *TAG. Theoretical and applied genetics. Theoretische und angewandte Genetik*, **106**, 846-857.
- Bennett, T., Sieberer, T., Willett, B., Booker, J., Luschnig, C. and Leyser, O.** (2006) The Arabidopsis MAX pathway controls shoot branching by regulating auxin transport. *Current biology : CB*, **16**, 553-563.
- Bittner, F., Oreb, M. and Mendel, R.R.** (2001) ABA3 is a molybdenum cofactor sulfurase required for activation of aldehyde oxidase and xanthine dehydrogenase in Arabidopsis thaliana. *J Biol Chem*, **276**, 40381-40384.

- Booker, J., Auldridge, M., Wills, S., McCarty, D., Klee, H. and Leyser, O. (2004)** MAX3/CCD7 is a carotenoid cleavage dioxygenase required for the synthesis of a novel plant signaling molecule. *Current Biology*, **14**, 1232-1238.
- Booker, J., Sieberer, T., Wright, W., Williamson, L., Willett, B., Stirnberg, P., Turnbull, C., Srinivasan, M., Goddard, P. and Leyser, O. (2005).** MAX1 encodes a cytochrome P450 family member that acts downstream of MAX3/4 to produce a carotenoid-derived branch-inhibiting hormone. *Developmental cell*, **8**, 443-449.
- Brewer, P.B., Dun, E.A., Ferguson, B.J., Rameau, C. and Beveridge, C.A. (2009)** Strigolactone acts downstream of auxin to regulate bud outgrowth in pea and Arabidopsis. *Plant Physiol*, **150**, 482-493.
- Brewer, P.B., Koltai, H. and Beveridge, C.A. (2013)** Diverse roles of strigolactones in plant development. *Molecular plant*, **6**, 18-28.
- Bruno, M. and Al-Babili, S. (2016)** On the substrate specificity of the rice strigolactone biosynthesis enzyme DWARF27. *Planta*, 1-12.
- Bruun-Rasmussen, M., Madsen, C. T., Jessing, S. and Albrechtsen, M. (2007).** Stability of Barley stripe mosaic virus-induced gene silencing in barley. *Molecular Plant-Microbe Interactions*, **20**, 1323-1331.
- Bu, Q., Lv, T., Shen, H., Luong, P., Wang, J., Wang, Z., Huang, Z., Xiao, L., Engineer, C., Kim, T.H., Schroeder, J.I. and Huq, E. (2014)** Regulation of drought tolerance by the F-box protein MAX2 in Arabidopsis. *Plant Physiol*, **164**, 424-439.
- Cardoso, C., Zhang, Y.X., Jamil, M., Hepworth, J., Charnikhova, T., Dimkpa, S.O.N., Meharg, C., Wright, M.H., Liu, J.W., Meng, X.B., Wang, Y.H., Li, J.Y., McCouch, S.R., Leyser, O., Price, A.H., Bouwmeester, H.J. and Ruyter-Spira, C. (2014)** Natural variation of rice strigolactone biosynthesis is associated with the deletion of two MAX1 orthologs. *Proceedings of the National Academy of Sciences of the United States of America*, **111**, 2379-2384.
- Chatfield, S.P., Stirnberg, P., Forde, B.G. and Leyser, O. (2000)** The hormonal regulation of axillary bud growth in Arabidopsis. *The Plant journal : for cell and molecular biology*, **24**, 159-169.
- Cheng, W.H., Endo, A., Zhou, L., Penney, J., Chen, H.C., Arroyo, A., Leon, P., Nambara, E., Asami, T., Seo, M., Koshiba, T. and Sheen, J. (2002)** A unique short-chain dehydrogenase/reductase in Arabidopsis glucose signaling and abscisic acid biosynthesis and functions. *The Plant cell*, **14**, 2723-2743.
- Cheng, X., Ruyter-Spira, C. and Bouwmeester, H. (2013)** The interaction between

- strigolactones and other plant hormones in the regulation of plant development. *Front Plant Sci*, **4**.
- Chernys, J.T. and Zeevaart, J.A.** (2000) Characterization of the 9-cis-epoxycarotenoid dioxygenase gene family and the regulation of abscisic acid biosynthesis in avocado. *Plant Physiol*, **124**, 343-353.
- Chetty, V.J., Ceballos, N., Garcia, D., Narvaez-Vasquez, J., Lopez, W. and Orozco-Cardenas, M.L.** (2013) Evaluation of four *Agrobacterium tumefaciens* strains for the genetic transformation of tomato (*Solanum lycopersicum* L.) cultivar Micro-Tom. *Plant cell reports*, **32**, 239-247.
- Chong, L.** (2001) Molecular cloning - A laboratory manual, 3rd edition. *Science*, **292**, 446-446.
- Christmann, A., Hoffmann, T., Teplova, I., Grill, E. and Muller, A.** (2005) Generation of active pools of abscisic acid revealed by in vivo imaging of water-stressed *Arabidopsis*. *Plant Physiol*, **137**, 209-219.
- Cline, M.G. and Oh, C.** (2006) A reappraisal of the role of abscisic acid and its interaction with auxin in apical dominance. *Annals of botany*, **98**, 891-897.
- Clough, S.J. and Bent, A.F.** (1998) Floral dip: a simplified method for *Agrobacterium*-mediated transformation of *Arabidopsis thaliana*. *The Plant journal : for cell and molecular biology*, **16**, 735-743.
- Counce, P.A., Siebenmorgen, T.J., Poag, M.A., Holloway, G.E., Kocher, M.F. and Lu, R.F.** (1996) Panicle emergence of tiller types and grain yield of tiller order for direct-seeded rice cultivars. *Field Crop Res*, **47**, 235-242.
- Cutler, S.R., Rodriguez, P.L., Finkelstein, R.R. and Abrams, S.R.** (2010) Abscisic acid: emergence of a core signaling network. *Annual review of plant biology*, **61**, 651-679.
- Dabbert, T., Okagaki, R.J., Cho, S., Boddu, J. and Muehlbauer, G.J.** (2009) The genetics of barley low-tillering mutants: absent lower laterals (als). *TAG. Theoretical and applied genetics. Theoretische und angewandte Genetik*, **118**, 1351-1360.
- Dabbert, T., Okagaki, R.J., Cho, S., Heinen, S., Boddu, J. and Muehlbauer, G.J.** (2010) The genetics of barley low-tillering mutants: low number of tillers-1 (lnt1). *TAG. Theoretical and applied genetics. Theoretische und angewandte Genetik*, **121**, 705-715.
- DeCook, R., Lall, S., Nettleton, D. and Howell, S.H.** (2006) Genetic regulation of gene expression during shoot development in *Arabidopsis*. *Genetics*, **172**, 1155-1164.

- Domagalska, M.A. and Leyser, O.** (2011) Signal integration in the control of shoot branching. *Nature reviews. Molecular cell biology*, **12**, 211-221.
- Drummond, R.S.M., Martinez-Sanchez, N.M., Janssen, B.J., Templeton, K.R., Simons, J.L., Quinn, B.D., Karunairetnam, S. and Snowden, K.C.** (2009) Petunia hybrida CAROTENOID CLEAVAGE DIOXYGENASE7 Is Involved in the Production of Negative and Positive Branching Signals in Petunia. *Plant Physiol*, **151**, 1867-1877.
- Dun, E.A., de Saint Germain, A., Rameau, C. and Beveridge, C.A.** (2012) Antagonistic action of strigolactone and cytokinin in bud outgrowth control. *Plant Physiol*, **158**, 487-498.
- Endo A, Okamoto M and Koshiba T.** (2014) ABA Biosynthetic and Catabolic Pathways. In Abscisic Acid: Metabolism, Transport and Signaling (pp. 21-45). Springer Netherlands.
- FAOSTAT** (2013) <http://faostat.fao.org/>
- Ferguson, B.J. and Beveridge, C.A.** (2009) Roles for auxin, cytokinin, and strigolactone in regulating shoot branching. *Plant Physiol*, **149**, 1929-1944.
- Gocal, G.F., Pharis, R.P., Yeung, E.C. and Pearce, D.** (1991) Changes after Decapitation in Concentrations of Indole-3-Acetic Acid and Abscisic Acid in the Larger Axillary Bud of Phaseolus vulgaris L. cv Tender Green. *Plant Physiol*, **95**, 344-350.
- Gomez-Roldan, V., Fermas, S., Brewer, P.B., Puech-Pages, V., Dun, E.A., Pillot, J.P., Letisse, F., Matusova, R., Danoun, S., Portais, J.C., Bouwmeester, H., Becard, G., Beveridge, C.A., Rameau, C. and Rochange, S.F.** (2008) Strigolactone inhibition of shoot branching. *Nature*, **455**, 189-194.
- Gonzalez-Grandio, E., Poza-Carrion, C., Sorzano, C.O. and Cubas, P.** (2013) BRANCHED1 promotes axillary bud dormancy in response to shade in Arabidopsis. *The Plant cell*, **25**, 834-850.
- Gonzalez-Guzman, M., Apostolova, N., Belles, J.M., Barrero, J.M., Piqueras, P., Ponce, M.R., Micol, J.L., Serrano, R. and Rodriguez, P.L.** (2002) The short-chain alcohol dehydrogenase ABA2 catalyzes the conversion of xanthoxin to abscisic aldehyde. *The Plant cell*, **14**, 1833-1846.
- Grant, S.G.N., Jessee, J., Bloom, F.R. and Hanahan, D.** (1990) Differential Plasmid Rescue from Transgenic Mouse Dnas into Escherichia-Coli Methylation-Restriction Mutants. *Proceedings of the National Academy of Sciences of the United States of America*, **87**, 4645-4649.

- Greb, T., Clarenz, O., Schafer, E., Muller, D., Herrero, R., Schmitz, G. and Theres, K.** (2003) Molecular analysis of the LATERAL SUPPRESSOR gene in Arabidopsis reveals a conserved control mechanism for axillary meristem formation. *Genes & development*, **17**, 1175-1187.
- Guo, D., Zhang, J., Wang, X., Han, X., Wei, B., Wang, J., Li, B., Yu, H., Huang, Q., Gu, H., Qu, L.J. and Qin, G.** (2015) The WRKY Transcription Factor WRKY71/EXB1 Controls Shoot Branching by Transcriptionally Regulating RAX Genes in Arabidopsis. *The Plant cell*, **27**, 3112-3127.
- Ha, C.V., Leyva-Gonzalez, M.A., Osakabe, Y., Tran, U.T., Nishiyama, R., Watanabe, Y., Tanaka, M., Seki, M., Yamaguchi, S., Dong, N.V., Yamaguchi-Shinozaki, K., Shinozaki, K., Herrera-Estrella, L. and Tran, L.S.** (2014) Positive regulatory role of strigolactone in plant responses to drought and salt stress. *Proceedings of the National Academy of Sciences of the United States of America*, **111**, 851-856.
- Hamiaux, C., Drummond, R. S., Janssen, B. J., Ledger, S. E., Cooney, J. M., Newcomb, R. D. and Snowden, K. C.** (2012) DAD2 is an  $\alpha/\beta$  hydrolase likely to be involved in the perception of the plant branching hormone, strigolactone. *Current Biology*, **22**, 2032-2036.
- Hayward, A., Stirnberg, P., Beveridge, C. and Leyser, O.** (2009) Interactions between Auxin and Strigolactone in Shoot Branching Control. *Plant Physiol*, **151**, 400-412.
- Holzberg, S., Brosio, P., Gross, C. and Pogue, G.P.** (2002) Barley stripe mosaic virus-induced gene silencing in a monocot plant. *The Plant journal : for cell and molecular biology*, **30**, 315-327.
- Hussien, A., Tavakol, E., Horner, D.S., Munoz-Amatriain, M., Muehlbauer, G.J. and Rossini, L.** (2014) Genetics of Tillering in Rice and Barley. *Plant Genome-Us*, **7**.
- Ishikawa S., Maekawa M., Arite T., Onishi K., Takamure I., Kyojuka J.** (2005) Suppression of tiller bud activity in tillering dwarf mutants of rice. *Plant Cell Physiol*, **46**, 79-86.
- Iuchi, S., Kobayashi, M., Taji, T., Naramoto, M., Seki, M., Kato, T., Tabata, S., Kakubari, Y., Yamaguchi-Shinozaki, K. and Shinozaki, K.** (2001) Regulation of drought tolerance by gene manipulation of 9-cis-epoxycarotenoid dioxygenase, a key enzyme in abscisic acid biosynthesis in Arabidopsis. *The Plant journal : for cell and molecular biology*, **27**, 325-333.
- Jamil, M., Charnikhova, T., Houshyani, B., van Ast, A. and Bouwmeester, H.J.** (2012) Genetic variation in strigolactone production and tillering in rice and its effect on *Striga hermonthica* infection. *Planta*, **235**, 473-484.



- Janssen, B.J. and Snowden, K.C.** (2012) Strigolactone and karrikin signal perception: receptors, enzymes, or both? *Front Plant Sci*, **3**, 296.
- Jiahn Ch. G., Karen E. Koch, Masaharu S., Shan W., Susan L., Tanya P., Charles G., Harry J. K., and Donald R. Mc.**(2012) Diverse Roles of Strigolactone Signaling in Maize Architecture and the Uncoupling of a Branching-Specific Subnetwork. *Plant physiology*, **160**, 1303-1317.
- Jiang, L., Liu, X., Xiong, G., Liu, H., Chen, F., Wang, L., Meng, X., Liu, G., Yu, H., Yuan, Y., Yi, W., Zhao, L., Ma, H., He, y., Wu, Z., Melicher, K., Q.Q., Xu, H., Wang, Y., Li, J.** (2013). DWARF 53 acts as a repressor of strigolactone signaling in rice. *Nature*, **504**, 401-405.
- Jiao, Y., Wang, Y., Xue, D., Wang, J., Yan, M., Liu, G., Dong, G., Zeng, D., Lu, Z., Zhu, X., Qian, Q. and Li, J.** (2010) Regulation of OsSPL14 by OsmiR156 defines ideal plant architecture in rice. *Nature genetics*, **42**, 541-544.
- Johnson, X., Brcich, T., Dun, E.A., Goussot, M., Haurogne, K., Beveridge, C.A. and Rameau, C.** (2006) Branching genes are conserved across species. Genes controlling a novel signal in pea are coregulated by other long-distance signals. *Plant Physiol*, **142**, 1014-1026.
- Kebrom, T.H., Spielmeyer, W. and Finnegan, E.J.** (2013) Grasses provide new insights into regulation of shoot branching. *Trends in plant science*, **18**, 41-48.
- Keller, T., Abbott, J., Moritz, T. and Doerner, P.** (2006) Arabidopsis REGULATOR OF AXILLARY MERISTEMS1 controls a leaf axil stem cell niche and modulates vegetative development. *The Plant cell*, **18**, 598-611.
- Kirby E. J. M., Appleyard M.** (1987). Cereal Development Guide. Kenilworth: Arable Unit.
- Knox, J.P. and Wareing, P.F.** (1984) Apical Dominance in Phaseolus-Vulgaris L - the Possible Roles of Abscisic and Indole-3-Acetic-Acid. *J Exp Bot*, **35**, 239-244.
- Komatsuda, T., Pourkheirandish, M., He, C., Azhaguvel, P., Kanamori, H., Perovic, D., Stein, N., Graner, A., Wicker, T., Tagiri, A., Lundqvist, U., Fujimura, T., Matsuoka, M., Matsumoto, T. and Yano, M.** (2007) Six-rowed barley originated from a mutation in a homeodomain-leucine zipper I-class homeobox gene. *Proceedings of the National Academy of Sciences of the United States of America*, **104**, 1424-1429.
- Kong, L.S., Abrams, S.R., Owen, S.J., Graham, H. and von Aderkasi, P.** (2008) Phytohormones and their metabolites during long shoot development in Douglas-fir

- following cone induction by gibberellin injection. *Tree Physiol*, **28**, 1357-1364.
- Koornneef, M., Jorna, M.L., Brinkhorst-van der Swan, D.L. and Karssen, C.M.** (1982) The isolation of abscisic acid (ABA) deficient mutants by selection of induced revertants in non-germinating gibberellin sensitive lines of *Arabidopsis thaliana* (L.) heynh. *TAG. Theoretical and applied genetics. Theoretische und angewandte Genetik*, **61**, 385-393.
- Koornneef, M., Leon-Kloosterziel, K.M., Schwartz, S.H. and Zeevaart, J.A.D.** (1998) The genetic and molecular dissection of abscisic acid biosynthesis and signal transduction in *Arabidopsis*. *Plant Physiol Bioch*, **36**, 83-89.
- Koppolu, R., Anwar, N., Sakuma, S., Tagiri, A., Lundqvist, U., Pourkheirandish, M., Rutten, T., Seiler, C., Himmelbach, A., Ariyadasa, R., Youssef, H.M., Stein, N., Sreenivasulu, N., Komatsuda, T. and Schnurbusch, T.** (2013) Six-rowed spike4 (Vrs4) controls spikelet determinacy and row-type in barley. *Proceedings of the National Academy of Sciences of the United States of America*, **110**, 13198-13203.
- Le Bris, M., Michaux-Ferriere, N., Jacob, Y., Poupet, A., Barthe, P., Guigonis, J.M. and Le Page-Degivry, M.T.** (1999) Regulation of bud dormancy by manipulation of ABA in isolated buds of *Rosa hybrida* cultured in vitro. *Aust J Plant Physiol*, **26**, 273-281.
- Li, X., Qian, Q., Fu, Z., Wang, Y., Xiong, G., Zeng, D., Wang, X., Liu, X., Teng, S., Hiroshi, F., Yuan, M., Luo, D., Han, B. and Li, J.** (2003) Control of tillering in rice. *Nature*, **422**, 618-621.
- Lichtenthaler, H.K.** (1999) The 1-Deoxy-D-Xylulose-5-Phosphate Pathway of Isoprenoid Biosynthesis in Plants. *Annual review of plant physiology and plant molecular biology*, **50**, 47-65.
- Liller, C.B., Neuhaus, R., von Korff, M., Koornneef, M. and van Esse, W.** (2015) Mutations in Barley Row Type Genes Have Pleiotropic Effects on Shoot Branching. *Plos One*, **10**.
- Lin, H., Wang, R., Qian, Q., Yan, M., Meng, X., Fu, Z., Yan, C., Jiang, B., Su, Z., Li, J. and Wang, Y.** (2009) DWARF27, an iron-containing protein required for the biosynthesis of strigolactones, regulates rice tiller bud outgrowth. *The Plant cell*, **21**, 1512-1525.
- Liu, J., He, H., Vitali, M., Visentin, I., Charnikhova, T., Haider, I., Schubert, A., Ruyter-Spira, C., Bouwmeester, H.J., Lovisolo, C. and Cardinale, F.** (2015) Osmotic stress represses strigolactone biosynthesis in *Lotus japonicus* roots: exploring the interaction between strigolactones and ABA under abiotic stress. *Planta*, **241**, 1435-1451

- Liu, W., Kohlen, W., Lillo, A., Op den Camp, R., Ivanov, S., Hartog, M., Limpens, E., Jamil, M., Smaczniak, C., Kaufmann, K., Yang, W.C., Hooiveld, G.J., Charnikhova, T., Bouwmeester, H.J., Bisseling, T. and Geurts, R.** (2011) Strigolactone biosynthesis in *Medicago truncatula* and rice requires the symbiotic GRAS-type transcription factors NSP1 and NSP2. *The Plant cell*, **23**, 3853-3865.
- Ljung, K., Bhalerao, R.P. and Sandberg, G.** (2001) Sites and homeostatic control of auxin biosynthesis in *Arabidopsis* during vegetative growth. *The Plant journal : for cell and molecular biology*, **28**, 465-474.
- Lopez-Raez, J.A., Kohlen, W., Charnikhova, T., Mulder, P., Undas, A.K., Sergeant, M.J., Verstappen, F., Bugg, T.D.H., Thompson, A.J., Ruyter-Spira, C. and Bouwmeester, H.** (2010) Does abscisic acid affect strigolactone biosynthesis? *New Phytologist*, **187**, 343-354.
- Mader, J.C., Emery, R.J.N. and Turnbull, C.G.N.** (2003) Spatial and temporal changes in multiple hormone groups during lateral bud release shortly following apex decapitation of chickpea (*Cicer arietinum*) seedlings. *Physiol Plantarum*, **119**, 295-308.
- Marin, E., Nussaume, L., Quesada, A., Gonneau, M., Sotta, B., Hugueney, P., Frey, A. and Marion-Poll, A.** (1996) Molecular identification of zeaxanthin epoxidase of *Nicotiana plumbaginifolia*, a gene involved in abscisic acid biosynthesis and corresponding to the ABA locus of *Arabidopsis thaliana*. *The EMBO journal*, **15**, 2331-2342.
- McSteen, P. and Leyser, O.** (2005) Shoot branching. *Annual review of plant biology*, **56**, 353-374.
- Muller, D. and Leyser, O.** (2011) Auxin, cytokinin and the control of shoot branching. *Annals of botany*, **107**, 1203-1212.
- Muller, D., Schmitz, G. and Theres, K.** (2006) Blind homologous R2R3 Myb genes control the pattern of lateral meristem initiation in *Arabidopsis*. *The Plant cell*, **18**, 586-597.
- Nambara, E. and Marion-Poll, A.** (2005) Abscisic acid biosynthesis and catabolism. *Annual review of plant biology*, **56**, 165-185.
- Oikawa, T. and Kyojuka, J.** (2009) Two-Step Regulation of LAX PANICLE1 Protein Accumulation in Axillary Meristem Formation in Rice. *The Plant cell*, **21**, 1095-1108.
- Pacak, A., Geisler, K., Jorgensen, B., Barciszewska-Pacak, M., Nilsson, L., Nielsen, T.H., Johansen, E., Gronlund, M., Jakobsen, I. and Albrechtsen, M.** (2010)

Investigations of barley stripe mosaic virus as a gene silencing vector in barley roots and in *Brachypodium distachyon* and oat. *Plant Methods*, **6**.

- Pallotta, M.A., Graham, R.D., Langridge, P., Sparrow, D.H.B. and Barker, S.J.** (2000) RFLP mapping of manganese efficiency in barley. *Theoretical and Applied Genetics*, **101**, 1100-1108.
- Prusinkiewicz, P., Crawford, S., Smith, R.S., Ljung, K., Bennett, T., Ongaro, V. and Leyser, O.** (2009) Control of bud activation by an auxin transport switch. *Proceedings of the National Academy of Sciences of the United States of America*, **106**, 17431-17436.
- Qin, X. and Zeevaart, J.A.** (2002) Overexpression of a 9-cis-epoxycarotenoid dioxygenase gene in *Nicotiana plumbaginifolia* increases abscisic acid and phaseic acid levels and enhances drought tolerance. *Plant Physiol*, **128**, 544-551.
- Raman, S., Greb, T., Peaucelle, A., Blein, T., Laufs, P. and Theres, K.** (2008) Interplay of miR164, CUP-SHAPED COTYLEDON genes and LATERAL SUPPRESSOR controls axillary meristem formation in *Arabidopsis thaliana*. *The Plant journal : for cell and molecular biology*, **55**, 65-76.
- Ramsay, L., Comadran, J., Druka, A., Marshall, D.F., Thomas, W.T., Macaulay, M., MacKenzie, K., Simpson, C., Fuller, J., Bonar, N., Hayes, P.M., Lundqvist, U., Franckowiak, J.D., Close, T.J., Muehlbauer, G.J. and Waugh, R.** (2011) INTERMEDIUM-C, a modifier of lateral spikelet fertility in barley, is an ortholog of the maize domestication gene TEOSINTE BRANCHED 1. *Nature genetics*, **43**, 169-172.
- Rani, K., Zwanenburg, B., Sugimoto, Y., Yoneyama, K. and Bouwmeester, H.J.** (2008) Biosynthetic considerations could assist the structure elucidation of host plant produced rhizosphere signalling compounds (strigolactones) for arbuscular mycorrhizal fungi and parasitic plants. *Plant Physiol Bioch*, **46**, 617-626.
- Ray, D.K., Ramankutty, N., Mueller, N.D., West, P.C. and Foley, J.A.** (2012) Recent patterns of crop yield growth and stagnation. *Nature communications*, **3**, 1293.
- Schmittgen, T.D. and Livak, K.J.** (2008) Analyzing real-time PCR data by the comparative C-T method. *Nat Protoc*, **3**, 1101-1108.
- Schmitz, G. and Theres, K.** (2005) Shoot and inflorescence branching. *Current opinion in plant biology*, **8**, 506-511.
- Schmitz, G., Tillmann, E., Carriero, F., Fiore, C., Cellini, F. and Theres, K.** (2002) The tomato Blind gene encodes a MYB transcription factor that controls the formation of

- lateral meristems. *Proceedings of the National Academy of Sciences of the United States of America*, **99**, 1064-1069.
- Schwartz, S.H., Leon-Kloosterziel, K.M., Koornneef, M. and Zeevaart, J.A.** (1997a) Biochemical characterization of the *aba2* and *aba3* mutants in *Arabidopsis thaliana*. *Plant Physiol*, **114**, 161-166.
- Schwartz, S.H., Qin, X. and Zeevaart, J.A.** (2003) Elucidation of the indirect pathway of abscisic acid biosynthesis by mutants, genes, and enzymes. *Plant Physiol*, **131**, 1591-1601.
- Schwartz, S.H., Tan, B.C., Gage, D.A., Zeevaart, J.A. and McCarty, D.R.** (1997b) Specific oxidative cleavage of carotenoids by VP14 of maize. *Science*, **276**, 1872-1874.
- Seiler, C., Harshavardhan, V.T., Rajesh, K., Reddy, P.S., Strickert, M., Rolletschek, H., Scholz, U., Wobus, U. and Sreenivasulu, N.** (2011) ABA biosynthesis and degradation contributing to ABA homeostasis during barley seed development under control and terminal drought-stress conditions. *J Exp Bot*, **62**, 2615-2632.
- Seiler, C., Harshavardhan, V.T., Reddy, P.S., Hensel, G., Kumlehn, J., Eschen-Lippold, L., Rajesh, K., Korzun, V., Wobus, U., Lee, J., Selvaraj, G. and Sreenivasulu, N.** (2014) Abscisic acid flux alterations result in differential abscisic acid signaling responses and impact assimilation efficiency in barley under terminal drought stress. *Plant Physiol*, **164**, 1677-1696.
- Seo, M., Hanada, A., Kuwahara, A., Endo, A., Okamoto, M., Yamauchi, Y., North, H., Marion-Poll, A., Sun, T.P., Koshihara, T., Kamiya, Y., Yamaguchi, S. and Nambara, E.** (2006) Regulation of hormone metabolism in *Arabidopsis* seeds: phytochrome regulation of abscisic acid metabolism and abscisic acid regulation of gibberellin metabolism. *The Plant journal : for cell and molecular biology*, **48**, 354-366.
- Seto, Y. and Yamaguchi, S.** (2014) Strigolactone biosynthesis and perception. *Current opinion in plant biology*, **21**, 1-6.
- Simons, J.L., Napoli, C.A., Janssen, B.J., Plummer, K.M. and Snowden, K.C.** (2007) Analysis of the DECREASED APICAL DOMINANCE genes of petunia in the control of axillary branching. *Plant Physiol*, **143**, 697-706.
- Sorefan, K., Booker, J., Haurogne, K., Goussot, M., Bainbridge, K., Foo, E., Chatfield, S., Ward, S., Beveridge, C., Rameau, C. and Leyser, O.** (2003) MAX4 and RMS1 are orthologous dioxygenase-like genes that regulate shoot branching in *Arabidopsis* and pea. *Genes & development*, **17**, 1469-1474.

- Sreenivasulu, N. and Schnurbusch, T.** (2012) A genetic playground for enhancing grain number in cereals. *Trends in plant science*, **17**, 91-101.
- Stirnberg, P., Furner, I. J. and Ottoline Leyser, H. M.** (2007) MAX2 participates in an SCF complex which acts locally at the node to suppress shoot branching. *The Plant Journal*, **50**, 80-94.
- Sussex, I.M.** (1989) Developmental programming of the shoot meristem. *Cell*, **56**, 225-229.
- Tamas, I.A., Ozbun, J.L. and Wallace, D.H.** (1979) Effect of Fruits on Dormancy and Abscisic Acid Concentration in the Axillary Buds of *Phaseolus vulgaris* L. *Plant Physiol*, **64**, 615-619.
- Tamura, K., Stecher, G., Peterson, D., Filipinski, A. and Kumar, S.** (2013) MEGA6: Molecular Evolutionary Genetics Analysis version 6.0. *Molecular biology and evolution*, **30**, 2725-2729.
- Tan, B.C., Joseph, L.M., Deng, W.T., Liu, L., Li, Q.B., Cline, K. and McCarty, D.R.** (2003) Molecular characterization of the Arabidopsis 9-cis epoxycarotenoid dioxygenase gene family. *The Plant journal : for cell and molecular biology*, **35**, 44-56.
- Tavakol, E., Tavakol, E., Verderio, G., Shariati, J.V., Hussien, A., Bilgic, H., Scanlon, M.J., Todt, N.R., Close, T.J., Druka, A., Waugh, R., Steuernagel, B., Ariyadasa, R., Himmelbach, A., Stein, N., Muehlbauer, G.J. and Rossini, L.** (2015) The Barley Uniculme4 Gene Encodes a BLADE-ON-PETIOLE-Like Protein That Controls Tillering and Leaf Patterning. *Plant Physiol*, **168**, 164-U877.
- Tilman, D., Balzer, C., Hill, J. and Befort, B.L.** (2011) Global food demand and the sustainable intensification of agriculture. *Proceedings of the National Academy of Sciences of the United States of America*, **108**, 20260-20264.
- Tucker, D.J.** (1977) Effects of Far-Red Light on Lateral Bud Outgrowth in Decapitated Tomato Plants and Associated Changes in Levels of Auxin and Abscisic-Acid. *Plant Sci Lett*, **8**, 339-344.
- Tucker, D.J. and Mansfield, T.A.** (1971) Effects of light quality on apical dominance in *Xanthium strumarium* and the associated changes in endogenous levels of abscisic acid and cytokinins. *Planta*, **102**, 140-151.
- Tuteja, N.** (2007) Abscisic Acid and abiotic stress signaling. *Plant signaling & behavior*, **2**, 135-138.
- Umehara, M., Hanada, A., Yoshida, S., Akiyama, K., Arite, T., Takeda-Kamiya, N.,**

- Magome, H., Kamiya, Y., Shirasu, K., Yoneyama, K., Kyojuka, J. and Yamaguchi, S.** (2008) Inhibition of shoot branching by new terpenoid plant hormones. *Nature*, **455**, 195-200.
- Waters, M.T., Brewer, P.B., Bussell, J.D., Smith, S.M. and Beveridge, C.A.** (2012) The Arabidopsis ortholog of rice DWARF27 acts upstream of MAX1 in the control of plant development by strigolactones. *Plant Physiol*, **159**, 1073-1085.
- Wen, C., Zhao, Q., Nie, J., Liu, G., Shen, L., Cheng, C., Xi, L., Ma, N. and Zhao, L.** (2016) Physiological controls of chrysanthemum DgD27 gene expression in regulation of shoot branching. *Plant cell reports*, **35**, 1053-1070.
- Xie, X., Yoneyama, K. and Yoneyama, K.** (2010) The strigolactone story. *Annual review of phytopathology*, **48**, 93-117.
- Yao, C. and Finlayson, S.A.** (2015) Abscisic Acid Is a General Negative Regulator of Arabidopsis Axillary Bud Growth. *Plant Physiol*, **169**, 611-626.
- Yoneyama, K., Xie, X.N., Kusumoto, D., Sekimoto, H., Sugimoto, Y., Takeuchi, Y. and Yoneyama, K.** (2007) Nitrogen deficiency as well as phosphorus deficiency in sorghum promotes the production and exudation of 5-deoxystrigol, the host recognition signal for arbuscular mycorrhizal fungi and root parasites. *Planta*, **227**, 125-132.
- Yoneyama, K., Xie, X., Yoneyama, K. and Takeuchi, Y.** (2009) Strigolactones: structures and biological activities. *Pest Manag Sci*, **65**, 467-470.
- Zhang, Y., van Dijk, A.D., Scaffidi, A., Flematti, G.R., Hofmann, M., Charnikhova, T., Verstappen, F., Hepworth, J., van der Krol, S., Leyser, O., Smith, S.M., Zwanenburg, B., Al-Babili, S., Ruyter-Spira, C. and Bouwmeester, H.J.** (2014) Rice cytochrome P450 homologs catalyze distinct steps in strigolactone biosynthesis. *Nature chemical biology*, **10**, 1028-1033.
- Zheng, K., Wang, X., Weighill, D.A., Guo, H.B., Xie, M., Yang, Y., Yang, J., Wang, S., Jacobson, D.A., Guo, H., Muchero, W., Tuskan, G.A. and Chen, J.G.** (2016) Characterization of DWARF14 Genes in Populus. *Scientific reports*, **6**, 21593.
- Zimmermann, P., Hennig, L. and Gruijssem, W.** (2005) Gene-expression analysis and network discovery using Genevestigator. *Trends in plant science*, **10**, 407-409.
- Zou, J., Abrams, G.D., Barton, D.L., Taylor, D.C., Pomeroy, M.K. and Abrams, S.R.** (1995) Induction of Lipid and Oleosin Biosynthesis by (+)-Abscisic Acid and Its Metabolites in Microspore-Derived Embryos of Brassica napus L.cv Reston (Biological Responses in the Presence of 8[prime]-Hydroxyabscisic Acid). *Plant*

*Physiol*, **108**, 563-571.

**Zou, J.H., Zhang, S.Y., Zhang, W.P., Li, G., Chen, Z.X., Zhai, W.X., Zhao, X.F., Pan, X.B., Xie, Q. and Zhu, L.H.** (2006) The rice HIGH-TILLERING DWARF1 encoding an ortholog of Arabidopsis MAX3 is required for negative regulation of the outgrowth of axillary buds. *Plant Journal*, **48**, 687-696.

**Zhou, R., Cutler, A.J., Ambrose, S.J., Galka, M.M., Nelson, K.M., Squires, T.M., Loewen, M.K., Jadhav, A.S., Ross, A.R., Taylor, D.C. and Abrams, S.R.** (2004) A new abscisic acid catabolic pathway. *Plant Physiol*, **134**, 361-369.

**Zwanenburg, B., Mwakaboko, A.S., Reizelman, A., Anilkumar, G. and Sethumadhavan, D.** (2009) Structure and function of natural and synthetic signalling molecules in parasitic weed germination. *Pest Manag Sci*, **65**, 478-491.



## 8. Appendix

### A. Nucleotide sequences associated with strigolactone synthesis and signaling in barley

>*HvD27*, AK358967

ATGGAGGCCACCGCACTTGTGCTCCTCCCTCACAGTCACAGCGGCCTCACGGTCA  
GAGCACCGTCTTCCGTGGGTGGAAGCTCCGTGACGAAGAAGAGCTACGCGAGGA  
GGATCAAGCGGAGCTCCACGGTGCAGGGGGTTCATGGCGAGGCCACAGGAGGCCA  
CTCTAGCTCGGGTCCCGGCACCGGCGCCAACAAGGCCGGTGAGAGAGACAGCCG  
CGGCAACGACGACGGTGTACCACGACACTTGGTTCGACAACCTCGCCATTGGCTA  
CCTGTCCAGGAACTTCAAGAAGCTTCCGGGATAAAGAACGGGAAACATGGCTAC  
CAAGGATTAATAGAGGCCGCTGTGGCAATCTCCAGAATCTTCAGGCTCGACACACA  
GTGCGAGATTGTGGCCGGTGTCTCGAACGAGCTATGCCAAGCTACATCGTCACAA  
TGATAAAGGTGATGATGCCACCTTCAAGATTTCCAGGGAGTACTTTGCTGCCTTC  
ACCACCATATTCTTCCCTTGGCTCGTCGGACCATGTGAGGTCAGGGAATCTGAAGT  
CGATGGAACGAGAGAGAAGAATGTGGTGTACATTCCCAAATGCAGGTTTCTGGAA  
AGCACCAACTGTGTCCGTATGTGCACGAACCTTTGCAAGATCCCATCCCAGAAGTT  
TATGCAAGATTCACCTCGGAGTTTCTGTGTACATGTCACCCAATTTTGAAGACATGA  
GCTGCGAGATGATCTTTGGACAGCAACCTCCTGAAGATGACCCAGCACTGAAGCA  
GCCCTGCTTCAGCACGAAATGTATCGCGAAGCAGGACTATGGTGTGAGTTGCTAG

>*HvCCD7*, MLOC\_55474.1

ATGATCCACGACTGGGGCTTCACCGACTCGCACTACGTCGTCCTGGGCAACAGGA  
TCAGGCTCGACATCCCGGGGTCCGGTGTGGCCATGACGGGCACGCACCCCATGAT  
CGCGGCGCTGGCGCTGGACCCGAGCAGCCGGACCACGCCGGTCTACCTGCTGCCG  
CGCTCCACGGAGGCCGTGGCCAGCGGCCCGCGACTGGACCGTGCCCGTCGAGGCG  
CCGGCGCAGATGTGGTTCGCTGCACGTCGGCAACGCCTTCGAGGAGGACAACGGC  
CGCGGCGGCCTGGACCTGCACCTGCACATGTCGGGCTGCTCCTACCACTGGTTCCA  
TTTCCACAGGATGTTCCGGTTACAACCTGGAAGAACAAGAAGCTGGACCCTTCCTTC  
ATGAACACGGTGAAGACCAAGGAGTTGCTGCCTCGGCTCGTCAAGGTGGCAATTG  
AGCTCGACAAGAGAGGAGGAGCATAACCGGAGATGCTCCGTGAAGAGACTGTCCG  
ATCAGTGGAACAGGCCGGCGGATTTCCCTGCGATAAATCCGAGCTATGCCAACAAG  
AGGAATAGGTTCAATTTACGCGGGCGCTGCATCCGGTTCGCGCAAATTAATCCCATAT  
TTCCATTTGACAGTGTGTGAAGGTTCGATGTCTCGAATGGGTCCGGCGAGGCGGGT  
GTCTTCCGAGGGCCGCAAGTTCGTCGGGGAGCCCGTCTTCATCCCCACCGGCGGT  
GGGGAGGATCACGGCTATGTTCTTCTTGTAGAGTATGCAGTCTCCGAAGACAGATG  
CCACCTGATGGTGTGGATGCAAGAAAGATAGGGAAAAGAGGTGCACTTGTGGCA  
AACTTGAAGTGCCAAAGCACCTCACCTTCCAATGGGATTCATGGGTTCTGGGC  
AGATGAA

>*HvCCD8*, MLOC\_66551.1

ATGTCCTTCGTCGGGCAAATGGCGAGCCTTTCTCCGGCAAACCTCCCTCACCGATAA  
CTCCAACACCGGCGTCGTCAGGCTCGGCGACGGCCGCGTGCTCTGCCTCACGGAG  
ACCGTCAAGGGGTCCATCGTCATCGACCCGGACACGCTGGACACGGTGAGCAAGT  
TCGAGTACGAGGACAAGCTGGGCGGGCTGATCCACTCGGCGCACCCGATCGTCAC  
CGACACCGAGTTCTGGACGCTGATCCCGGACCTGATCCGGCCCCGGCTACGTGGTG  
GCGAGGATGGAGGCCGGGAGCAACGAGAGGCAGTTCGTGGGCAGGGTGGACTGC  
CGCGGCGGACCGGCGCCCCGGGTGGGTGCACTCGTTCCCGGTCACCGAGAACTACG  
TGGTCGTGCCGGAGATGCCGCTCCGGTACTGCGCCGCGAACCTCCTACGCGCCGA  
GCCACGCCTCTCTACAAGTTCCAGTGGCACCTCGAGTCCGGGAGCTACATGCAC  
GTCATGTGCAAGGCCAGCGGCAAGATCGTGGCGAGCGTGGAGGTGCCGCCGTTTCG  
TGACGTTCCACTTCATCAACGCGTACGAGGAGAAGGACGAGGAGGGGCGTGTGA  
CGGCGATCATCGCCGACTGCTGCGAGCACAACGCCGATACTCCATCCTCGACAAC  
CTCCGTCTCCACAATCTCCGGGCATTCACCGGCGAGGACGTCCTCACCGATGCCAG  
GGTGGGGCGGTTTCAGGATACTGGACGGCAGCCCGTTCGGGGAGCTGGAGGC  
GGCGCTGGACCCGGAGGAGCACGGGCGCGGCATGGACATGTGCAGCATCAACCC  
CGCCCACCTCGGCAAGGAGTACCGCTACGCCTACGCCTGCGGCGCGCGCCGGCCC  
TGCAACTTCCCCAACACGCTCACCAAGATCGACCTGGTGGAGAAGACGGCCAAG  
AACTGGCACGAGGAGGGCGCCGTGCCGTCCGAGCCCTTCTTCGTGCCGCGCCCCG  
GCGCCGTCGAGGAAGACGACGGCGTGGCGATATCCATGGTGAGCGCCAAGGACG  
GGTCGGGCTACGCGCTGGTGCTGGACGCCAAGACCTTCAAGGAGATTGCCAGGGC  
CAAGTTCCCCTACGGGCTGCCCTACGGCTTGCACTGCTGCTGGGTGCCAGGGAC  
AAG

>*HvMAX1*, AK367034

ATGGAGGGGGCGGGAGCAGCACCAGTGTGGGGCCAGCCGCCATCGTTCCCGGCG  
ATGCTGTTACGGTGGCGGCCATGGCCGCCGGCGCGTTAGCCGTACTGTACTTCTA  
CGCGCCGTCGTGGCGCCTGCGCAGGGTCCCCGGGCCCTCGCCTACGGCCTCGTC  
GGCCACCTGCCGCTGCTGGACAAGCATGGCTCTCAGGCGTTCGGCGTCCTCGCGA  
AGAAATACGGGCCCATCTATAGGTTTTACATGGGCAGGCAGCCGCTGGTGGTGCTC  
GCGGACCCGGAGCTGTGCAGGGAGGCCGGCATCAAGAAGTTCAAGAGTATCACC  
GACAGGAGCGTGCCGGTCACCATCGCTAGCTCGCCATCCACTACAAGAGCCTCC  
TCTTACCAAAGGCTCGACATGGCAAGCCATGCGGAACGTGATCATCTCCATCTAC  
CAGCCGTCGCACCTGGCGAGCCTCATCCGGCGATCCAGCCATACATCGAGCGGG  
CGGGTAGCCTGTTCTGCCCGGCGAGGAGATCACCTTCTCCGACGTCTCCATCAGG  
CTCTTACCGACGTCATCGGCCAGGCCGCTTCGGCGTCGACTTCGGGCTCACCA  
AGGACGCCGACGACGCCGAGAAGATCATCCACGACGCGCCCCGCGACTTCATCCA  
GAAGCACCTCTACGCCACCACGTCCCTCAAGATGGACACGTCGGGCTCGCTGTCC  
ATGCTCGTCGGCACCTTCTGCGGCGCTCCAGAAGCCGCTGCGGAAGCTGATGC  
TGAGCGTGCCGGGATCCATGGACCGGCGGATGGACGACACCAACTCGGCCCTCAG  
CGGCGAGCTCGACGTTATCGTGGCGGAGCGGGCGGCGCAGGCCGACAGGGGCCA  
GAAGAACTTCTCTCCGTGCTCCTCAACGGCATCGACACCAGCGACGCCATGAGG  
AAGCTCTTACGCCGGACTACGTCAGCGCGCTCACCTACGAGCACCTGCTCGCCG

GCTCCGGCACCATGTCCTTCACGCTGTCGAGCCTGGTGTACCTCGTGTCCACGCAC  
CCGGAGGTGGAGGAGAAGCTGCTGCAGGAGATCGACGCGTTCGGGCCCCAAGGAC  
GTGGTGCCCCGACGCCGACGACCTCCGCACCAAGTTCACCTACCTGGAGCAGGTCC  
TGAAGGAGACCATGCGATACTTCCCCGGCTCCCCGGTGGTCTCAAGGGAGGCAAC  
CGCCGACGTCGAGATCGGAGGCTACCTCCTGCCCAAGGGGACGTGGGTGTGGCTG  
GCGACGGCGGTGCTGGGGAGGGACCCGGAGCAGTTCCCGGAGCCCCGAAGCGTTC  
CGGCCGGAGCGGTTTGACCCGGAGAGCGAGGAGTGCAAGAGGAGGCACCCCTAT  
GCCTACATCCCCTTCGGCATCGGCCACGGGCGTGCCCCGGCCAGAAGTTCGCGTT  
CCAGCAGCTCAAGCTCACCTCATCCACCTCTACCGCCGCTACGTCTTCAGGCACT  
CGCCCAGAATGGAGTCCCCCTGAAGCTGCAGTTCTCCATCGTCAACCACTTTAAG  
AACGGTGTCAAGCTCCAGGTCCTTGAAAGGAACAATAA

>*HvD14*, AK363454

ATGATCCGGTCCACGCATCCCCTCAGCCCCAGCAGCAGCAGCAGTAGCGGGCGGCA  
GCAGCCCGGCCCCGGCGTCCGGCTCCGGCGAGACGATGGTTCGGGGGCGCGCCGA  
GCGGGGCGAAGCTGCTGCAGATCCTGAACGTGCGGGTGGTGGGCACCGGCGAGC  
GCGTGGTGGTGTGTCGCACGGCTTCGGCACGGACCAGTCCGCGTGGAGCCGCGT  
GCTGCCGTACCTGACCCGCGACCACCGCGTGGTGTCTACGACCTCGTCTGCGCC  
GGCAGCGTCAACCCGGACCACTTCGACTTCCGCCGCTACAACAACCTGGACGCCT  
ACGTGGACGACCTGCTCTCCATCCTCGACGCGCTCCGCATCCCGCGCTGCGCCTTC  
GTCGGCCACTCCGTCTCCGCCATGATCGGCATCCTCGCCTCCATCCGCCGCCCGA  
CCTCTTCGCCAAGCTCGTCTCATCGGCGCCTCGCCTAGGTTCTTGAACGACAGCG  
ACTACCACGGCGGGTTCGAGCTGGAGCAGATCCAGCAGGTGTTTCGACGCGATGTC  
GGCCAACACTACGCGGCGTGGGCGACGGGGTACGCGCCGCTGGCGGTGGGCGCGGA  
CGTGCCGGCGGCGGTGCAGGAGTTCAGCCGGACGCTGTTCAACATGCGGCCGGAC  
ATCTCGCTCCACGTCTGCCAGAGCGTGTTCAGACCGACCTCCCGGGCGTGTGG  
GCATGGTGCAGGCGCCGTGCGTCGTGTCAGACCACCCGCGACGTCTCCGTGCC  
GGCCTCCGTGCGCGGTACCTCAAGGCCACCTCGGCGGCCGACCAACATCGAG  
CCCCTGCCGACGGAGGGCCACCTCCCCACCTCAGCGCCCCAGCCTCCTCGCCC  
AGGTGCTCCGCCGCGCGCTCGCCCGGTTCTAG

>*HvMAX2*, MLOC\_4044.5

ATGGCGGAGGCGGGGGCGTCGGCGCTGATGGACCTGCCGGAGCCGCTGCTGCTGC  
ACATCATGGGATACCTGGCGGACCCGCGGTGCGGGCACAGCGCATCGATGGCGTG  
CCGGAGGACGCTGGCGGGCGGAGCGGGCGACGCGGGCGGGCGATGGCGTCCGGGG  
GGACCCGAGGACGCCGACTTCTGCTGCTCCCGCCGGCCTTCTGCTTCCCGGCG  
CTCCGCCGCTCGACCTCTCGCTCGCCTCGCCCTGGGGCCACCCGCTGCTCTCCTC  
CGCCTCGCGGGTTCGCGGGGGCGCCCGCCTCCGCCTCCTCCAACCACCTCCCGCTC  
ACCCCGGAGGAGGCCGCGGAGCGCAACGCCTTCGTGCGCCGCCGCTCGCCGCT  
ACTTCCCCGCCGTCGCCCGCCTCGCCGTCTACTGCCGCGACCCCTCCACGCTCGCC  
AGCCTCGCCCCCTGCTGGCGCGCCACGCTCCGCGCCGTCCGCCTCGTGCCTGGC  
ACCAGCGGCCCTCGACCTCCCCGCGGGCGCGGATCTCGAGCCGCTGCTCGCCTC

CTGCCCAACCTCGCCGAGCTCGACCTCTCCGACTTCTACTGCTGGACGGAGGAC  
GTGCTGCCGGCCCTCGCCGCGCACCCCGCCGCCGCCAGGCTCACCGACCTCG  
ACCTCGGCCTCGCCGGCGCCTCCAACGGCTTCCACGCCGCCGAGCTCGGGGCCAT  
CGCCGCCGCCTGCCCCGCCCTGCGGAGGCTCGTCGCGCCCTGCGTCTTCAACCC  
CGCTACGTGACCATGTGCGGACGCAGCTCTGCTCGCGCTCGCCTCCAGCTGCCC  
CTCCTCACCGTCTGCGCCTCAGCGAGCCCTTCGAGCCGGCCTCCACCAGCCAG  
CGGGAGCAGGCGGGCATCACCGCCATGGGGCTCGTCGAGTTCTTTGCCGCGCTCC  
CTGGGCTGGAGGACCTCATGCTCGACCTCCAGCACAAATGTGCTCGAGGCAGCTCC  
GGCCATGGAGCTGCTCGCACGCAGGTGCCCGCGGATCAAGGTCCTGACATTGGGG  
TGCTTTCAGGGGTTGTGCAAGGCCGCCTGGTTGTATCTCGACGGCGTTGCGGTGTG  
CGGTGGGCTGGAGTCCCTCTGCATCAAGAATTGCGAGGATCTCACCGACGCCAGC  
CTTGGGGCGATCGGGCGTGGGTGTGGGAGGCTTGCCAAGTTTGCCATCCAAGGAT  
GCGATCTTGTCACGGCAGCTGGGATCAGGACGCTGGCGAAGGCGCTTCGGCCTAC  
ATTGAAGGAGGTTAGCGTGTGCACTGCCGGTTTCTGCACACTGCAGCCTGCCTTG  
CTGCTCTGAATCCGATACGCGATCGGATTGAGAGTCTTGAGATCAACTGTGACTGG  
GAGGAGGTTGAACAACCCAGCTCCAGCTGTGTGGCCAATGGCACAACCGGATGCG  
ATCATGAGGATGATGAGCCTGATGAAATGGCGTACCAGTCCGCGCCCAAGAAATGC  
AGGTTCTCCTACATGGAAATGGATAATTATGAAAGCTGGGAAATGCTCCGCTCACT  
CTCCCTTTGGTGCCCTGCTGGTCAGTTGCTCTCCCCGCTCATTCTGCCGGGCTCGA  
TAGCTGCCCTGTGCTTGAGAAGATCTCAATTAAGGTGGAGGGCGATCTTCGGACTT  
GTCCGCGGCCATTTACGGGTCAGCTTTTGGCTTGAGCGACCTTGAGCCTTCCAA  
GCACTGGCCAAGATGAAGCTGGACCTCAGCGAGGCGGTGGGTTATGCACTCACCG  
CGCCAACGGGGCACATGGATCTTTCACAGTGGGAGCGATTTTATTTGAGTGGCATT  
GAATCATTGCTGAGTTTGTATGAGCTGGACTACTGGCCGCCCAAGACAAGGATGT  
GAATCACCGGAGCCTGTCGCTGCCAGCGGTGCGACTGTTCCAGCACTCCATTGGA  
CTCAGGAAGCTCTTCATCCATGGCACCACACGAGCACTTCATGAGCTTCTTTCA  
GAAAATGCCAACTTTCGCGGACGTGCAGCTAAGGGAGGACTATTATCCAGCACCG  
GAGAACGACATGATGATCACAGAGATGCGGGCTGAATCTTGCTCCTCGGTTCGAGC  
AGCAGCTGAACAACCGGCAATTCGGCAAATTCCTGATTAG

>HvD53, AK372211

ATGCCACGCCGGTGCCCGCGGCGAGGCAGTGCCTGTGCGCCGGCGGCCGTGACGG  
CGCTCGACGCCGCGGTGCTCTCCGCGCGCCGCAGGGTGCACGCGCAGACCACGTC  
GCTGCACCTCGTCGCCGCGCTGCTGGCGCAGCAGGCCCCCGCCGCTCCTGCGCGAC  
GCGCTCGCGCGGGCCCGCAGCGCCGCTACTCCCCGCGCGTGCAGCTCAAGGCGC  
TCGAGCTCTGCTTCGCCGTCTCCCTCGACAGGCTCCCTCCGCTCCTCCGCGTCC  
GCGTCGACGTCGGCCTCGGGCGCGGACGAGCAGCCGGAGCCGCCCCTGTCCAAC  
TCGCTCATGGCCGCCATCAAGCGCTCGCAGGCCAACCAGCGCCGCAACCCGGACA  
CCTTCCACTTCTACCACCAGGCCGCGTTCCAGGCCGCCACCGCCGCCTCGCAGGT  
CAGGGTCGAGCTCTCGCAGCTCCTGCTCGCCATCCTCGACGACCCCGTTCGTCAGC  
CGCGTATTCGACGACGCCGGCTTCCGCAGCGCCGACATCAAGCTCGCCATCCTCCG  
CCCCGCGCCGCCATGCCGCTGCTCGGCCGCTCCCCACGCGGGCACGCCCGCCG  
CCTCTCTCCTCTGCAGCTTCGCCGCCGGCGACGACGCCGACGTGCCTTCGCCCGC

CGGGAGCGCCGCCGGCGCCGGCGAGGAGAACGGCCGCCGCATCGCCGAGATCCT  
CGCCCGGGGCGCAACCCCATGCTCGTAGGTGTTGGGGCAGCGTCCGCCGCAGCC  
GACTTCGCCCGCGGCTCGCCGTACCGCGTCCTCCCCGTCGGTCCAAACTCCATCGA  
CCAAACACAACCTCAGCGTGGCGGGCGGCGATGGCTAGCGCCACCTCCGGCCTCGTC  
ATAAGCGTCGGCGACCTCAGAGAACTGGTCCCCGATGACGGCGAGCTCCAGGAAC  
GAGGGCGCCGAGTGGTGGCGGAGGTGACGCGGGTGTGGAGACGCACAGAGAG  
GGGCGTGTCTGGGTGATGGGGTGGTTCGGCCACCTACGAGACCTACCTCACCTTCCT  
CTCCAAGTTCCCCTTGGTTGACAAGGACTGGGAGCTCCAGCTGCTGCCGATCAG  
GCGGTGCGCGCCGGAGGACTCATGCCTCCGGCAACCACGCCACCTGCTTTATCCA  
AGTCCGCTAGCTTGGTGGAAATCGTTTAGTCCTTTTGGTGGACTTGTCAACAATACCT  
ACGACTCTAACAGCCTCGCAGTGCATCCTGGCCCCAGACGCTCCGGTGTCAACA  
GTGCAATGATAGATGTGAGCAAGAAGTCACAACAATCGTTAAAGGGAGTGGCATT  
ACAGCTGACCAGGGAGGTCTGCCTTCCCTGCTTCAGAATGGCAGCATGATGGGTC  
TTAACAATGGACTTGATGTAATCAAGGTTAGAGATGATCAGATGGTGTGAAGTCA  
AAAATATTGAATCTGCAGAAGAAGTGGAACGAGTACTGCCTGCGGCTCCACCAAG  
GATCCAGAGGATCAACACAGGTCTTACCAGTTATTTCCAAATTATGCTGCTGTTC  
CAGTTGACACAGAAAGAGCAACAATTCTGAGCAAAGGTTCCGAGTCGGTTACT  
TCAAAGGGATGTTATTAGGCCTTCTGCAGTGTCTGCTACTCAAACGAATGCAACCC  
CCAAAAGAGTGTTTCACCTCCATCTATCTCAAACCAAAGGAACGAAGGCCTTGT  
GTTGAATCTTCAAGGGAGGCATTTCGAAGGGTGTGAGCAATTTCAAGACAGGCAT  
GCACAGTTGCGACAAGAACAACACTTGTCAAGCTGCCATGATCGCGAAGATCACATGT  
CGCCATCCGCTGCTGCATCCGTGGCAACGGACTTGGTGTGAGCACGCCTCGTGGA  
TCTTCTTCCAAGGGTACAAGTTCTGTGAGCTGGAAACATGCAGTGGATGCAGAGA  
AGTCTACCCACCTGACACCCAATAAGGTTGATGATTTGAATATGGAGCCCCACAG  
CCCTTTGCACAACCTTACAGCTCCAGGAGTTCCACAAATATGGGGCAAACATCACC  
TAGTGCTTTGCATTCACCAGCTTCAGGAGGCGTGTCTGCCTTTGGCCAATGGAGGC  
AAAAGCCCTCACAGCTTGCAGCACAAGGTTCTGATTTGAGCGACTACAAGCTACT  
CGTGGAACGCCTGTTCAAGGTAGTTGGAAGGCAGGAGGAAGCCCTGAGTGCTATC  
TGTGGATCCATTGTTGGCTGCCAGTCAACAGAGAGGCGCCGCGGCGCAAGCAGGA  
AGAACGACATCTGGTTCAGCTTTCATGGTTTCGACAGCGTGGCCAAGCGGAGAGT  
TGCCGTGGCGCTGGCAGAGCTCGTGCACGGCAGCCAAGACAGCTTCATTCATCTG  
GACCTGAGCCTCCAGGACTGGGGCGGCTCAAGTTTCAGAGGAAAGACTGGCATA  
GATTGCATCGTCGAGGAGTTGAGCAAGAAACGGCGCTGTGTCATCTTCTCGACA  
ACATTGATAAAGCTGACTGCCTCGTTCAGGACAGCCTCTCCCATGCCGTTGACACC  
GGAAGATTCCGGGACATGCGCGGCAAGGAAGTTGCCATTAATGACTCCATAGTAAT  
ACTGTCAACAAGATTGGCGCGATGCAGCAAAAATGCCTCGGTTGGGGTGGAAAGAG  
GGGCATATCTTCTCCGAAGAGAAGATCCTGGCTGCTAGAGGACAACAACCTCAAGA  
TCTTGATAGAATCAGGCACGGTGATCACCAGCAGAGGCTCTCCTAGTAGCAGCAA  
GGTGGCAGCTTCCCCAAGTCACCTCTCACCAAATTCAAACTTCCGTGTACTCTG  
GTTGCGTCAGTAAGCGGAAGCTTGACATTTCTGACGACCGTGAAAAGCTGCTAGA  
ATCACCGAGCAATCCCAAGCGGCCGCACAGAACCTCAAGTGTGCCGTTTCGACCTG  
AACCTCCCCGTCGGCGAGGACGGATCCAGTGACGCTGACGGCGACGACAGCAGC  
AGCAACGACAGTCCAGATGAGTCCATCGACAGCCTCCTGGGTTTGGTCGACAGAG  
CGATCGAATTCAAGGCGTTCGACTTTGGGAAGCTCGCCAACGACATCCTGCAGGA

GCTGAGCAACGTGCTCGGCAACATCATGGGCCCCGGGCAGCACGCTGGAGGTCGGC  
GATGGCGCGATGGAGCAAATGCTTGCGGCGTCATGGGTATCGGAGGACAGGCGGC  
GCCCTCTGCAGGCCTGGCTGGAGCAGGTGTTCCGCCAGGAGCCTCGAGGAGCTGA  
AGCTCAAGCACAGTAAGCCTGCGGGCAACTCTGCTCTTAGGCTAGTGGCCTGTGA  
CTGTGAGGACGGCAAAGCAGCAGCGACGGCGGCTAAGGAAGACGGCGGTTTTGG  
ACCGCTGCTCCCCTCGAGAATAATTCTGGAGTGGCGATGA

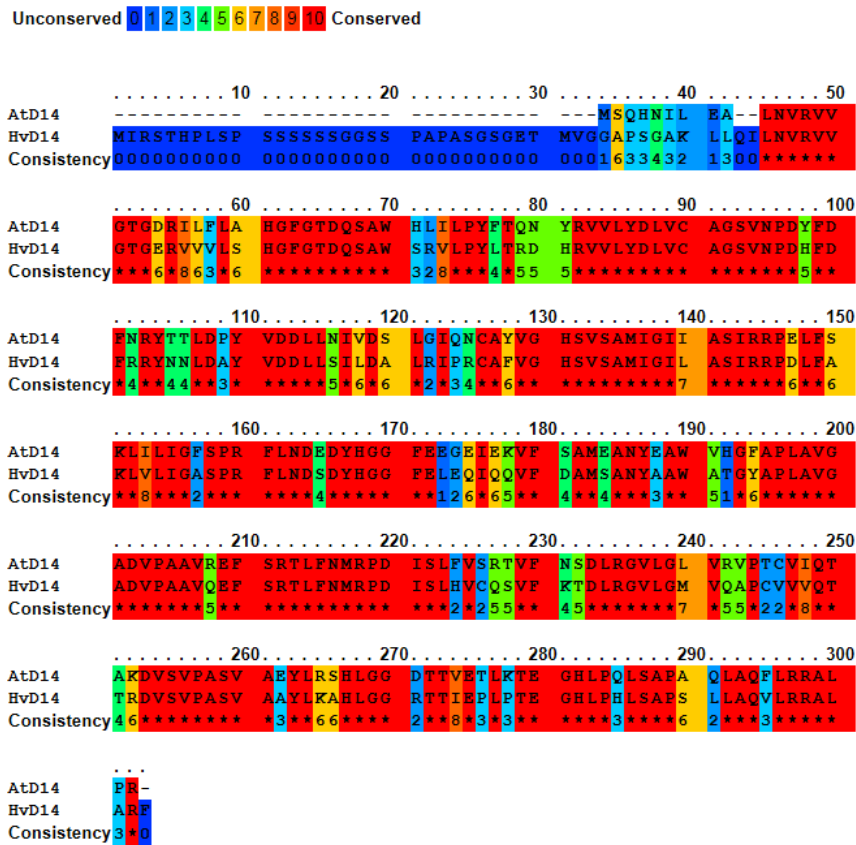
B. Nucleotide sequences of *AtD27* promoter used in this study

>*AtD27* promoter region, -709

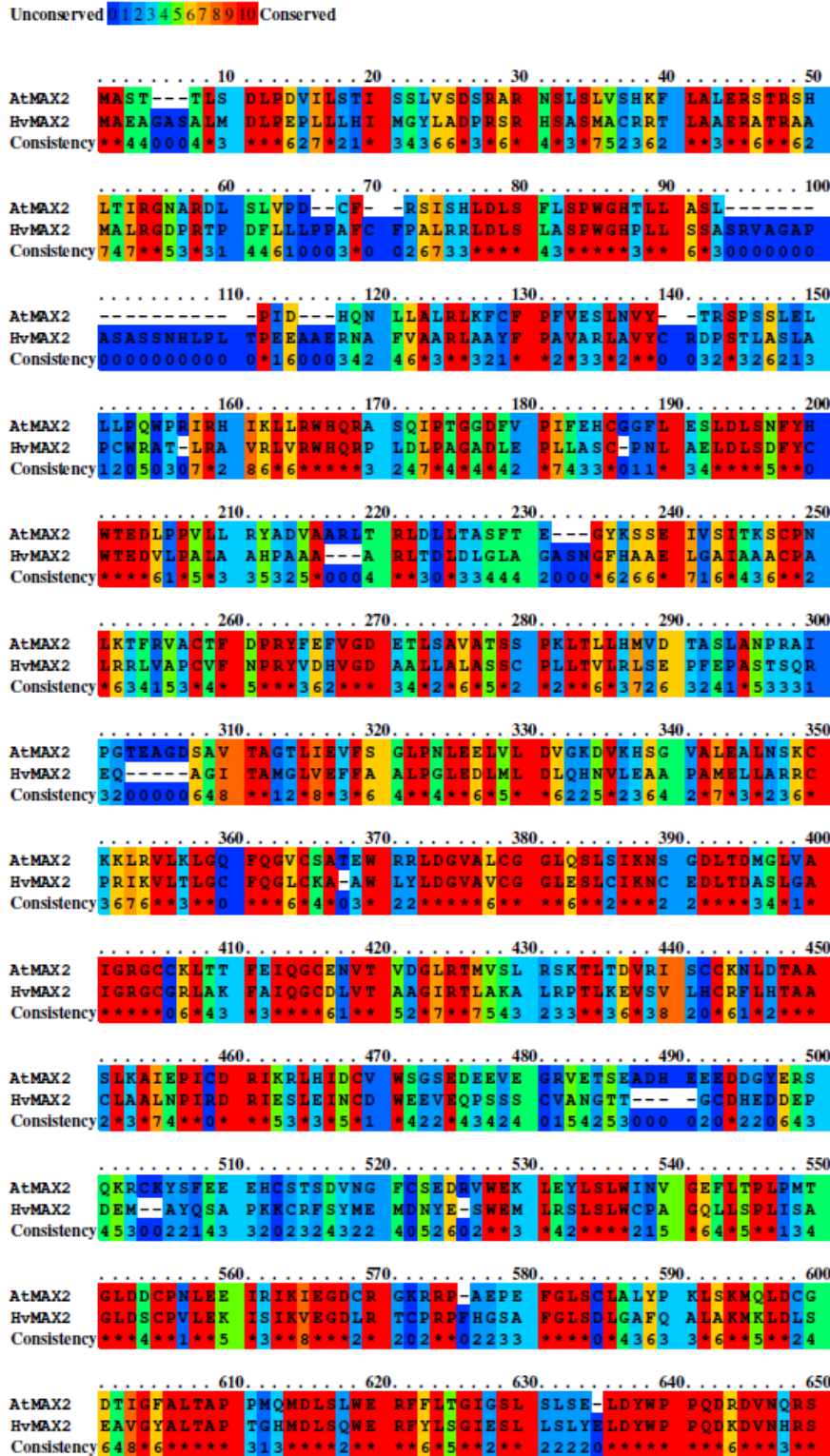
GTTCTTGAGTGAGAAAGAGAGATGGTTTGTGGGAATCTCATATATCAAGTATATGAT  
ATATTTAGTAGATCAACAAGTAAACAAAAGACAACATACCACAGAGAAGAAAAGA  
AATACGACCCGTAATTATATAATTCAACGAGATTATTTTTTGCTGTCAAATGCTTAAA  
GAATAATTTTTCTAAATACTACATCTTAATTTACTAGAGTAATATGTGTTTATCTTGT  
ATTATATATGTGATATTTATGTTTCTTCATATAATAATGATTTTATAGCTAATCAAATT  
GATATAAATGATATTTTAACTTTTGCAGATTTTACCGGAAAAAATAAGATTAGATAC  
CATTTTAAACACTTTAACCATTCAGCCTTTTGAAAAGATCTATGATCATAAATTGAA  
AGAGAGAGAGAGAACAATATCTTCCAAAAGATAGAAACATGAGAATTGTCTAAAT  
TCTTCATTGTTTTCTCGTTTTAACTTTCCTAGAAAGGACTGTCTTTACCGGAGAAAA  
GGGTCTTTTTAATAAAAAGAGAAAGAAATTTTTTAATAAAAAGATAGAGACAAAAT  
AAAATACAGGCATTCAAGGCCATATATATATATACTTTGGAGACGTCAATTAATGTC  
CTTAGAAAATTAACACAGAGAAACCTGCAACAAAATTTCTGCCAAAACCTCTTCT  
TCTACCCAAAAAAAACAAAAGAT

C. Alignments of the HvD14, HvMAX2 and HvD53 protein sequences with AtD14, AtMAX2 and AtD53 (SMXL6)

C.1 Alignment of the HvD14 protein sequence with AtD14

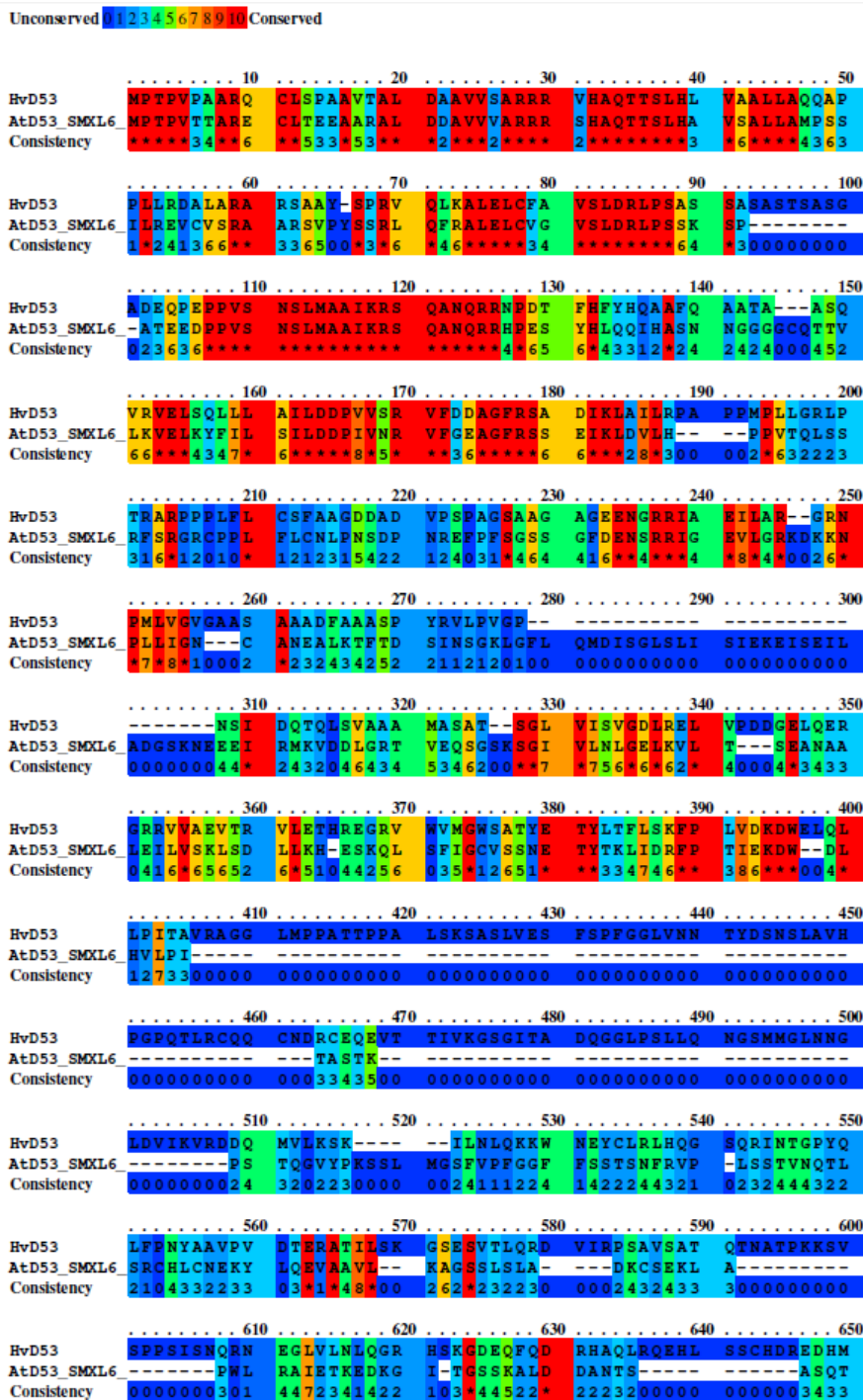


## C.2 Alignment of the HvMAX2 protein sequence with AtMAX2





### C.3 Alignment of the HvD53 protein sequence with AtD53 (SMXL6)



	660	670	680	690	700
HvD53	SPSAAA SVAT	DLVLS TPRGS	SSKGTSSV SW	KHAVDA EKST	HLTPNKVDDL
AtD53_SMXL6	AALQKKNDNI	CQSIHH--TP	AFPKLGFQSV	SPQFPVQTEK	SVRTPTSYLE
Consistency	6323330123	0227310023	62323422*0	4133256343	3633132001
	710	720	730	740	750
HvD53	NMEPPQPTAQ	PYS-----	-----SR	STNMGQTSP	SALHSPA SGC
AtD53_SMXL6	TPKLLNPPIS	KPKPMEDLTA	SVTNRTVSLP	LSCVTTDFGL	GVIYASKNQE
Consistency	425114*034	3040000000	0000000022	2*21324241	4575633522
	760	770	780	790	800
HvD53	VSAFG-QWRQ	KPSQLAAQGS	DLSDYKLLVE	RLFKVVGRRQE	EALSAICGSI
AtD53_SMXL6	SKTTRKPKML	VTLNSLLEHT	YQKDFKSLRE	ILSRKVAWQT	EAVNAISQII
Consistency	2442205032	2324263615	024*6*2*1*	1*262*40*3	*65*222*
	810	820	830	840	850
HvD53	VGCQSTERRR	GASRKNDIWF	S-FHGFDSVA	KRRVAVLAE	LVHGSQDSFI
AtD53_SMXL6	CGCKTD---S	TRRNQASGIW	LALLGFDKVG	KKKVAMTISE	VFFGGKVNYI
Consistency	2*45530003	2334524004	2041*0*4*4	*66*54*6*	632*45156*
	860	870	880	890	900
HvD53	HLDSLQDWG	GSFRGKTGI	---DCIVEEL	SKRRRCVIFL	DNIDKADCLV
AtD53_SMXL6	CVDFGAHC--	SLDDKFRGK	TVVDYVTGEL	SRKPHSVVLL	ENVEKAEFPD
Consistency	06*4436210	0*212213*1	000*1842**	*6*232*84*	6*86*6111
	910	920	930	940	950
HvD53	QDSLSHAVDT	GRFRDMRGKE	VAINDSIVIL	STRLARCSKN	ASVGVREGHI
AtD53_SMXL6	QMRLSEAVST	GKIRDLHGRV	ISMKNVIVVV	TSGIAKDNAT	DHVIKPKVFP
Consistency	*13*3*4*	*64*73*62	865452**86	5527*60534	23*0232221
	960	970	980	990	1000
HvD53	FSEKILAAAR	GQQLKILIES	GT-VITSRGS	PSSSKVAASP	SHPLTKIQTS
AtD53_SMXL6	EEQVLSARSW	KLQIKLGDAT	KFGVNRKRYE	LETAQRAVKV	QRSYLDLNL
Consistency	1462223360	22*7*70135	220*133604	145651*542	4333337433
	1010	1020	1030	1040	1050
HvD53	VYSGCVSRRK	LDISDDREKL	LESPSNPKRP	HRTSSVPPDL	NLPVGEDGSS
AtD53_SMXL6	VNE----TE-	-----F-	-----SPDHE	AED	-----
Consistency	*140000340	0000000010	000005*333	2430000000	0000000000
	1060	1070	1080	1090	1100
HvD53	DADGDDSSSN	DSPDESIDSL	LGLVDRAIEF	KAFDFGKLAN	DILQELSNVL
AtD53_SMXL6	-----	--RDANFDEF	IEKVDGKVTF	KPVDFDELAK	NIQEKIGSHF
Consistency	0000000000	002*304*44	722**2383*	*33**35**4	5*26574514
	1110	1120	1130	1140	1150
HvD53	GNIMGPGSTL	EVGDGAMEQM	LAASVVEDR	RRP-LQAWLE	QVFARSLEEL
AtD53_SMXL6	ERCFGSETHL	ELDKEVILQI	LAASWSLSS	GEEGRTVVD	QWMQTVLARS
Consistency	2424*3251*	*6332551*5	***2*143	2430054066	*04332*342
	1160	1170	1180	1190	
HvD53	KLKHSKPAGN	SALRLVACDC	EDGKAAATAA	KEDGGFGPLL	FSRIILEWR
AtD53_SMXL6	FAEAKQKYG	-NPMLGVK--	---LVASSSG	LAS---GVEL	PAKVDVIN-
Consistency	13924532*5	0213*13000	00025*6564	234000*21*	*668161*0

## 9. Abbreviations

<b>Abbreviation</b>	<b>Full Name</b>
%	Percent
°C	Celsius
μl	Microliter
μm	Micrometer
μM	Micromolar
AABO	Absciscic aldehyde oxidase
ABs	Axillary buds
ABA	Absciscic acid
ABA1	ABA deficient 1; Zeaxanthin epoxidase
ABA2	ABA deficient 2; Short chain dehydrogenase reductase
ABA3	ABA deficient 3; Molybdenum co-factor sulfurase
ABA8'OH	ABA 8' hydroxylase
ABA-GE	Absciscic acid glucose ester
ABI1	ABA-insensitive 1
ABAl	Absciscic aldehyde
Amp <sup>r</sup>	Ampicillin resistance
ANOVA	Analysis of variance
At	<i>Arabidopsis thaliana</i>
AXMs	Axillary meristems
BG	Beta-glucosidase
bp	base pair
BRC1	Branched1
BSMV	Barley stripe mosaic virus
CCD	Carotenoid cleavage deoxygenase
cDNA	Complementary DNA
CK	Cytokinins
Col-0	Columbia
cv.	cultivar
DAG	Days after germination
dNTP	deoxy-ribonucleoside triphosphate
CL	Carlactone
DNA	Deoxy ribo nucleic acid
DNase	deoxyribonucleases
DPA	Dihydro phasc acid
D27	Dwarf27
EDTA	Ethylenediaminetetraacetic acid
FW	Fresh weight
g	Gram
h	Hour
HD-ZIP	Homeodomain-leucine zipper

Hv	<i>Hordeum vulgare</i>
ID	Identifier
IPA	Idealized plant architecture
IPK	Leibniz Institute of Plant Genetics and Crop Plant Research
IPP	Isopentenyl pyrophosphate
LBO	Lateral branching oxidoreductase
LC-MS/MS	Liquid chromatography-tandem mass spectrometry
Lea	Late embryogenesis abundant
LOHi	<i>HvLea::HvABA 8'-hydroxylase</i> RNAi
MAX1	More axillary growth1
MEP	Methylerythritol phosphate
min	Minute (s)
ml	Milliliter
mM	Millimolar
MoCo	Molybdenum co-factor
MOSU	Molybdenum co-factor sulfurase
NCED	9- <i>cis</i> -epoxycarotenoid dioxygenase
nm	nanometer
Os	<i>Oryza sativa</i>
PA	Phaseic acid
PATS	Polar auxin transport stream
PCR	Polymerase chain reaction
PINs	Pin-formed auxin transport proteins
PP2A	Type 2A protein phosphatase
qRT-PCR	Quantitative real time polymerase chain reaction
RNA	Ribo nucleic acid
RNase	Ribonuclease
RT-PCR	Reverse Transcription Polymerase Chain Reaction
NaCl	Sodium chloride
NSY	Neoxanthin synthase
R:FR	Red to far-red
RT	Retention time/Room temperature
s	Second
SAM	Shoot apical meristem
SDR	Short chain dehydrogenase
SE	Standard error
siRNA	Small interfering RNA
SLs	Strigolactones
Spec <sup>r</sup>	Spectinomycin resistance
T-DNA	transfer DNA
TFs	Transcription factors
TCP	Teosinte branched1-Cycloidea-Proliferating cell factor
UDP	Uridine diphosphate
UGT	Uridine diphosphate (UDP) glucosyltransferase

v/v	volume by volume
VDE	Violaxanthin de-epoxidase
VIGS	Virus-induced gene silencing
WAG	Weeks after germination
WT	Wild type (Golden promise)
w/v	weight by volume
ZEP	Zeaxanthin epoxidase

## 10. Acknowledgements

I would like to express my deepest appreciation to all those who provided me the possibility to complete this dissertation. First and foremost, I have great exhilaration to express my deepest thanks to Prof. Dr. Nicolaus von Wirén for accepting me as a PhD candidate and providing a supportive and trustful environment with opportunities, challenges and also enough freedom to develop as a researcher.

For financial support during my PhD I would like to acknowledge the Leibniz Graduate School "Yield Formation in cereals-overcoming yield-limiting factors" and the IPK Gatersleben. I thankfully acknowledge Dr. Nese Sreenivasulu, Dr. Markus Kuhlmann and Dr. Christiane Seiler for being my scientific mentor for excellent discussion and valuable suggestion. I also appreciate Prof. Dr. Harro J. Bouwmeester (Chair of Laboratory of Plant Physiology, Wageningen University) for valuable suggestion and excellent cooperation.

I am grateful to all the members of the Department of Molecular Genetics for their technical support and for sharing devices as well as giving friendly and positive atmosphere. Special thanks to Dr. Vokkaliga T. Harshavardhan for experimental help. I am also very grateful to all the efforts from my work partners. I would like to appreciate Dr. Kai Eggert and Dr. Mohammad-Reza Hajirezaei for hormone measurement, Dr. Wanxin Chen and Dr. Patrick Schweizer for VIGS experiment, Dr. Twan Rutten for his assistance with the histological analysis, Dr. Götz Hensel for providing plasmids for vector construction, Sabine Skiebe and Elke Liemann for their help with complementation experiment. I would like to express my thanks to each of all, past and present members of our Department, Dr. Rajesh Kalladan, Korana Surdonja and Thirulogachandar Venkatasubbu, for their support and their help, for encouraging me through this time and for creating such a pleasant working atmosphere.

For technical assistances I will give special thanks to Jana Lorenz and Mandy Pueffeld for their kindness and perfect assistance on most of my laboratory work, and Gabriele Einert for wonderful greenhouse work. I also would like to give many thanks to Dr. Britt Leps for her efforts that made my daily life convenient in Gatersleben.

Last but not least I want to thank my family and all my friends. I cannot be grateful enough for your continuous love and support in so many ways. I want to thank to my wife Huijuan Yan for supporting me during every step of the way. She made me happy since we have been together and she has taken great care of me.

I wish to express my sincere gratitude to everyone who, in their own way, helped me to complete this dissertation.

## 11. Curriculum Vitae

**Family name:** Wang      **First name:** Hongwen

**Address:** Leibniz Institute of Plant Genetics and Crop Plant Research (IPK), OT Gatersleben, Corrensstrasse 3, D-06466 Stadt Seeland, Germany

**E-mail:** wanhg@ipk-gatersleben.de, whw19850210@126.com

**Date of Birth:** 10/02/1985

**Place of Birth:** Gaomi city / Shandong province / China

**Nationality:** Chinese    **Gender:** Male    **Marital status:** Married

### Education:

Oct. 2012 – present      **Ph.D.** Enrolled at Martin Luther University, Halle, Germany, and the thesis was prepared at: Leibniz Institute of Plant Genetics and Crop Plant Research (IPK), Gatersleben, Germany

Sep. 2008–July. 2011    **M.Sc.** Biochemistry and Molecular Biology, China-UK HUST-RRes Crop Genetics Engineering and Genomics Joint Laboratory, Huazhong University of Science and Technology (HUST), Wuhan, China

Sep. 2004–Jul. 2008    **B.Sc.** Laboratory of Molecular Biology, Department of Biology, College of Life Sciences, Weifang University (WFU), Weifang, China

### Academic researches:

1, Genetic manipulation of the crosstalk between abscisic acid and strigolactones and their biosynthetic link during late tillering in barley (PhD thesis) (Oct. 2012 – Sep. 2016).

2, Identification of new low-molecular-weight glutenin subunit genes in wheat (Master dissertation) (Sep. 2008 – July. 2011).

### Publications:

1, Ma, F., Li, M., Yu, L., Li, Y., Liu, Y., Li, T., Liu, W., **Wang, Hongwen.**, Zheng, Q. and Li, K. (2013) Transformation of common wheat (*Triticum aestivum* L.) with avenin-like b gene improves flour mixing properties. *Molecular Breeding*, **32**, 853-865.

2, Cui Cuiju, Ma Fengyun, **Wang Hongwen**, Mao Yuejian, Wang Yuesheng, He Guangyuan. (2009) Identification of new genes encoding the low-molecular-weight glutenins in wheat. *Molecular Plant Breeding*; 2009-04.



### **Conferences - poster:**

1, **Hongwen Wang**, Markus Kuhlmann, Vokkaliga Thammegowda Harshavardhan, Twan Rutten, Christiane Seiler, Nese Sreenivasulu. Regulation of tiller formation by abscisic acid in barley. Plant Science Student Conference, Halle, Germany, 2013.

2, **Hongwen Wang**, Christiane Seiler, Vokkaliga Thammegowda Harshavardhan, Nese Sreenivasulu, Tatsiana Charnikhova, Harro J. Bouwmeester, Markus Kuhlmann. The Effect of Abscisic acid-Strigolactones Crosstalk on Tillering in Barley. 1st International Congress on Strigolactones, Wageningen, Netherlands, 2015.

Hongwen Wang  
Gatersleben, 15<sup>th</sup> September, 2016

## 12. Affirmation/Eidesstattliche Erklärung

Hongwen Wang

Leibniz Institute of Plant Genetics and Crop Plant Research (IPK)  
OT Gatersleben, Corrensstrasse 3,  
D-06466 Stadt Seeland,  
Germany

I hereby declare that the submitted thesis has been completed by me, the undersigned, and that I have not used any other than permitted reference sources or materials or engaged any plagiarism. All the references and the other sources used in the presented work have been appropriately acknowledged in the work. I further declare that the work has not been previously submitted for the purpose of academic examination, either in its original or similar form, anywhere else.

Hiermit erkläre ich, dass ich diese eingereichte Dissertation selbständig angefertigt und keine anderen als die angegebenen Quellen und Hilfsmittel verwendet habe. Die den benutzten Hilfsmitteln wörtlich oder inhaltlich entnommenen Stellen habe ich unter Quellenangaben kenntlich gemacht. Die vorliegende Arbeit wurde in gleicher oder ähnlicher Form noch keiner anderen Institution oder Prüfungsbehörde vorgelegt.

I hereby declare that I have no criminal record and that no preliminary investigations are pending against me.

Des Weiteren erkläre ich, dass ich weder vorbestraft bin noch dass gegen mich Ermittlungsverfahren anhängig sind.

Gatersleben, 15<sup>th</sup> September, 2016

Hongwen Wang